

**Adaptive Antenna Arrays
for
Satellite Personal Communication Systems**

by

Keng Jin Lian

Thesis submitted to the Faculty of the
Virginia Polytechnic Institute and State University
in partial fulfillment of the requirements for the degree of

MASTER OF SCIENCE

IN

ELECTRICAL ENGINEERING

APPROVED:

Dr. Timothy Pratt, Chair

Dr. Charles Bostian

Dr. Brian Woerner

January 27, 1997

Blacksburg, Virginia

ADAPTIVE ANTENNA ARRAYS
FOR
SATELLITE PERSONAL COMMUNICATION SYSTEMS

by

Keng-Jin Lian

Committee Chairman: **Timothy Pratt**
Department of Electrical Engineering

ABSTRACT

Since about the turn of the decade, several proposals have come forth for personal communication services implemented by means of multiple satellite systems. These satellite systems are similar to current terrestrial cellular technologies, which are still relatively new and have numerous technical problems associated with them. As a result, these satellite systems will also experience some of the similar problems. Two of such problems are the issue of multipath and interference. These problems may result in significant link degradation and affect overall capacity. To overcome this problem, adaptive antenna arrays on handheld terminals are proposed. This technique is believed to be better than omnidirectional antennas which radiate in all directions. Adaptive antenna arrays have the ability to adapt to the changing environment and null out the interference. The LMS algorithm was investigated and used in the simulation of the adaptive array. The performance of the LMS array was discussed in detail. In the case of a multipath, an alternate approach was proposed where a diversity combiner is used to phase shift the multipath and combine the Signal of Interest and multipaths constructively.

Acknowledgments

First, I would like to thank God for His blessings and for giving me wonderful parents whose love, encouragement and support have been my source of inspiration. I am eternally grateful to them for the sacrifices that they went through to send me abroad.

I would like to express my heart-felt thanks to Dr. Timothy Pratt, whose insights and invaluable advice have helped me arrive at this important milestone. He has been a mentor and friend in guiding me throughout my graduate career. I would also like to express my deepest gratitude to Dr. Charles W. Bostian who has been a respectful employer by providing me with a research assistantship for which many would say that I am unqualified. I would like to thank Dr. Brian Woerner for serving on my committee and providing me with valuable technical advice. I appreciate all their help in carefully reviewing this thesis report.

I also wish to thank the STARR foundation for their financial support throughout my years at Virginia Tech.

I wish to express my sincere gratitude to Jesse, Mansoor, Ivanna, George, Farooq, Nim, Nishith, Melanie, Angie, Elvin and Tor for their help during this past one and a half years. Also, to all my friends from the Chinese Bible Study Group for their prayers and support.

Last but not least, I would like to thank my sister Pin Pin for her patience and for putting up with me during difficult times.

Table of Contents

CHAPTER 1 INTRODUCTION	1
CHAPTER 2 PERSONAL COMMUNICATION SATELLITES	4
2.1 Motivation	4
2.2 Historical Perspectives	5
2.3 Satellite Cellular Integration	5
2.4 Geometrical Analysis	6
2.4.1 Estimation of number of satellites and orbits	7
2.5 Orbits and Characteristics of Mobile Satellite Services	11
2.5.1 ORBCOMM	11
2.5.2 IRIDIUM	13
2.5.3 GLOBALSTAR	14
2.5.4 ODYSSEY	15
2.5.5 Inmarsat P (ICO Global)	16
2.5.6 AMSC	17
2.5.7 Teledesic	18
2.5.8 Others	19
2.6 Summary	19

CHAPTER 3 NETWORK RESOURCE MANAGEMENT AND LINK ANALYSIS	23
3.1 Personal Communication Network	23
3.2 Antenna Beams	24
3.2.1 Multibeam Coverage:	24
3.2.2 Intersatellite links:	24
3.3 Doppler Effect	25
3.4 Handoff	25
3.5 Channel Assignments	27
3.6 Call Setup	29
3.6.1 IRIDIUM [Swa 93] [Rod 96] [Gru91]	30
3.6.2 ORBCOMM [Par et al. 96]	30
3.7 Routing Considerations	31
3.7.1 Centralized Adaptive Routing	31
3.7.2 Distributed Adaptive Routing	31
3.7.3 Flooding	32
3.8 Link Analysis	32
3.8.1 IRIDIUM Link Budgets	33
3.8.2 GLOBALSTAR Link Budgets	35

3.9 Summary	37
CHAPTER 4 ADAPTIVE ANTENNA ARRAYS	38
4.1 Motivation	38
4.2 Antenna Arrays for Suppression of Interference and Multipath	41
4.3 Array Classification	42
4.4 Array Design Architecture	42
4.5. Grating Nulls [Sko80]	51
4.6 Practical Limitations	52
4.6.1 Degrees of Freedom	53
4.6.2 Array Null Depth	56
4.7 Adaptive Algorithms	64
4.8 Adaptive Arrays and SatPCS	64
4.9 Summary	65
CHAPTER 5 ADAPTIVE ALGORITHMS, SIMULATIONS AND RESULTS	67
5.1 The Least Mean Square (LMS) Algorithm	67
5.1.1 Introduction	67
5.1.2 Minimum Mean Square Error (MMSE)[Wid67],[Com88]	69

5.1.3 Basic Description	72
5.1.4 The Convergence Rate of the LMS Algorithm	73
5.2 Simulation Assumptions	73
5.3 Simulations & Results	74
5.3.1 LMS Algorithm in a TDMA System	74
5.3.1.1 Adaptive Array in the Presence of Interference (Uncorrelated)	75
5.3.1.2 Adaptive Array in the Presence of Multipath (Correlated)	86
5.4 Adaptive Array for Combating Multipath	89
5.5 Conclusion	91
CHAPTER 6 CONCLUSIONS AND FUTURE WORK	93
6.1 Summary and Conclusions	93
6.2 Future Work	94
REFERENCES	96
VITAE	103

List of Figures

FIGURE 1 CENTRAL ANGLE	8
FIGURE 2 CELL COVERAGE (<i>FOOTPRINTS</i>)	9
FIGURE 3 NUMBER OF SATELLITES VERSUS ORBIT HEIGHTS	10
FIGURE 4 NUMBER OF ORBITS VERSUS ORBIT HEIGHTS	11
FIGURE 5 SATPCS USER IN THE PRESENCE OF INTERFERENCE AND MULTIPATH	39
FIGURE 6 AN EXAMPLE OF AN ADAPTIVE ANTENNA ARRAY	43
FIGURE 7(A). VOLTAGE PATTERN OF AN LMS ARRAY, DOA(DESIRED) = 0°; DOA(INTERFERER) = 45°; SIR(DB) = -10; ITERATION = 1	46
FIGURE 7(B). VOLTAGE PATTERN OF AN LMS ARRAY, DOA(DESIRED) = 0°; DOA(INTERFERER) = 45°; SIR(DB) = -10; ITERATION = 70	47
FIGURE 7(C). VOLTAGE PATTERN OF AN LMS ARRAY, DOA(DESIRED) = 0°; DOA(INTERFERER) = 45°; SIR(DB) = -10; ITERATION = 350	48
FIGURE 7(D). VOLTAGE PATTERN OF AN LMS ARRAY, DOA(DESIRED) = 0°; DOA(INTERFERER) = 45°; SIR(DB) = -10; ITERATION = 750	48
FIGURE 7(E). VOLTAGE PATTERN OF AN LMS ARRAY, DOA(DESIRED) = 0°; DOA(INTERFERER) = 45°; SIR(DB) = -10; ITERATION = 1200	49
FIGURE 7(F). VOLTAGE PATTERN OF AN LMS ARRAY, DOA(DESIRED) = 0°; DOA(INTERFERER) = 45°; SIR(DB) = -10; ITERATION = 3000	49
FIGURE 8 WEIGHTS OF THE ADAPTIVE ARRAY VS. NUMBER OF ITERATIONS	50
FIGURE 9(A) 2 ELEMENT ARRAY VOLTAGE PATTERN; DOA(DESIRED)=45°; DOA(INTERFERER)=0°; SIR(DB)=10	55

FIGURE 9(B) 4 ELEMENT ARRAY VOLTAGE PATTERN; DOA(DESIRED)=45°;	
DOA(INTERFERER)=0°; SIR(DB)=10	55
FIGURE 9(C) 6 ELEMENT ARRAY VOLTAGE PATTERN; DOA(DESIRED)=45°;	
DOA(INTERFERER)=0°; SIR(DB)=10	55
FIGURE 9(D) 8 ELEMENT ARRAY VOLTAGE PATTERN; DOA(DESIRED)=45°;	
DOA(INTERFERER)=0°; SIR(DB)=10	56
FIGURE 10(A) 2 ELEMENT ARRAY VOLTAGE PATTERN; DOA(DESIRED) = 30°;	
DOA(INTERFERER) = 0°; SIR(DB) = -20	57
FIGURE 10(B) 2 ELEMENT ARRAY VOLTAGE PATTERN; DOA(DESIRED) = 30°;	
DOA(INTERFERER) = 0°; SIR(DB) = -10	57
FIGURE 10(C) 2 ELEMENT ARRAY VOLTAGE PATTERN; DOA(DESIRED) = 30°;	
DOA(INTERFERER) = 0°; SIR(DB) = 0	58
FIGURE 10(D) 2 ELEMENT ARRAY VOLTAGE PATTERN; DOA(DESIRED) = 30°;	
DOA(INTERFERER) = 0°; SIR(DB) = 10	58
FIGURE 11 WEIGHTS CONVERGING AS INR OF SNOI ₂ INCREASES	62
FIGURE 12 THE LMS ADAPTIVE ANTENNA ARRAY	69
FIGURE 14(A) VOLTAGE PATTERN OF AN ADAPTIVE ARRAY DOA(DESIRED)=45°;	
DOA(INTERFERER)=0°; SIR(DB) = 5	76
FIGURE 14(B) OUTPUT SINR VERSUS NUMBER OF ITERATIONS (TRAINING	
SEQUENCES)	77
FIGURE 15(A) 2 ELEMENT ARRAY VOLTAGE PATTERN; DOA(DESIRED) = 30°;	
DOA(INTERFERER) = 0°; SIR(DB) = -20	77

FIGURE 15(B) 2 ELEMENT ARRAY VOLTAGE PATTERN; DOA(DESIRED) = 30°;	
DOA(INTERFERER) = 0°; SIR(DB) = -10	78
FIGURE 15(C) 2 ELEMENT ARRAY VOLTAGE PATTERN; DOA(DESIRED) = 30°;	
DOA(INTERFERER) = 0°; SIR(DB) = 0	78
FIGURE 15(D) 2 ELEMENT ARRAY VOLTAGE PATTERN; DOA(DESIRED) = 30°;	
DOA(INTERFERER) = 0°; SIR(DB) = 10	79
FIGURE 16(A) OUTPUT SINR VERSUS NUMBER OF ITERATIONS. $\mu = 0.1480$	80
FIGURE 16(B) OUTPUT SINR VERSUS NUMBER OF ITERATIONS. $\mu = 0.0001$	81
FIGURE 17 OUTPUT SINR VERSUS NUMBER OF INTERFERERS FOR SEVERAL	
DIFFERENT ARRAYS	83
FIGURE 18(A) 2 ELEMENT ARRAY WITH SIR = 20 DB VOLTAGE PATTERN;	
DOA(DESIRED)=30°; DOA(INTERFERER)= 0°	84
FIGURE 18(B) 4 ELEMENT ARRAY WITH SIR = 20 DB VOLTAGE PATTERN;	
DOA(DESIRED)=30°; DOA(INTERFERER)= 0°	84
FIGURE 18(C) 6 ELEMENT ARRAY WITH SIR = 20 DB VOLTAGE PATTERN;	
DOA(DESIRED)=30°; DOA(INTERFERER)= 0°	85
FIGURE 18(D) 8 ELEMENT ARRAY WITH SIR = 20 DB VOLTAGE PATTERN;	
DOA(DESIRED)=30°; DOA(INTERFERER)= 0°	85
FIGURE 19(A) VOLTAGE PATTERN OF ADAPTIVE ARRAY (WITH MULTIPATH	
PHASE SHIFTED BY $\pi/2$)DOA(DESIRED) = 30°; DOA(INTERFERER) = 0°;	
SIR(DB)=3	87
FIGURE 19(B) OUTPUT SINR VERSUS NUMBER OF ITERATIONS	88

FIGURE 20(A) VOLTAGE PATTERN OF ADAPTIVE ARRAY (WITH MULTIPATH PHASE SHIFTED BY π)	89
DOA(DESIRED) = 30° ; DOA(INTERFERER) = 0° ; SIR(DB)=3	89
FIGURE 20(B) OUTPUT SINR VERSUS NUMBER OF ITERATIONS	89
FIGURE 21 A BLOCK DIAGRAM OF THE TWO ELEMENT PHASED ARRAY [BER96]	90

List of Tables

TABLE 1. SYSTEM PARAMETERS OF SOME OF THE PROPOSED CONSTELLATIONS[VAT ET.AL.95].	9
TABLE 2. ORBCOMM'S CHANNEL REQUIREMENTS[PAR ET AL. 96]	12
TABLE 3. IRIDIUM'S FREQUENCY & CHANNEL ASSIGNMENTS [SOURCE: MOTOROLA 1992]	13
TABLE 4. GLOBALSTAR'S FREQUENCY ASSIGNMENTS	15
TABLE 5. ODYSSEY'S FREQUENCY ASSIGNMENTS	16
TABLE 6. AMSC-1'S FREQUENCY ASSIGNMENTS	17
TABLE 7A. SELECTED BIG LEOS [ABR 96] [TOR96] [LIA96]	21
TABLE 7B. SELECTED LITTLE LEOS [ABR 96] [TOR96] [LIA96]	22
TABLE 7C. SELECTED GEOS [ABR 96] [TOR96] [LIA96]	22
TABLE 8. LINK BUDGET FROM HANDHELD TO IRIDIUM [<i>SOURCE: MOTOROLA</i> <i>1992</i>]	33
TABLE 9. LINK BUDGET OF INTERSATELLITE LINKS FOR IRIDIUM [<i>SOURCE:</i> <i>MOTOROLA 1992</i>]	34
TABLE 11. LINK BUDGET CALCULATION FOR TYPICAL ORBCOMM SUBSCRIBER EQUIPMENT UPLINKS (VHF-1, 148 MHZ BAND)[HOW96]	36
TABLE 12. LINK BUDGET CALCULATION FOR TYPICAL ORBCOMM SUBSCRIBER EQUIPMENT DOWNLINKS (VHF-3, 137 MHZ--UHF)[HOW96]	36
TABLE 13. SATELLITE CHARACTERISTICS	64

Chapter 1 Introduction

“Just as human beings once dreamed of steam ships, railroads and superhighways, we now dream of the global information infrastructure that can lead to a global information society.”

~ Vice President Al Gore, Brussels, February 25, 1995

Since about the turn of the decade, several proposals have come forth for personal communication services implemented by means of multiple satellite systems. It appears that at least one such system, and perhaps more than one, will be launched before the turn of the century. The challenges surrounding these systems are many. However, the rewards are equally great [Enr95]. These challenges range from choosing a suitable modulation technique that will provide reasonable capacity, isolation of users from each other, resistance to channel impairments, to networking issues such as access techniques, delivery time analysis, and channel allocation. The rewards will be a communication system that will provide data and voice links to virtually anywhere at anytime.

Satellite Personal Communication Systems (SatPCS) have been touted as being able to provide communication services to vast regions of the Earth that lack adequate infrastructure for commercial telephony services. Whether this is indeed the backdrop for such systems will depend on many factors, not the least important of which is cost. Also of grave importance is the successful integration of SatPCS with the land-mobile and fixed networks. However, judging from the explosive growth of such systems as PCSs, it seems a safe bet that mobile user satellite systems will enjoy an equally rapid growth into markets not yet entirely foreseen. Satellite Personal Communication Services are comparable to moving cellular technology into space.

The existing terrestrial cellular system is viewed as a relatively new technology and there are still numerous technical problems associated with it. Moving cellular communications into space poses additional complications for system designers. Some of these complications include shadowing effects, power control, soft-handoff, multipath fading, capacity and cost. Most existing cellular systems use simple arrays or antennas transmitting in a fixed direction or all directions (omnidirectional). This causes a lot of interference between the subscribers. Interference on voice channels causes cross-talk, where the subscriber hears interference in the background. On control channels, interference will lead to missed or blocked calls due to errors in digital signaling. With the rapid increase in cellular subscription, capacity will be an issue in future communication systems. One approach to increase capacity is to reduce interference, and a cost effective method of achieving this is diversity.

Diversity is a powerful communication receiver technique that provides wireless link improvements, and exploits the random nature of radio propagation by finding independent (or at least highly uncorrelated) signal paths for communication [Rap96]. There are many diversity technique variations: spatial diversity, selection diversity, polarization diversity, frequency diversity and time diversity. However, the most popular technique that is being used is spatial diversity.

Space diversity (sometimes known as antenna diversity) is widely used in wireless systems. Recent trends in mobile communications have shown that adaptive (smart) antenna arrays have tremendous potential for increasing the capacity of mobile communications by reducing co-channel interference, multipath and noise. The focus of this thesis is to look at the impact of using adaptive antenna arrays on handheld communicators for SatPCS.

This thesis will start with an overview of the proposed SatPCSs such as IRIDIUM, GLOBALSTAR and ODYSSEY. Next, an analysis on the tradeoffs between the different proposed constellations, minimum elevation angle, inclined orbit and capacity will be presented. In addition, details related to network architecture, i.e. channel assignment strategies, handoff and compatibility with existing terrestrial systems will be discussed.

Subsequent to providing a brief introduction on SatPCS, the focus will shift toward antenna diversity. A quick introduction on adaptive antenna arrays will be presented and some basic and one of the more popular algorithms will be discussed.

Later, a simulation of a linear adaptive algorithm will be conducted to demonstrate the self-steering capability of an adaptive antenna array. The thesis will demonstrate how adaptive

antennas can be used to combat both interference and multipath fading. An analysis of the simulation results will then be presented.

After this, the impact of using adaptive antenna arrays on handheld communicators will be discussed. The thesis will attempt to show that apart from reducing interference, adaptive antennas can offer multipath immunity and immunity to the fast changing effects of the environment. Finally, some issues that had to be extracted from the thesis due to time constraints will be mentioned and possible solutions will be briefly stated.

Chapter 2 Personal Communication Satellites

2.1 Motivation

Wireless personal communications is one of the fastest growing fields in the engineering world. However, the wireless industry is still in its infancy. While this might seem to be a rash statement, considering the fact that more than a century has passed since Guglielmo Marconi first demonstrated radio's ability as a means of communications [Rap 95], most of the technologies dealing with cellular communications are less than a decade old. In the past decade, the phenomenal growth in the wireless industry is due in part to the improvements of microelectronics, better fabrication techniques, and new large-scale circuit integration.

The United States, like the rest of the world, is sorting through the options of this information revolution. At this point in time, the "information superhighway" is more like an unmarked country road. As a result, everyone is scrambling to find a way to mesh disparate technologies into forms that will yield a workable road map.

The issue of standards is by far one of the more difficult roadblocks facing all participants in the communications industry. For instance, in the US, the cellular telephony and PCS market are suffering from the early success of analog systems, namely the Advanced Mobile Phone Service (AMPS).

2.2 Historical Perspectives

AMPS was first developed by AT&T Bell Laboratories back in the late 1970s [You79] [Rap95]. This system was first deployed in late 1983 in Chicago by Ameritech; a total of 40 MHz of spectrum in the 800 MHz band was allocated by the Federal Communications Commission (FCC) [Rap 95]. Six years later, the demand for the cellular market had grown and an additional 10 MHz of spectrum was extended to existing cellular communication services.

There are currently two digital cellular communications standards in various stages of technical development. The technologies are Global System for Mobile communications (GSM), and Code Division Multiple Access (CDMA). GSM is currently adopted by 86 countries and 156 operating companies and was first commercially available in Europe in 1992 [Ire96]. On the other hand, CDMA is new, and many claim that it is unproven and is a multibillion-dollar technology gamble.

In any event, there will be an estimated 210 million cellular subscribers in the world by the year 2000, with Asia leading the rest of the world in terms of subscribers [ABI 96]. Consequently, the demand for a seamless wireless market will be created.

2.3 Satellite Cellular Integration

In the last couple of years, numerous proposals have come forth for a wireless satellite network that will provide subscribers with continuous coverage anywhere and anytime. Some of these systems, also known as the “Big LEOs”, will forever revolutionize the way we communicate and perceive the world. The technology involved is, in general, a migration of terrestrial cellular technology into space. In many ways, these personal communication satellites are meant to complement current terrestrial networks and not compete with them. In other words, this can be seen as an integration of satellite and cellular technology.

Many feel that one of the factors driving the integration of these two are that terrestrial systems are more suitable for urban and suburban regions, while satellites are more suitable for rural areas [Bos95]. An integrated system will not only provide the subscribers with one-number service and unrestricted roaming, but satellites can be used as a backup for terrestrial systems when needed.

In order for this “marriage” to work, numerous technical issues have to be considered. Some of these issues include: (a) The air interface - modulation, multiple access, link budgets, (b) Traffic modeling, including estimating the demand for satellite PCN, (c) Radio resource management - user mobility, handoff management, both between satellite and routing strategies,

(d) Terminal technology, and (e) Networking features. Unfortunately, due to time constraints, only some of the issues mentioned will be examined in this thesis.

The development detail of the concepts, the planning of services, as well as the production of the hardware have been started by a number of industries from the US, Europe and other regions of the world.

On the regulatory front, initial frequency bands were set aside at the 1992 World Administrative Radio Conference (WARC-92) while the US FCC has issued orders licensing several data communications systems as well as three voice communications systems.

2.4 Geometrical Analysis

Circular orbits can be classified according to the satellite altitude, H , as: low-altitude earth orbits, having $500 < H < 2000$ km; medium-altitude earth orbits (MEO), having $5000 < H < 20000$ km; the geostationary orbit (GEO), having $H = 35800$ km. Figure 1 shows the lower limit on the number of satellites required to provide global Earth coverage (polar regions excluded) as a function of H and with the minimum elevation angle, α , as a parameter. A detailed derivation is discussed in section 2.4.1. The advantages of going from LEOs to GEOs are: (a) Shorter delays (better transmission quality), (b) Ability to reuse frequency and increase capacity, (c) Smaller and lighter radio handsets since less power is required, (d) Handsets can use low power and non-directive antennas, (e) World-wide coverage, (f) More fail-safe due to greater number of satellites, and (g) Provide position location. Nevertheless, LEOs are not without their own disadvantages; for instance: (a) Large numbers of satellites are needed at high cost, (b) Relatively complex satellites: (i) On-board switching, routing, (ii) Multihop operation for long distance calls, (iii) Handoff, (iv) Cross-links, (v) Power management during orbit, (c) Complex Network Operations: (i) Satellite monitoring, (ii) Control Replenishment, and (iii) Individual satellites spend a large percentage of time over areas with little traffic.

Consequently, MEO constellations look for a compromise between LEOs and GEOs. They require a limited number of satellites for global coverage by employing intermediate elevation angles ($\alpha \geq 20^\circ$, or so). Also, the propagation delay and attenuation due to free space are also intermediate.

The identification of the optimum satellite constellation relies on the analysis of a number of mutually linked factors, such as: (a) type of service(s), (b) maximum transmission delay, (c) minimum elevation angle, (d) service quality and availability specifications, (e) extent and distribution of the expected user population, (f) number and class of satellites, and (g) types of mobile terminals, etc.

Comparison of alternatives is difficult due to the complex interaction between these elements [Vat et al. 95]. As a consequence, the main system parameters are the number of communications satellites, gateway earth-stations (network nodes), and the number and kind of communication links in the network [Lutz 93]. In terms of performance measures, some geometrical considerations will play a role in affecting the coverage areas, handoff times, and link analysis [Cor et.al 95][Vat et.al 95][Cor et.al 93][Böt 95].

A high degree of connectivity within a LEO/ICO satellite network can be achieved by a sufficient number of such network nodes and corresponding links between them [Lutz 93]. The higher the degree of connectivity, the more alternatives for routing are given, and therefore the better the traffic flow distribution. Moreover, it enhances the flexibility of the network to cope with link or node failures. On the other hand, construction and positioning of more gateways and/or satellites means higher fixed costs, and the permanent supply of large capacity means high recurring costs. These factors show that optimization of the whole system is a central task in the initial state of system planning.

2.4.1 Estimation of number of satellites and orbits

In this section, a simple derivation for the necessary number of satellites and orbits will be shown. The most crucial parameter that determines these quantities is the orbit height, which will be the starting point of our analysis.

The *footprint* is that part of the surface of the earth where a satellite can be seen under a certain elevation angle $\geq \varphi$. Thus the *footprint* is a spherical segment of the Earth with the central angle ψ (Figure 1). The central angle is given as follows (see also reference 2):

$$\psi = \frac{r}{R} - \varphi - \arcsin\left(\frac{r \cos(\varphi)}{r + h}\right) \quad (2.1)$$

If at anytime at least one satellite has to be seen from any point of the Earth, the *footprints* must overlap. The effective *footprint* of a single satellite is then equivalent to the largest inscribed hexagon (Figure 2). This hexagon consists of six spherical triangles with one angle of 60° and two identical angles α . The area A of the hexagon is

$$A = 6r^2 \epsilon \quad (2.2)$$

Here, ρ denotes the mean radius of the Earth and ϵ the spherical excess of one of the six isosceles triangles:

$$\alpha = 2\theta + \frac{\theta}{3} - \theta = 2\theta + \frac{2\theta}{3} \quad (2.3)$$

Furthermore, the angle α is given by

$$\begin{aligned} \cos \alpha &= -\cos \theta \cos \frac{\theta}{3} + \sin \theta \sin \frac{\theta}{3} \cos \psi \\ \Rightarrow \alpha &= \tan^{-1} \frac{\sqrt{3}}{\cos \psi} \end{aligned} \quad (2.4)$$

To cover the total surface of the Earth, at least

$$n = \frac{4\pi R^2}{A} \quad (2.5)$$

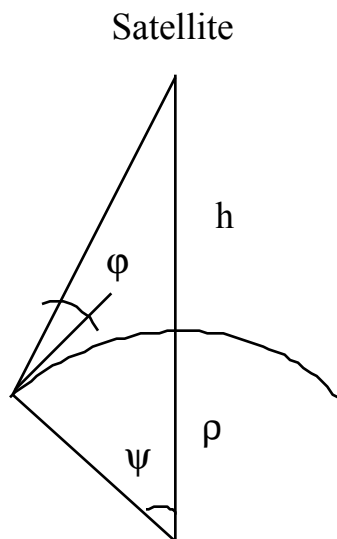


Figure 1 Central Angle

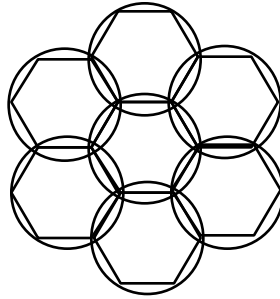


Figure 2 Cell Coverage (*Footprints*)

hexagons, and thus the same number of satellites, are necessary. Figure 3 shows the number of required satellites versus the orbit height. For the example systems of Table I, the chosen values are also given.

Table 1. System parameters of some of the proposed constellations[Vat et.al.95].

System	Height (km)	Nominal α ($^{\circ}$)	Number of Satellites	Number of Orbital planes	Inclination ($^{\circ}$)
<i>Iridium</i>	780 (795)	10	66	6	90
<i>Globalstar</i>	1400	10/15	48	6	47/52
<i>Teledesic</i>	700	N/A	840-924	21	N/A
<i>Odyssey</i>	10354	22	12	3	55

Besides the number of satellites, the minimum number of orbits Ω is also important. At least for great orbit heights, one launcher has to be used for each orbit. In order to determine the necessary number of orbits it is sufficient to consider the satellite coverage at the equatorial coverage depicted in Figure 2. On the condition that in every orbit there are at least two satellites, each orbit covers $3\rho\psi$ of the equator [Lutz 93]. Therefore, at least

$$\Omega = \frac{2x}{3\psi} \quad (2.6)$$

orbits are necessary to guarantee global coverage. The quantity Ω versus the orbit height is depicted in Figure 4. Again, the values of the example systems are presented for comparison reasons.

Title: fig23. eps
Creator: MATLAB, The Mathworks, Inc
CreationDate: 01/18/97 11:13:31

Figure 3 Number of Satellites versus orbit heights

Title: fig24.eps
Creator: MATLAB, The Mathworks, Inc
CreationDate: 01/18/97 11:16:32

Figure 4 Number of Orbits versus Orbit heights

2.5 Orbits and Characteristics of Mobile Satellite Services

As mentioned in Section 2.4, GEO satellites are located in orbits farthest from the Earth. The time delay experienced by the communications link for a GEO is 250 msec (one way) or more when processing delays are added. Most of the non-geostationary satellites are located in LEO orbits, between the Earth's atmosphere and inner Van Allen Belt. Medium Earth orbit (MEO) systems take advantage of a gap between the inner and outer Van Allen belts and place the satellites in inclined orbits.

2.5.1 ORBCOMM

The ORBCOMM system will be the world's first low-Earth orbit (LEO) satellite system to provide high availability, low-cost, two-way, mobile communications over the entire globe. Orbcomm is one of the major players among the little LEOs and has recently launched two

satellites. This system will provide real time messaging at data rates of 2400 bps from user to satellite and up to 4800 bps back to the user [Har 95]. The satellites are designed to relay messages throughout the world by means of on-board processing.

The ORBCOMM system consists of a constellation of LEO satellites launched on a phased basis. The primary constellation will be comprised of three orbital planes with eight satellites per plane, inclined with respect to the equator at an angle of 40-60 degrees. The supplemental constellation will be four satellites in orthogonal polar orbits flying 180 degrees apart. The ORBCOMM satellites will operate simultaneously in two frequency bands. The VHF band will be used for the transmission and reception of all message traffic, and the UHF band will be for the transmission of time signals, standard frequency, and satellite ephemeris (position) information required for enhanced position determination. Each satellite will have 20 uplink messaging channels operating in the 148 - 149.9 MHz frequency range, 19 downlink message channels operating in the 137 - 138 MHz frequency range, one downlink channel operating in the UHF band at 400.1 MHz, and an inter-satellite link to receive GPS time/positioning information in the L-band at 1575.42 Mhz. Table 2 outlines the channel requirements. Transmit polarization for both the VHF band and UHF band downlinks will be circular. The subscriber terminal transmit polarization will be linear. The ORBCOMM satellites located in the same plane are spaced so as to eliminate mutual visibility at any point on the Earth. This allows all satellites in the same plane to employ the same frequency plan with no interference. The single time and frequency channel needs to be transmitted by all planes. A TDMA approach is used to overcome intrasystem interference. The regional gateway links must also be shared on a similar simple TDMA basis.

Table 2. ORBCOMM's Channel Requirements[Par et al. 96]

	Frequency (MHz)	Channels	BW/Channel (kHz)	Total Bandwidth
Downlink				
Subscriber Term.	137.2-138.0	18	15	270
Regional Gateway	137.0-137.050	1	50	50
Time/Freq.	400.075-400.125	1	50	50
Uplink				
Subscriber Term	148.0-148.850	74	10	740
Regional Gateway	148.850-148.900	1	50	50
Inter-Satellite Link				
GPS Sat	1575.42 (Rx only)			

The ground segment supporting the ORBCOMM satellite system will be initially comprised of a network of regional Gateway Earth Stations (GES) interconnected with ORBCOMM headquarters [Hara 94]. The ground segment is comprised of Network Control Centers (NCC) and GES. The “intelligent” ground stations allows for simple satellites thus reducing the cost of the overall system.

2.5.2 IRIDIUM

IRIDIUM was one of the earliest systems to consider voice communications from non-geostationary orbits. IRIDIUM is designed to provide global communications by means of state of the art electronics [Har 95], and each satellite has a special design feature where each satellite has four crosslinks per satellite. Because the satellites operate from relatively low altitude (740 km), each satellite can only observe about 2% of the Earth's surface at a given time. Consequently, 66 satellites are needed to provide the service. The satellites therefore are frequently out of contact with land facilities which could carry transmissions into the terrestrial wireline infrastructure. IRIDIUM would overcome this obstacle by passing communications between satellites until a land Earth station can make the terrestrial connection. This architecture provides a space network which links the entire IRIDIUM system to the Public Switched Telephone Network (PSTN).

IRIDIUM uses a GSM based telephony architecture to provide digitally switched telephone network and global dial tone call - and receive calls - from any place in the world [Swa 95]. This system has a built in roaming feature and each subscriber is assigned a single phone number throughout the entire world, thus the subscriber will only receive one bill no matter what country he or she visits whenever placing or receiving a phone call. The IRIDIUM system is fully digital and utilizes high-quality vocoded messages at 4.8 kbps with Forward Error Correction (FEC) coding. The vocoding technique used is called Vector Sum Excited Linear Prediction (VSELP). Besides this, IRIDIUM also provides data communication at 2.4 kbps, paging, two-way messaging and position location services. In Figure 10, illustrates one of the sixty-six satellites that makes up of the constellation. Table 3 summaries the frequency assignment adopted by IRIDIUM.

Table 3. IRIDIUM’s Frequency & Channel Assignments [source: Motorola 1992]

	Frequency	Assignment	Max. Number of Channels per satellite
Mobile-to-Satellite	L-Band	1616 - 1626.5 MHz	3840

Gateway-to-Satellite	Ka-Band	27.5 - 30.0 GHz 18.8 - 20.2 GHz	3000
Satellite-to-Satellite	Ka-Band	22.55 - 23.55 GHz	6000

Sixty-six operational satellites are configured in six-near polar orbital planes, in which 11 satellites circle in one plane [Swa 95]. The satellites are phased appropriately in co-rotating planes up to one side of the Earth. The first and last planes rotate in opposite directions, creating a “seam” [Swa 95]. Corotating planes are separated by 31.6 degrees, and the seam planes are 22 degrees apart [Rod 96].

The IRIDIUM project will have a satellite and network control facility in Landsome, Virginia, with a backup facility in Italy [Swa 95]. A third engineering control complex is at Motorola’s SATCOM location in Chandler, Arizona. This site is estimated to handle the first 40 satellites before transferring full operations to the Virginia Center.

2.5.3 GLOBALSTAR

GLOBALSTAR is in some ways similar to IRIDIUM. The GLOBALSTAR space segment consists of a constellation of 48 LEO satellites in circular orbits with 1389 km altitude (750 nautical miles) from the Equator to 70° latitude. This constellation belongs to what is known as a “Walker Constellation” and provides 100% global coverage [Maz93]. Unlike IRIDIUM, the GLOBALSTAR satellites can observe as much as 5% of the surface of the Earth at a time. As a result, services can be provided with a somewhat smaller constellation (48). Each satellite is less complex than the IRIDIUM satellites, since GLOBALSTAR does not use intersatellite links (ISLs).

In this constellation, six satellites are equally spaced in an orbit and occupy each of the eight planes. This design was chosen in an attempt to provide double coverage with large angular separation in order to eliminate the problem of long term blockage and shadowing effects. Each orbital plane has an inclination angle of 52 degrees. Each satellite has a 7.5 degree phase shift to the satellite in the adjacent orbital plane [Maz93].

The six spot isoflux antenna beams of the satellite generate elliptical coverage on the surface of the earth [Maz 93][Har 95]. The major axes of these elliptical coverage cells are aligned with the velocity vector of the satellite movement, so that the time a user stays within the same satellite beam cell is increased and the number of call hand-off operations among the satellite beam cells are reduced.

The system uses CDMA, but the satellites do not have on-board processing capabilities; it can be considered as a “bent pipe” system. Each satellite projects 16 beams to the Earth. GLOBALSTAR employs spatial diversity by transmitting signals through two satellites. This Qualcomm technique reduces the amount of power required for transmission, thus, each handset communicates through two satellites. The two CDMA signals are combined in each handset using RAKE receivers (which add the two CDMA signals constructively). This technique provides the most robust service when two satellites are available. The double path provides a "soft" handoff from beam to beam and satellite to satellite as the constellation of satellites moves overhead [Har 95]. The GLOBALSTAR satellite spot beam antennas are also designed to compensate for the difference in the satellite-to-user link losses between the “near” and the “far” users so that the power flux density of the far “users” is about the same as the “near” users (i.e. isoflux design) [Maz 93]. Hence, the “near-far” effect experienced in terrestrial cellular systems is eliminated. This design reduces and helps eliminate harmful interference and thus increases the overall capacity of the system. Table 4 shows the four segments proposed for GLOBALSTAR.

Table 4. GLOBALSTAR’s Frequency Assignments

Links	Frequency Assignment	
User	1610-1626.5 MHz	Mobile-to-Satellite
	2483.5-2500 MHz	Satellite-to-Mobile
Feeder	5091-5250 MHz	Gateway-to-Satellite
	6700-7075 MHz	Satellite-to-Gateway

2.5.4 ODYSSEY

ODYSSEY was the first system design which would employ orbiting satellites in Medium Earth Orbit or Intermediate Circular Orbits (ICO) for mobile satellite service [Lutz 93]. The designers recognized that a small constellation would be cost effective because a smaller number of Earth stations and less complex operations are required and minimal speech delay is achieved. However, this would mean that the satellites would operate inside the Van Allen Belts. By operating in this region, the radiation experienced by the satellites is reduced, thus requiring less shielding on the satellite. This environment allows a longer lifetime (15 years) compared to LEOs, which have a lifetime of about 5-7 years.

These considerations led to the selection of the MEO, which can furnish initial service with only 6 satellites and full global coverage with only 9 satellites. With 12 satellites, at least two satellites would be visible from any point in the world. ODYSSEY also provides the highest elevation angles of all the mobile satellite systems proposed for voice service. The ODYSSEY

constellation provides continuous global coverage with a high degree of dual satellite visibility. This means a mobile subscriber has at least one satellite in view above 20 degrees elevation angle at all times, and two satellites in view above 20 degrees elevation angle more than 88% of the time, virtually guaranteeing link completion [Bai96]. The propagation time delay experienced is as low as 100 msec, much shorter than the 250 msec for GEO systems.

Since two or more satellites are available for service anywhere in the world, service can be routed through whichever satellite provides better transmission. This type of diversity service provides very high availability for the user. The system is also designed with directed coverage to concentrate capacity into the regions where demand is the greatest.

Each satellite's 61 multibeam antenna pattern divides its assigned coverage region into a set of contiguous cells. The total area visible to a satellite will typically include one or more regions of significant population density [Bai96]. Table 5 lists the frequency assignments for ODYSSEY.

Table 5. ODYSSEY's Frequency Assignments

Links	Frequency Assignment	
User	1610-1626.5 MHz	Mobile-to-Satellite
	2483.5-2500 MHz	Satellite-to-Mobile
Feeder	Ka-Band	Satellite-to-Satellite

The ODYSSEY system will utilize the CDMA multiple access technique. As seen from the tabulated data above, the ground station(s) and the satellites take place at Ka-band. The frequency plan divides the feeder link spectrum into groups of sub-bands called channels, and the channels can be dynamically switched between the feeder links and the mobile link beams (or cells). In the return direction the comprised signals received from the different cells are frequency division multiplexed prior to translation from L-band to Ka-band. Conversely, in the forward direction, the satellite duplexes the FDM uplink transmission into its component sub signals following translation from Ka-band to S-band. The feeder link bandwidth is 300 MHz in both the forward and return directions.

2.5.5 Inmarsat P (ICO Global)

This Inmarsat Affiliate system is very similar to the ODYSSEY constellation and ground infrastructure. I-CO has adopted the same altitude, nearly the same inclination, multibeam antennas, and service features [Har 95]. Both systems orbit 12 satellites, but I-CO only operates 10 satellites and has two nonoperating spares in orbit [Tor 96] [ICO 96] [Har 95] [INM 95].

This ICO system has an altitude of 10355 km and provides for slow-moving satellites, thus requiring fewer handoffs compared to the LEO systems. The satellites relay calls between the mobile terminal and an earth station. Twelve Earth stations and the subscriber databases are interconnected using terrestrial facilities to form a network. The Earth stations are linked to the public switched telephone network (PSTN) through gateways which are owned and operated by third parties. ICO is also a member of the GSM MoU group, and ICO plans to reuse as much as possible the GSM technology in a narrowband TDMA satellite environment. The mobile terminals are planned in both the single and dual modes, where the mobile terminals will work with both the ICO standard and regional terrestrial cellular standard (GSM in Europe, JDC in Japan, DAMPS in North America) [Tor 96].

Inmarsat has elected to use TDMA access, the 2.0 / 2.2 GHz frequencies (which require a large number -163 smaller beams). The argument was that TDMA allows for power efficient modulation schemes, and promises to support peak traffic capabilities by increasing and switching the capacity within a beam to cover real life traffic distributions.

ICO's focus will be primarily on users from the existing terrestrial cellular market who travel to places where terrestrial cellular coverage is incomplete, patchy or non-existent.

2.5.6 AMSC

American Mobile Satellite Corporation (AMSC) is a geosynchronous orbit satellite system that is meant to provide coverage for northern America. The system is a "bent pipe" design that receives each transmission directly from the Earth and retransmits it back again, hence the real "intelligence" of this system is on the ground. Table 6 illustrates the frequency assignment for AMSC-1. Mobile units communicate in the L-band and the satellite converts it to Ku-band, which then transmits the signal to the control center and vice versa. A phone call via AMSC-1 requires a 12 kHz channel of the L-band, six kilohertz for transmitting and another six for receiving. According to company estimates, each 12 kHz channel can carry 2000 simultaneous phone calls.

Table 6. AMSC-1's Frequency Assignments

Links	Frequency Assignment	
User	1645.5 - 1660.5 MHz	Mobile-to-Satellite
	1544-1599 MHz	Satellite-to-Mobile
Feeder	13.2-12.35 GHz	Earth Station-to-Satellite
	10.75 - 10.95 GHz	Satellite-to-Earth Station

At launch, the satellite's antennas were configured into six spot beams that tightly focus the satellite signal on particular geographic regions. The spot beams allow the satellite to communicate with relatively low-powered mobile units. AMSC-1 is currently operating with five spot beams. This is because of a test conducted in 1995 that damaged an amplifier on the satellite and made the Eastern spot beam unstable. In March 1996, AMSC reconfigured the three beams to compensate for the loss experienced by the Eastern beam [Sau 96].

2.5.7 Teledesic

Unlike all the other previously mentioned systems, the Teledesic system is not meant for voice communication but rather for purely data communication. To date, Teledesic has received most of its funding from Bill Gates - the founder of Microsoft, the world's largest computer software company - and Craig McCaw - who founded McCaw Cellular, the world's largest cellular communications service provider before its sale to AT&T in 1994. Teledesic offers several advantages over the other "Big LEOs" because it operates in the Ka-Band, allowing it to provide fiber-like capacity. The concept behind these hundreds of satellites is that even outside most advanced urban areas, most of the world will never get access to these technologies through conventional wireline means [GRI 95]. Consequently, if these powerful new technologies are available only in advanced areas, people will be forced to migrate to those areas in search of economic opportunity to fulfill other needs and desires. Based on this explanation, Teledesic is designed with the intention to bring the network infrastructure to people instead of having people move toward the infrastructure. This system also offers the advantage of using a decentralized network, which provides better system reliability compared to other centralized systems.

This satellite constellation is by far the most elaborate in terms of the number of satellites. The cost of the system is estimated to be around US \$9 billion for the 840 - 924 satellites in 21 planes in a sun-synchronous, inclined circular low earth orbit. Teledesic's objective is to provide high data rate services with fiber-like delay and a bit error rate of 10^{-10} [Tor96].

The Ka-Band mobile link was chosen to achieve sufficient bandwidth for the high bit rates Teledesic requires. In order to overcome the delay problems, a LEO constellation with an elevation angle of 40° was selected to overcome the shadowing effects. Each satellite has an intersatellite link with its eight adjacent neighboring satellites. All communication within the network is treated as streams of short, fixed length (512 bits) packets, and is based on Asynchronous Transfer Mode (ATM). Each ISL has a bit rate of 155.52 Mbps.

Teledesic uses steerable antennas and regional mapping to reduce the number of handoffs required due to the satellite's motion and the Earth's rotation. The Earth's surface is mapped to approximately 20000 supercells, each of which is again divided into 9 cells. The supercell is a square 160 km on each side. A satellite footprint encompasses a maximum of 64 supercells, or 576 cells, corresponding to one supercell per beam. The channel resources (frequencies and timeslots) are associated with each cell and are managed by serving satellites.

The multiple access method chosen by Teledesic is a combination of space, time and frequency division multiple access [Tor 96]. Teledesic proposes a wide variety of terminals, with bit rates ranging from a minimum of 16 kbps plus 2 kbps for signaling, up to 2.048 Mbps (128 basic channels of 16 kbps) for mobile subscriber terminals.

2.5.8 Others

There are still numerous proposed constellations which are not mentioned here partially because of time constraints and difficulty in obtaining information regarding these relatively new and proprietary systems. Some of the constellations includes Archimedes, ECCO, Ellipso, MSAT, Inmarsat-3, Mobilesat, EMS, LLM, GEMnet, VTAsat, Starsys, Optus B1, Solidaridad, INSAT, CCI, Celstar, SatPhone, Aces, APMT, Agrani, and African.

2.6 Summary

This chapter provides a basic overview of some of the existing and future mobile systems within the evolving global Personal Communication Systems. It was shown that different mobile satellite systems can be classified according to orbital altitude, spectrum allocation, and end user service provisions. From the discussions, we can see that four transmit and receive frequency bands are adopted (1.5/1.6 GHz, 1.6/2.4 GHz, 2/2.1 GHz, and 20/30 GHz), with approximately 30 MHz of bandwidth at each frequency except for Ka-band, which might be approximately 500 MHz. A summary of some known satellite characteristics are shown in Table 7.

This chapter serves to provide the necessary background to a later discussion in Chapter 4 and 5 about utilizing adaptive antenna arrays to combat interference and multipath in SatPCS. Most of these proposed satellite personal communication system uses low frequencies (L- and S-band), as a result, there will be some practical limitations with the spacing of adaptive antenna elements on a handheld unit. The issue of interference, multipath and adaptive arrays will be further discussed in Chapter 4.

Table 7a. Selected Big LEOs [Abr 96] [Tor96] [Lia96]

	IRIDIUM	GLOBALSTAR	ODYSSEY	Teledesic
Organization	Motorola	Loral/ Qualcomm	TRW	Teledesic Co.
Orbital type	LEO	LEO	MEO	LEO
No. of orbital planes	6	8	3	21
No. of satellites	48	66	12	840-924
Access Method	TDD/TDMA/ FDMA	CDMA	CDMA	FDMA/ ATDMA
Initial/full service	1998	1998	1998	2001

	Ellipso	ICO	Archimedes	ECCO
Organization	MCHI	ICO Global	ESA	Const. Comm./ Telebras
Orbital type	HEO/MEO	MEO	M-HEO	LEO
No. of orbital planes	2/1	2	6	1
No. of satellites	10/6	10	5-6	11
Access Method	CDMA	TDMA	FDMA/TDM/ COFDM	CDMA
Initial/full service	1998	1999	N/A	1999

Table 7b. Selected little LEOs [Abr 96] [Tor96] [Lia96]

	Orbcomm	Starsys	VITAsat	GEMnet
Organization	Orbital Comm.	Starsys Global Pos.	VITA/ Final Analysis	CTA Commerc. Systems
Orbital type	LEO	LEO	LEO	LEO
No. of orbital planes	6	6	1	5
No. of satellites	36	24	2	38
Access Method	FDMA	CDMA	FDMA	FDMA
Initial/full service	1995/1997	1998/2001	1996	1997

Table 7c. Selected GEOs [Abr 96] [Tor96] [Lia96]

	AMSC-1	MSAT	Mobilesat	EMS
Organization	AMSC	AMSC, TMI	Optus Comm.	ESA
Orbital type	GEO	GEO	GEO	GEO
No. of satellites	2	2	2	1
Access Method	FDMA/TDMA	FDMA	FDMA	CDMA/FDMA
Initial/full service	1995	1995	1994	1996

Chapter 3 Network Resource Management and Link Analysis

The purpose of this chapter is to discuss how handoff, channel assignments, call set-up and link budgets are handled in SatPCS. Similar to terrestrial networks, the voice and control channels in SatPCS will experience problems such as cross-talks or blocked/dropped calls if there is a threat of strong interference and multipath present. To overcome this problem, the proposal to use adaptive arrays on handheld units will be discussed in Chapter 4. However, before moving into the issue of interference and multipath, the discussion of issues related to the voice and control channel will be addressed in this chapter.

3.1 Personal Communication Network

The early design objective of most cellular services was to provide a large area of coverage by using a single, high powered transmitter with an antenna mounted on a tall tower [Rap95]. The drawback of this method is that it eliminates the possibility of reusing the same frequency within the same coverage area. Henceforth, a new cellular concept was developed to overcome the problem of congestion and to utilize the spectrum more efficiently.

As discussed in Chapter 2, satellite based personal communication systems are a migration of terrestrial cellular technology into space. The basic concepts applied in most cellular systems are adopted with the use of multibeam antennas and the satellite, where a *footprint* is generated by each beam and is comparable to cells in a terrestrial system. Unlike terrestrial cells which are stationary, these cells move with the satellite. The rate in which these cells move is dependent on the speed of the satellite, hence, the satellite systems will experience more handoffs compared to terrestrial systems. As a result, issues such as Doppler shift and

routing considerations for LEOs and MEOs will affect the trunking efficiency, grade of service (GOS) and overall capacity.

Trunking in cellular terms means trying to accommodate a large number of users in a limited radio spectrum. The concept of trunking allows a large number of users to share the relatively small number of channels in a cell by providing access to each user, on demand, from a pool of available channels [Rap95]. Trunking exploits the statistical behavior of users so that a fixed number of channels or circuits may accommodate a large number of users in a cell. Thus, trunking efficiency will decrease as the number of users increases in a limited channel environment. Most trunked radio systems are designed to handle a specific GOS, the level at which the system can handle a specific capacity. The GOS is a measure of the ability of the user to access a trunked system during the busiest hour and is usually given as the likelihood that a call is blocked [Rap95].

Consequently, the satellites used to provide cellular coverage will have highly directive multibeam antennas or adaptive antenna arrays to increase the number of footprints/cells to reuse frequency, thus increasing overall capacity. This chapter will basically cover areas such as frequency reuse, Doppler shift, handoff, routing considerations, channel assignment and network resource management of some of the proposed and existing systems.

3.2 Antenna Beams

3.2.1 Multibeam Coverage:

The advantages of a multibeam satellite antenna include high antenna gain within each individual beam but a more complex payload and greater antenna size. Having multibeam coverage also enables the possibility of frequency reuse if sufficient angular separation can be achieved between coverage. However, adjacent beams must use different frequency bands from one adjacent beam to another in order to avoid interbeam interference, and this is a drawback as it obliges the earth terminals to change frequency as the satellite passes overhead.

3.2.2 Intersatellite links:

These links are used for carrier transmission between satellites, and are usually operated using radio frequency links or optical links. Radio frequency links can use either omnidirectional antennas or directional antennas or a combination of both. The use of omnidirectional antennas obviates the task of locating the satellite but has low throughput. Directional antennas, on the other hand, allow high throughput but require a location determination system of some agility to find the destination satellite. Phased array antennas are

well adapted for agility and are highly directional. Phased array antennas will be discussed in Chapter 4.

3.3 Doppler Effect

Doppler effect is due to the relative radial velocity between the satellites and the user, between two satellites in the case of inter-satellite links. Doppler shift is a frequency shift of the transmitted carrier at the receiver end of the link. Moreover, this effect is time varying with the relative position of the transmitter and the receiver. If two transmitters are not separated by a sufficient frequency margin equivalent to the maximum possible Doppler shift, then the receiver will experience interference. The Doppler shift effect can be compensated for with either a sufficient frequency gap between carriers or by frequency tracking at the receiver end. The Doppler shift can also be used for position determination purposes. This implies that the earth terminal knows the satellite position with sufficient precision and that a computing facility is available.

For most of the proposed LEO constellations, the Doppler shift can reach values as high as ± 50 kHz (on satellite to mobile link) and ± 35 kHz (on mobile to satellite link) with Doppler rates up to 500 Hz/s. On the gateway/satellite link, knowledge of the satellite ephemeris is used to compensate the Doppler shift in a closed loop through the satellite at the gateway. The only remaining Doppler is the differential term due to the mobile distance to the gateway.

3.4 Handoff

There are generally two types of handoff; the call is either switched between two spot beams of the same satellite, or it is switched between two spot beams of different satellites. However, in most feeder links (where it involves the Earth stations), the handoff occurs between satellites since a multispot beam is generally not required.

Mobile handoff between spot beams occurs when the satellite remains in view but the communication needs to be supported by another spot beam. This either happens when the mobile user moves from one spot beam (cell or *footprint*) to another, or because of the motion of the satellite, the stationary (fixed) user needs to be transferred to another spot beam. This type of handoff could also be experienced when both the satellite and the user are in motion.

Mobile handoff between satellites occurs when the satellite is moving out of visibility and the communication needs to be switched to another satellite. In the case of an earth station handoff, the satellite moves out of visibility and communications (feeder) need to be switched to another earth station which provides the same coverage for the satellite. Alternatively, the communication can be handed over to a new satellite in visibility of the same earth station.

There are numerous reasons for handoffs to occur. First, they take place whenever the network needs to free up some of its resources in areas with high traffic load, usually by handoffs between antenna footprints. Secondly, they occur because the satellite is moving out of visibility of the user and in order to preserve the communication link, a handoff is required.

In a satellite communication system based on a non geostationary constellation, the network has to cope with the motion of the satellite as well as that of the mobile user. Location of the mobile provides the network with the necessary information to route calls. In a satellite system, this information is based on the terminal location (e.g. the longitude and latitude). Since the orbital parameters are known, it is always possible to identify the proper satellite and spot beams (for LEOs and MEOs) in order for the call to be routed

The handoff strategies do not apply to all of the proposed and existing constellations. For instance, ODYSSEY's system design does not provide for handoffs. The constellation has long visibility periods for each satellite (about two hours), and each satellite has a built-in overlap of 10 minutes for every user. The system designers do not anticipate a lot of traffic during these switch overs between the "old" and the "new" satellite. In any event, if a call is dropped, the users are allowed to reestablish communication on the "new" satellite free of charge. Furthermore, the ODYSSEY satellites have a built-in antenna steering capability, thus no spot beam handoffs are really necessary. Besides this, the cell coverage is also relatively large, approximately 500 miles (800 km). Because the system utilizes CDMA and large antenna footprints, the users at the edge of the beam will experience graceful degradation of link quality as the footprint moves away.

GLOBALSTAR is designed with the objective of minimizing handoffs between spot beams. The system uses active phased array antennas which have dedicated low noise amplifiers for receiving and dedicated high power amplifiers for transmitting for every antenna element. The phased array uses passive phase shifters for beam steering and a beam forming network. This characteristic allows the system to decrease the need for handoffs, thus a communication link starting in a beam can be supported by that beam until the satellite moves out of visibility. Earth station handoffs are also not allowed in this particular system, only mobile handoffs between satellites are allowed, and this can only be handled by the same earth station. The size of the cell is approximately 400 miles (650km).

GLOBALSTAR utilizes soft handoff; as a result, a new communication signal is passed to a new satellite while it continues to transmit to the original ("old") satellite. Simultaneously, in the forward direction a new radio link is established through the new satellite by the earth station. In this case, two links are both active in the forward and reverse directions. This system

makes use of the concept of path diversity [Rap95]. However, the two links will experience independent fading and shadowing if the separation angle is sufficiently large. In most communication systems, it is highly unlikely that both links will experience deep fades at the same time since they will have independent fading characteristics. Soft handoff and CDMA will thus allow for a RAKE receiver design on the handheld, where different multipath signals are combined to improve the quality of the link. Soft handoff can be exploited whenever the link quality is satisfactory, thus improving power and overall efficiency.

IRIDIUM has by far one of the most complicated network designs. This system together with its intersatellite links will allow all the handoffs (mobile handoff between types of two different spot beams and between two different satellites) to be implemented. This will significantly complicate the network structure and requires complex on-board processing, which might add to the delay of the communication link. However, because of IRIDIUM's low altitude, it is anticipated that this additional delay will not cause significant degradation in voice communications quality.

The idea behind IRIDIUM's handoff mechanism is that once the mobile terminal is turned on, the terminal will start monitoring the satellite links. The received signal at the mobile terminal will then be averaged over a period of time to minimize the effects of deep fades. When the averaged signal strength falls below a specified threshold, the terminal will switch the signal either to another satellite or to a terrestrial network depending on the channel availability.

In most of the systems, priority will be given to terrestrial networks to minimize the load on the satellite. In any event, the protocols will ultimately determine which is the best route for the call since the traffic intensity is also a major factor in the design. If the terrestrial signals are not strong enough, the mobile terminals will send out a request to the terrestrial base station for a channel assignment and wait for a confirmation. After a confirmation is received, the mobile terminal will then be assigned a channel to the user. However, if the terrestrial signals are not strong enough, and if the mobile terminal does not receive any confirmation within a specific time, the mobile terminal will assume the request is denied. Consequently, the mobile terminal will continue to monitor the signals on the satellite links.

3.5 Channel Assignments

One of the major issues in implementing an efficient mobile satellite service is to maximize the channel throughput with limited bandwidth while providing high quality service. In the case of a handoff, everytime a mobile user with a call in progress passes from one cell (*footprint*) to an adjacent one, a new channel is required in order to prevent call termination.

As mentioned earlier, most of the cells are illuminated by spot beams of the satellite. The difference between LEO, MEO and GEO satellites is the size of the cells. In the case of GEOs, the cells are larger in diameter compared to the LEOs. The latter case will allow the frequency to be reused more often, thus allowing more traffic to be handled by the network. However, the limiting factor will be co-channel interference.

Co-channel interference is defined as interference between signals from adjacent cells that reuse the same frequency. Unlike thermal noise, co-channel interference cannot be overcome by increasing the carrier transmitter power. This is because an increase in transmitter power will result in an increase in interference with neighboring co-channel cells [Rap95]. As a result, a minimum reuse distance is required between cells using the same set of frequencies. Rappaport [Rap95] talks in detail about the derivation of the minimum reuse distance, D^2 . The derivation of D^2 depends on the particular multiple access technique and modulation scheme used, the mobile environment and the acceptable voice quality.

In any event, an efficient channel allocation technique is required in order to utilize the spectrum efficiently and increase trunking efficiency. IRIDIUM, for instance, uses Fixed Channel Assignment (FCA) strategies. The drawback of this technique is that any call requests made by a subscriber can only be served by channels that are occupied at that particular cell, otherwise the call is blocked. ORBCOMM uses Dynamic Channel Assignment (DCA) strategies. This technique has no fixed number of channels assigned to a particular cell. All call attempts are referred to the Mobile Switching Center (MSC), which manages all channel assignments in its respective region. This responsibility could very well be shared with the earth station, adding to the complication of the network. In most terrestrial cases, the MSC assigns, on a call-by-call basis, channels with the minimum cost function. This cost function will depend on the future blocking probability, usage frequency of the particular channel, the reuse distance of the channel, and other factors. Fantacci [FAN93] did a study on the performance analysis of dynamic channel allocation techniques for satellite mobile cellular networks. According to his simulation results (with the assumption of a uniform load condition for each cell), he found that FCA in GEOs will experience a higher blocking probability as a function of traffic intensity per cell (Erlang). However, as the traffic intensity increases, the DCA technique will eventually experience the same blocking probability as FCA, perhaps even worse. As a result, there is a tradeoff in the system design, depending on the traffic load of a particular cell or the anticipated customer base. The system designer will have to make a decision as to which technique will be more favorable.

In the case of ORBCOMM, which uses DCA, each of its satellites allows the mobile terminals to communicate effectively in the presence of co-channel uplink interference. The subscriber uplink channels are continuously reassigned to accommodate the statistical variation

of the usage of the uplink band over time. The entire uplink band is scanned, at the satellite, in intervals using a given bandwidth. The power level of each slot is recorded. The slots are then ranked from the lowest to the highest power levels. The satellite sends this information to the user terminals to determine the best 20 uplink channels (out of 74) that can be used for transmission [Par et al. 96].

3.6 Call Setup

In general, there are numerous methods of designing a call setup. Frequently, the setup will be very similar to terrestrial systems. Basically, there are two types of call setup, fixed to mobile and mobile to fixed.

The fixed to mobile call set-up procedure [Cul93]:

- a) The fixed user will first dial the mobile user's number and will be connected to the PSTN.
- b) The PSTN will transfer the signal to the Primary Earth Station/controller (PES/c).
- c) The PES/c will then page the mobile terminal via the appropriate satellites and coverage zones through the last known location of the user.
- d) The paged mobile terminal then sends a channel request message to the PES/c (Random Access Channel, RACH).
- e) The PES/c that was 'randomly accessed' then returns an immediate assignment message, specifying a 'stand-alone dedicated control channel (SDCCH)' to the mobile terminal (Paging, broadcast and access grant channel, PBC).
- f) The mobile replies with a paging response which includes its international mobile subscriber identity/space (IMSI/s) number (SDCCH channel).

In the case of the mobile to fixed call setup [Cul93]:

- a) The mobile user will dial a number.
- b) The mobile terminal will then send a channel request message to the PES/c (RACH channel).
- c) The PES/c that was 'randomly accessed' will then return an immediate assignment message, specifying a 'stand-alone dedicated control channel' to the mobile terminal (PBC channel).
- d) The mobile replies with a paging response which includes its IMSI/s number (SDCCH channel).

The call setups mentioned above are just general techniques; in the following two subsections the call setup of IRIDIUM and ORBCOMM will be discussed.

3.6.1 IRIDIUM [Swa 93] [Rod 96] [Gru91]

As discussed earlier, the IRIDIUM system consists of 66 LEO satellites and uses intersatellite links. As a result, it has a very complicated network architecture compared to the other proposed constellations. Besides having 66 satellites and 12 spares, the IRIDIUM system will also have numerous gateways to monitor the activity of its subscribers, such as billing, last known location where a call via IRIDIUM was made and so on. In order for a call to be made, the IRIDIUM subscriber will only have to turn the mobile terminal on.

Once the IRIDIUM subscriber unit is turned on it enters a standby mode where it locks onto the strongest spacecraft signaling channel. To place a telephone call, the IRIDIUM user will dial the number and depress the send button to start the call setup mode. The unit then sends its own phone number, the registration number, and the number being called directly to the satellite. The satellite then passes that information to the regional gateway. The regional gateway looks into its database and then sends this information to the home gateway of the user to verify the validity of the caller. After validation, the regional gateway determines the proper routing to the destination. If the destination is another IRIDIUM subscriber, its own home gateway must validate the called user and provide his or her location. Both the caller and destination information is sent to the regional gateway which will provide the final routing to the satellite. The entire call setup procedure should take no more than 30 seconds.

A public telephone user can also direct dial an IRIDIUM subscriber unit's number. This call will enter the IRIDIUM system through the caller's closest regional gateway. The IRIDIUM user's home gateway will validate that the user is still current and provide the user's last known location. The remainder of the call setup proceeds as explained above.

Once the call is setup there is constant synchronization and handoff from cell to cell as the satellite moves rapidly above the earth. Cell-to-cell handoffs take place about every two minutes and satellite-to-satellite handoffs will occur about every nine minutes. Once either party disconnects, billing and location information is updated at the gateway(s).

3.6.2 ORBCOMM [Par et al. 96]

Unlike IRIDIUM, ORBCOMM is designed for paging services. For this particular system, there are two methods of processing messages which depend on the messages' point of origin. First, a subscriber will initiate the message which will flow from his or her terminal through the satellite and a Regional Gateway to the Network Master Control Center (NMCC), where it is either printed out for delivery by mail or routed based on pre-determined protocols through packet switched networks. Emergency messages will be passed directly through to

service providers or to ORBCOMM's Customer Service activity where each message will be individually managed until confirmed as cleared. Emergency messages will be handled on a priority basis over all other traffic.

Secondly, an off-network message may enter the system through the Service Operation Center (SOC) via several different media, e.g., electronical, hard copy or verbal. The Service Operations Center will enter the message into the system computers, which in turn will forward it to the NMCC. The NMCC will then provide the proper structure and addressing and route it to the designated subscriber via the appropriate Regional Gateway and satellite based on the subscriber's last known position.

3.7 Routing Considerations

The network topology of a LEO satellite is dynamic since the satellites move in accordance with the law of orbital mechanics and the Earth stations rotate with the Earth's surface. The nodes of the network move in and out of range of each other or are eclipsed by the Earth. Therefore, as connectivity is time-varying and the routing table is not fixed, it seems inevitable to use adaptive routing.

3.7.1 Centralized Adaptive Routing

A central control facility (probably a relay Earth-station) where all of the routing information is stored continually checks the location of the terminals and satellites. This can be done by means of specific signaling channels. A continually updated routing in the central control facility provides information as to the location of the destination, decides upon the route for onward transmission, then proceeds to transmit it around the network. This method of routing allows for a simpler routing algorithm, but the danger of the system is that it will result in high signaling traffic density and the requirement of a super-fast computing central controller. The system vulnerability to failure is also increased. The system relies on the correct operation of a single Earth-station. This vulnerability to failure may be reduced by having a back-up central control facility within the network.

3.7.2 Distributed Adaptive Routing

A dynamic routing mechanism via distributed processing can be used such that each node in the network (satellite or relay Earth stations) individually updates its routing table and selects the most cost-effective route. The 'local' routing table at each node would be updated depending on the effective connectivity at a given time with other nodes. The devolution of the routing

decision is then spread among the routing nodes. In such a way a decision could be made locally as to the direction that the message will take, and thus signaling capacity can be reduced. This, however, means that the satellites will be more complicated and more expensive, as they will require more memory and processing power to calculate message routes. To avoid this necessity, the routing could be performed at the relay Earth-stations only. Devolution of the routing decisions at 'local' level would reduce the likelihood of overall system failure if only one node should fail. The system will be able to adapt to a node failure and reroute the messages to the destination.

3.7.3 Flooding

Flooding consists of the forwarding of messages on all the possible links to the destination. There are, however, problems associated with this routing method. The message may be forwarded forever if it forms a loop in the network. The very nature of a flooding algorithm means that the message will be received by the destination at the earliest possible time at the expense of incurring very high traffic in the network. The occurrence of high traffic could in turn cause congestion if the network is not designed to cope with it. Work has been performed on the possibility of using flooding as a method for routing messages in a dynamic satellite communications network. In a network that is rapidly changing, the use of the flooding routing method greatly simplifies the problems of routing, as there is no necessity to keep track of different points in the network. If there is a large number of satellites (i.e. the network becomes complicated), then the flooding method may become a viable solution. The method requires very little overhead, as no routing method is gathered and put into the message header. Alternatively, flooding can be used only during initial route establishment of call.

Selective flooding uses the same methods as described in flooding above except that some information about the location of the destination terminal is already known by the routing node. This allows the node to flood only a certain section of the network in order to get the message to its destination.

3.8 Link Analysis

The design of a satellite communication system is a complicated process which involves making compromises between numerous factors in order to achieve the maximum performance at an acceptable cost [Pra86]. Some of these factors include rain attenuation, the effective isotropically radiated power (EIRP), receiving and transmitting antenna gain, frequency, shadowing effects, fading channel and multiple access techniques used. The design of a good communication link is critical in providing good reception to the user. If insufficient link

margins are provided to compensate for the shadowing effects and fading conditions, this will result in the call being dropped, adversely affecting the quality of the overall system.

Like all cellular radio communications, the signal is susceptible to multipath fading. Allnutt [All95] has done some studies where he reported that in certain instances, multipath fading will cause serious link reliability problems for L-Band satellite personal communication systems. He reported that in some occasions, multipath fading was in excess of 10 dB [All93] [Dis93]. The fading phenomena in mobile satellite systems are quite difficult to model because the user is located in an unknown environment. As a result, it is difficult to identify a single statistical model that is able to reproduce the actual situation [Cor92]. Moreover, because there is a rapid change in the satellite elevation angle, the channel is nonstationary in nature, even if the users are static.

Vatalaro et al. [Vat93] have simulated a mobile satellite communication channel model based on various assumptions. Vatalaro et al. [Vat93] assumed that all users are located in a continental region, are in a similar environment, and experience nonselective fading due to diffuse multipath, the latter having constant power relative to the direct component. This is equivalent to assuming a Ricean Distribution for the transfer function envelope of the propagation medium. Allnutt [All95] on the other hand found that in the case of a GEO, the multipath has numerous components but only one of them will be dominant. The adaptive antenna array simulation in this thesis will look at both cases and compare their results.

The following subsections show the link budget between the satellite and handheld communicator, satellite and the ground stations, and between the satellites.

3.8.1 IRIDIUM Link Budgets

Table 8 shows link budget calculations for the link between a handheld personal communicator and the satellite. In this particular calculation, we assumed that no shadowing loss occurs. Basically, this means that the subscriber has a direct LOS with the satellite and there are no trees, mountains or tall buildings blocking the communication link.

Table 8. Link budget from handheld to IRIDIUM [source: Motorola 1992]

(a) Uplink (Without Shadowing)

EIRP	(dBW)	- 4.2
SatelliteGr	dB)	24
Path Loss	(dB)	160
Noise Temperature (K)		500

(b) Downlink (Without Shadowing)

EIRP	(dBW)	27.7
Handheld Gr	(dB)	1
Path Loss	(dB)	160
Noise Temperature (K)		250

Noise Bandwidth(kHz)	31.5
CNR (dB)	16.42

Noise Bandwidth (kHz)	31.5
CNR (dB)	28.34

Table 9. Link budget of Intersatellite links for IRIDIUM [source: Motorola 1992]
Intersatellite Links (Without the Sun)

EIRP (dBW)	38.4
Satellite Gr (dB)	36.7
Path Loss (dB)	192.7
Noise Temperature (K)	720.3
Noise Bandwidth(MHz)	12.6
CNR (dB)	11.42

3.8.2 GLOBALSTAR Link Budgets

Table 10. Link budget calculation from handheld to satellite for GLOBALSTAR
 [source: *Applied Microwave & Wireless 1995*]

Parameter	Forward Link		Reverse Link		Units
	Satellite to Mobile	Gateway to Satellite	Mobile to Satellite	Gateway to Satellite	
Frequency	2.5	5	1.6	7	GHz
EIRP/User	1.1	36.4	-14.3	-33.3	dBW
Space Loss	163.4	169.7	159.6	172.3	dB
<i>Other Factors*</i>	1.40	7.90	2.10	1.60	dB
G/T (Handheld)	-26	-29.6	-14.25	27.5	dB/K
CNR _{overall}	5.1	24	4.5	15.1	dB

*Note: Other factors here refers to all of the aforementioned parametric factors in Chapter 2 and 3.

3.8.3 ORBCOMM Link Budgets

Table 11. Link budget calculation for typical ORBCOMM subscriber equipment uplinks (VHF-1, 148 MHz Band)[How96]

Parameter	Personal Terminal		Mobile
	Basic	Enhanced	
Tx Pwr	3.0 dBW	3.0 dBW	7.0 dBW
Ant Gain	-1.0 dB	2.0 dB	2.0 dB
EIRP	2.0 dBW	5.0 dBW	9.0 dBW
Free space loss	-145.7 dB	-145.7 dB	-145.7 dB
Atm loss	-3.2 dB	-3.2 dB	-3.2 dB
Polarization loss	-3.0 dB	-3.0 dB	-3.0 dB
Data rate	2400 bps	2400 bps	2400 bps
Satellite CNR	52.9 dB	55.9 dB	59.9 dB

Table 12. Link budget calculation for typical ORBCOMM subscriber equipment downlinks (VHF-3, 137 MHz--UHF)[How96]

Parameter	Basic (137 MHz)	Mobile	Time/Freq. Link
Satellite Tx Pwr	10 W	10 W	10 W
Ant Gain	0.7 dB	0.7 dB	0.0 dB
Satellite EIRP	10.7 dBW	10.7 dBW	13.0 dBW
Free space loss	-144.9 dB	-144.9 dB	-154.19 dB
Atm loss	-3.2 dB	-3.2 dB	-0.5 dB
Polarization loss	-3.0 dB	-3.0 dB	-3.0 dB
Data rate	4800 bps	4800 bps	4800 bps
Subscriber CNR	57.5 dB	63.6 dB	53.0 dB

From the tables shown above, we can see that different proposed constellations have different link requirements, based on the applications for which they are intended. Some of the factors and differences experienced in these numbers reflect the variation bit rates, link margin, power limitation on the handheld, and frequency at which the system is broadcasting.

In Table 8, we observed that the uplink and downlink carrier-to-noise ratio for IRIDIUM is 16.42 dB and 28.34 dB. These numbers are much higher compared to the carrier-to-noise ratio in the GLOBALSTAR system as seen in Table 10. This is because the EIRP for GLOBALSTAR is much lower (-14.3 for Mobile to Satellite) compared to IRIDIUM's, which is -4.2 dB. Furthermore, the tabular results for GLOBALSTAR do not specify the conditions/assumptions (i.e., shadowing effects) that were used when calculating the carrier-to-noise ratio. However, for the ORBCOMM system, Tables 11 and 12 clearly show a much higher carrier-to-noise ratio compared to the other two systems, namely IRIDIUM and GLOBALSTAR. ORBCOMM's high carrier-to-noise ratio is due to its operating frequency, which is in the VHF and UHF bands. At these frequencies, the path loss experienced by the signals will be much less compared to that at L and S Bands. Moreover, since ORBCOMM provides only messaging/data communications, it utilizes flexible or retractable antennas between 9 and 18 inches in length depending on the application. As a result, the system to has a much higher carrier-to-noise ratio.

3.9 Summary

This section examines some of the network management issues that the different constellations will be utilizing in order to manage the network resources more efficiently. Some of these issues discussed include choice of antenna beams, the Doppler effect due to satellite motion, handoff, channel assignment strategies, call setup, and routing considerations. Finally, several link analysis were shown for some of the proposed constellations.

Chapter 4 Adaptive Antenna Arrays

4.1 Motivation

In most satellite personal communication systems(SatPCS), interference and multipath fading remain a problem for reliable reception of signals. Interference sources include another user in the same coverage area, terrestrial base stations, and other satellites that are operating in the same frequency band. Multipath fading is a result of cancellation between signals transmitted from a satellite which reach a receiver via direct paths and reflected paths. Multipath can be caused by scattering surfaces such as the ground, buildings, and vehicles. Figure 5 illustrates the signals interfering with each other, resulting in the degradation of reception performance.

The antennas used for transmit and receive in most handheld terminals are ideally isotropic and circularly polarized. They are normally designed with a single low gain antenna element so that users are not required to point the antenna at the satellite. This is especially true in the case of a LEO system, where the satellite moves across the sky in a period of 8 to 15 minutes. Therefore, having the user point the antenna at the satellite is a difficult task. However, these single element units are particularly vulnerable to interference and multipath effects because they receive signals from all directions. One approach to alleviate this problem is to use an adaptive antenna array mounted on the handheld unit. The adaptive array, as will be discussed, will have the ability to reject interference and track the satellite automatically as it moves across the sky.

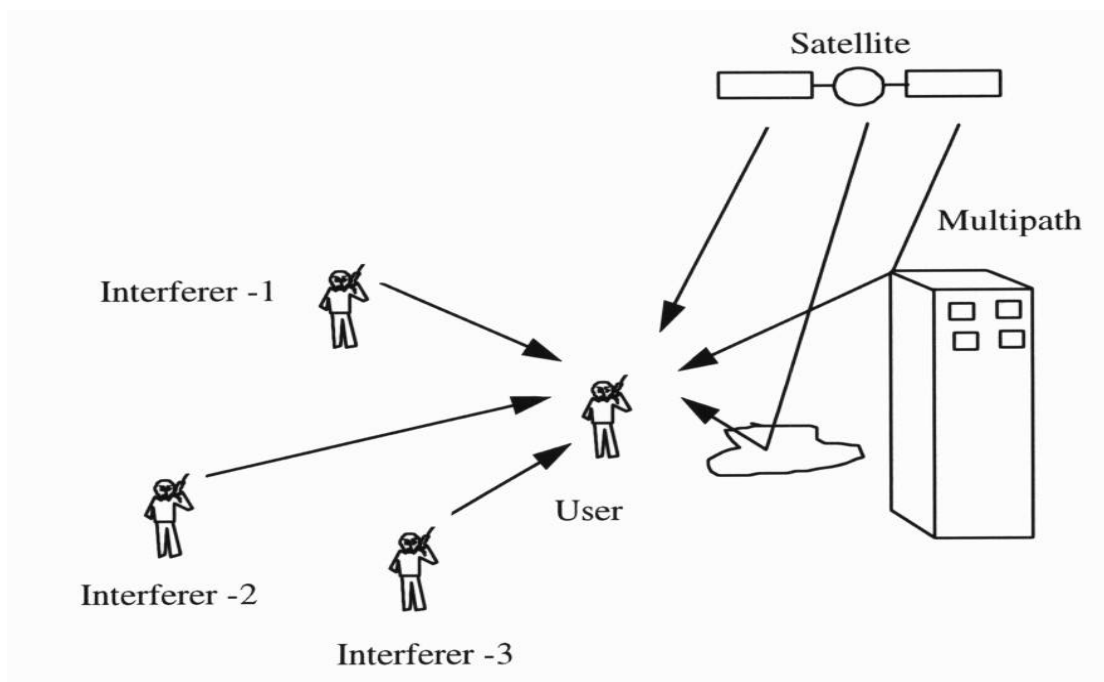


Figure 5 SatPCS User in the presence of interference and multipath

In a satellite personal communication (SatPCS) system, the channels contain noise which may arise from electrical disturbances (e.g. lightning) or from man made sources, such as high-voltage transmission lines, the circuit switching systems of a nearby computer, or the ignition system of a car [Cou93]. In addition, multiple copies of the Signal of Interest (SOI) might arrive at the receiver at different times and with different attenuation characteristics. These multipath elements may introduce intersymbol interference (ISI), which will eventually result in significant amplitude variation in the signal envelope and can also cause co-channel interference.

As mentioned in Chapter 3, several SatPCSs proposed the use of frequency reuse in order to maximize the system capacity. As a result, for a given coverage area, there will be several cells that use the same set of frequencies. The cells which reuse the same frequency are defined as co-channel cells. The interference between signals from these cells is defined as co-channel interference [Rap 95].

Consequently, ISI and co-channel interference are only two of the many factors that will affect system capacity, range of operation and carrier-to-noise ratio. Moreover, if the multipath elements vary in time and have different attenuation characteristics, the result will be different levels of fading experienced at the channel output. Hence, multipath fading, ISI and co-channel interference are key elements that will degrade the communication link and may cause significant link failure in a wireless mobile environment.

Numerous techniques have been used to combat interference and multipath fading; diversity and spread spectrum are just some of the widely used methods. Diversity is a commonly used technique in mobile radio systems to combat multipath signal fading. The basic principle of diversity can be explained as follows: several replicas of the same information carrying signal are received over multiple channels with comparable strengths and exhibit independent fading. As a result of this, there is a good likelihood that at least one or more of these signals will not be in a fade at any given instant of time, thus making it possible to deliver adequate signal level to the receiver by combining or switching between the channel outputs. Without diversity techniques, the transmitter will have to deliver a much higher power level to protect the link during the short intervals when the channel experiences a deep fade. However, in a satellite personal communication system, the power available is severely limited by the electrical power source on board the satellite. The more power required, the larger and heavier the satellite. Moreover, for a given satellite, low Carrier-to-Noise ratio is usually combated by narrowing the receiver bandwidth to reduce the effect of the noise level, N . This will result in lowering the data rate, and possibly more delays or longer time for the signals to arrive at the destination. In any case, diversity is very effective in reducing transmitter power. Diversity itself has numerous variations. These include polarization diversity, selection diversity, frequency/time diversity and space diversity. Adaptive arrays fall into the category of space diversity.

Space diversity has traditionally been the most common form of diversity in terrestrial mobile radio base stations. It does not require additional frequency spectrum and is easy to implement. Space diversity is exploited by spacing antennas (at the receiver side) apart so as to obtain sufficient decorrelation between the signals from each antenna. The key for obtaining uncorrelated fading of antenna outputs is adequate spacing of the antennas. The main goal of this technique is to minimize the effects of fading by the simultaneous use of two or more antennas that are spaced a number of wavelengths apart, which is a function of the frequency of operation.

Space diversity exploits the common polarization and spatial separation of two or more receiving antennas. Their signals may be combined at intermediate frequency (IF) or audio frequency (AF) stages to produce a single output signal. This technique makes use of the fact that fading is often a very localized phenomenon. The spacing of the antennas is usually 2 or 3 wavelengths for high-frequency (HF) systems.

Spacing between array elements is an important factor in designing antenna arrays. If the elements are spaced more than half a wavelength ($\lambda/2$) apart, *grating lobes* can appear in the antenna pattern (applies to a linear, equally spaced array) which are generally undesirable.

Similarly, for every null formed, a grating null may appear for element spacings that are greater than one half a wavelength ($\lambda/2$) [Com78][Stu81][Lib95]. The problem occurs because interference nulled by the array at one angle causes additional nulls (grating nulls) to appear at other angles. If the desired signals fall in a grating null, this will result in a low SINR [Com88][Lib95]. Therefore, it is generally advisable to maintain a small spacing ($0.5\lambda - 0.8\lambda$) between the array elements.

4.2 Antenna Arrays for Suppression of Interference and Multipath

When several antennas are arranged in space and interconnected to produce a directional pattern, an antenna array is formed [Stu81]. An antenna array can mimic the performance of a single large antenna and can often obtain the same level of performance. Large antennas produce narrow beams and must be mechanically steered to maintain maximum signal strength, while the antenna array can electronically scan the main beam of the antenna by phasing the elements in the array instead of mechanically moving the antenna.

Adaptive antenna arrays differ from conventional arrays in the sense that they are adaptive. An adaptive array is actually a phased array antenna that is capable of adjusting the phasing of elements automatically, thus controlling its own pattern. These antennas are used extensively in radar and communication systems that are subject to interference and jamming. They adjust their pattern automatically to the signal environment to reduce the level of interference. This is accomplished by optimizing the signal-to-interference-plus-noise ratio (SINR) at the array output. As a result, adaptive arrays are extremely effective in protecting radar and communication systems from interference and jamming.

There are several advantages of using an adaptive antenna array as opposed to a conventional array. Adaptive arrays are capable of sensing the presence of interference noise sources and are able to suppress the interference while simultaneously enhancing desired signal reception without prior knowledge of the signal/interference environment. Adaptive arrays can also be designed to complement other interference suppression techniques so that the actual suppression achieved is greater than that obtained solely through conventional means, for instance, by the use of spread spectrum techniques or the use of a highly directive antenna. In general, a null in an antenna pattern can be made very deep, even in a low gain array. A directional beam can only have high gain if the antenna is large (multiple wavelengths in diameter). Essentially, interference rejection works best on nulls. An adaptive array also offers enhanced reliability compared to a conventional array. When an element in a conventional array fails, the sidelobe structure of the array pattern may be significantly degraded as the sidelobes increase. However, in the case of an adaptive array, the response of the remaining operational elements in the array can be automatically adjusted until the array sidelobes are reduced to an

acceptable level. Hence, adaptive arrays fail gracefully compared to conventional arrays, and they increase reliability results.

The operation of an adaptive array can most easily be visualized by considering the response in terms of the array pattern. Interference signal suppression is obtained by appropriately steering the beam pattern nulls and reducing sidelobe levels in the direction of interfering sources, while desired signal reception is maintained by steering the main beam. Since an adaptive array is capable of forming deep nulls over a narrow angle region, very good interference suppression can be realized. As a result, interference suppression by null steering is a principal advantage of adaptive arrays.

Adaptive nulling is currently considered to be the principal benefit of adaptive techniques employed by adaptive array systems, and automatic cancellation of sidelobe jamming provides a valuable electronic-countermeasure (ECCM) capability for radar and communication systems [Mon90].

4.3 Array Classification

There are numerous ways of classifying antenna arrays. One of the most common ways is by geometrical configuration. The most elementary configuration is the linear array which can have equally or unequally spaced elements. A linear array is classified as having a single row of elements along a straight line. A planar array has several (or many) rows of elements in a plane. In this thesis, we will limit the discussion to linear receiving arrays for convenience, but because of the reciprocity principle, the results obtained apply equally well to transmitting arrays [Sko80][Col85].

The radiation pattern of an array is determined by the type of individual elements used, their orientations and position in space, and the amplitude and phase of the received signal [Stu81]. In order to simplify our discussion, we will assume that each element of the array is an isotropic point source. The resulting phase pattern is known as the array factor [Stu81]. The array may also be used for transmission by reciprocity, but we will only look at the case of receiving arrays [Com88] [Mon90].

4.4 Array Design Architecture

To analyze the antenna array, it is necessary to make several assumptions. We will first assume that there is a direct path for the signal from the satellite and there is also some form of interference, where the interfering signal is uncorrelated with the signal of interest. Furthermore, there also exist multipath components due to reflection, scattering and diffraction which are

incident on the antenna array. These incident waves are assumed to be plane waves. It is further assumed that the transmitter and any object which results in multipath components are in the far field of the receiver's antenna [Stu81]. Next, we will assume that all the array elements are placed closely enough such that there is no significant amplitude variation due to the difference in propagation path length for any two elements. Moreover, we will assume that there is no significant difference between the Direction-of-Arrival (DOA) of a particular plane wave at any two elements. Finally, we will assume that each of the antenna elements has the same pattern and the same orientation.

Figure 6 shows an example of an adaptive antenna array. This adaptive array architecture is based on the Least Means Square (LMS) algorithm. The figure shows plane waves arriving at the antenna elements. The signals are then downconverted to an Intermediate Frequency and sampled by an Analog to Digital (A/D) converter. The A/D converter converts the electrical signal from analog to digital form. Then, this input signal is multiplied with a variable weight and all the symbols are summed to produce an output, $y(k)$.

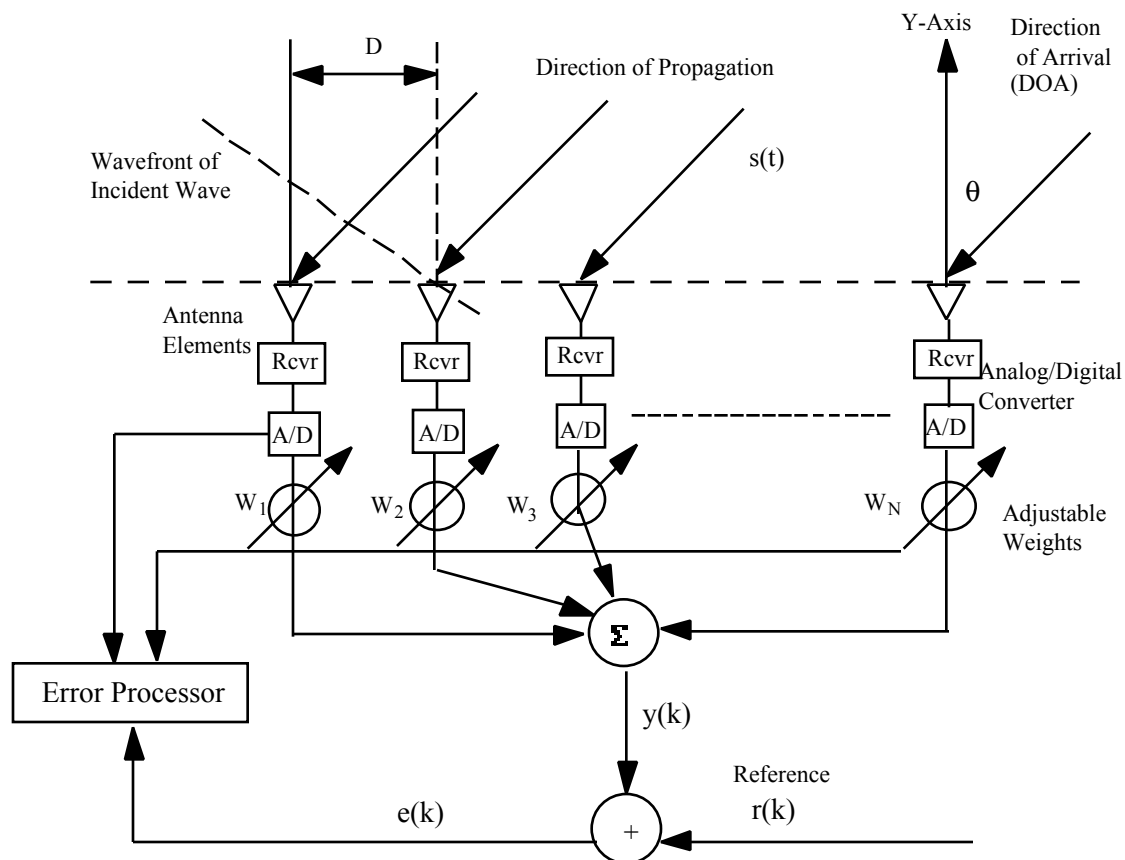


Figure 6 An example of an adaptive antenna array

The LMS algorithm, which will be discussed further in Chapter 5 requires the use of a reference signal, $r(k)$. There are numerous ways of generating this reference signal, however, this is beyond the scope of this thesis. Compton [Com 88] discusses numerous techniques for generating this reference signal. The error signal, $e(k)$ in the figure represents the difference between the summed output, $y(k)$ and the reference signal, $r(k)$. The error processor then computes the required weight adjustment necessary in order to null out the undesired signal (Section 5.1 will discuss more details about the error signal and how it works). This process is an iterative process and will continue until all the weights in the array converge. The issue of weight convergence will be addressed in Chapter 5.

In general, we model the system and all signals as follows:

$$s(t) = A e^{2\pi f_c t + \phi} \quad (4.1)$$

where A and ϕ carry the information of the transmission, while f_c represents the carrier frequency. Since the signals incident on all the antenna elements are of different phases due to the difference in distance traveled by the wave between two antenna elements, the phase difference between the incident waves at successive elements is given by

$$\phi = \frac{2\pi d \sin(\theta)}{\lambda} \quad (4.2)$$

where d is the distance between successive antenna phase centers, θ is the DOA with reference to the y-axis (See Figure 6), and λ is the wavelength. The output of each element is a phase shifted version of the same signal, shifted by phase angle ϕ with respect to the previous element. The reference is usually taken as the center element of the antenna or the first element. In this case, we will follow the latter convention. Hence, the phase shift of the i_{th} element can be formulated by multiplying this signal by $e^{j\theta i}$.

Using this notation, the phase shift factors of all the elements can be modeled as a vector. [Col85]

$$\mathbf{U} = [1 \quad e^{j\theta} \quad e^{j2\theta} \quad \dots \quad e^{jN\theta}]^T \quad (4.3)$$

This vector is known as the steering vector, which basically controls the direction of the antenna beam [Col85]. The direction of the antenna beam is controlled by null steering. With reference to Figure 18, the signal induced at the N_{th} element of the array is denoted by $S_N(t)$, and the received signal with noise is denoted by $d_N(t)$. Assuming that a single plane wave source is

transmitting a signal that remains stationary during the period when the wavefront crosses all elements, we get the signal vector induced in all elements as

$$\mathbf{S} = s(t)\mathbf{U} \quad (4.4)$$

After adding Additive White Gaussian Noise(AWGN), (4.4) becomes the data vector available at the outputs of the elements and is given by

$$\mathbf{D} = \mathbf{S} + \mathbf{AWGN} \quad (4.5)$$

Where **AWGN** is a vector of the noises in each element/receiver branch. Assuming omnidirectional antenna elements and a single plane wave incident on the array, the response of the array is given by weighting the output of each element by the corresponding weight and summing all the weighted outputs. This is given by

$$y(t) = \mathbf{W}^T \mathbf{D} \quad (4.6)$$

where \mathbf{W}^T is the weight vector given by

$$\mathbf{W} = [w_1 \quad w_2 \quad \dots \quad w_N]^T \quad (4.7)$$

These weights are adjustable as shown in Figure 6. The purpose of the weights is essentially to determine the radiation pattern or array factor of the adaptive antenna. For instance, if the signal arriving at element-1 has a stronger component of the desired signal (determined by analyzing the error signal, $e(k)$, where $e(k)$ is complex), then a higher numerical value will be assigned to w_1 . In the case where the signal incident on element-2 has a stronger component from an undesired user (by measuring the $e(k)$), a smaller value is assigned to the w_2 . This process repeats until the weights converge under a given specification.

Take for example a two element LMS adaptive antenna array. Let us assume that the user's BPSK modulated signal is arriving from an angle of 0° . There exists an interference signal (uncorrelated) arriving from the 45° angle. This signal is also a BPSK signal. Given a Signal-to-Interference ratio(SIR) of -10 dB, the strength of the interference is 10 times stronger than the SOI, we will demonstrate how the adaptive array adjusts its weight as the number of samples/iterations increases. An E_b/N_0 of 10 dB was used and a bit rate of 200 kbps was chosen. A training sequence of 3000 was selected to train the weights of the adaptive array. The noise is assumed to be independent between the antenna elements; therefore, it is generated separately and independently for each element. The convergence factor, μ , of 0.001 was selected to control the rate of convergence of the weights (Section 5.1 will discuss more on the

convergence factor). The array voltage patterns are plotted in Figure 7. The different voltage patterns will illustrate how the antenna pattern changes as the training sequences are used to vary the weights.

The plots in Figure 7 are all voltage patterns drawn to the same absolute scale; the magnitude is normalized for simplicity. The labels surrounding the diagram are the angles of arrival. Figure 7 shows the array voltage pattern changing with respect to the training sequences or the number of iterations, k . The pattern at any given iteration is computed using the Least-Mean Square (LMS) algorithm. Figure 7(a) shows the initial pattern at iteration = 0; Figure 7(b) through 7(f) show the patterns at iteration = 10 and iteration = 3000; Figure 7(f) shows the final pattern, which is also the steady state computed pattern. Note that the shape and the magnitude both change with the number of iterations. A close analysis of the final antenna pattern demonstrates that the beam is directed toward the desired user while a null is placed at 45° . The magnitude of the initial pattern is determined by the initial (arbitrary) choice of weights, \mathbf{W} , whereas the magnitude of the final pattern is determined by the strength of the desired signal, the direction and strength of the interfering signal and the noise in the system.

Figure 7 demonstrates that as the training sequences are corrupted by the noise in the environment, the adaptive array will be able to utilize the information contained in these corrupted training sequences. The adaptive arrays will then adjust the weights and steer the null of the array in the direction of the interferer.

From Figure 7, we know that as the iterative process progresses, the voltage pattern will change to null out the interfering signal and focus on the SOI. This is a direct effect from the change in the weights of the adaptive antenna array.

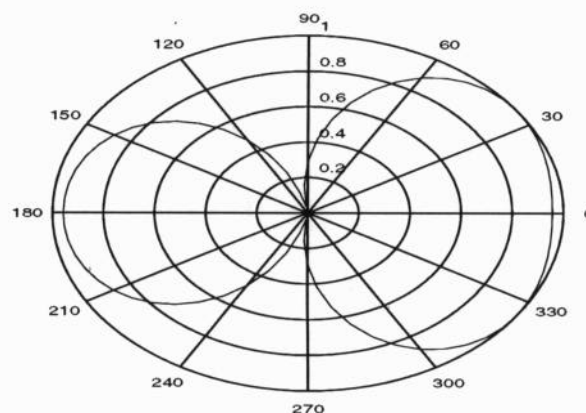


Figure 7(a). Voltage Pattern of an LMS Array, DOA(desired) = 0° ; DOA(interferer) = 45° ; SIR(dB) = -10; Iteration = 1

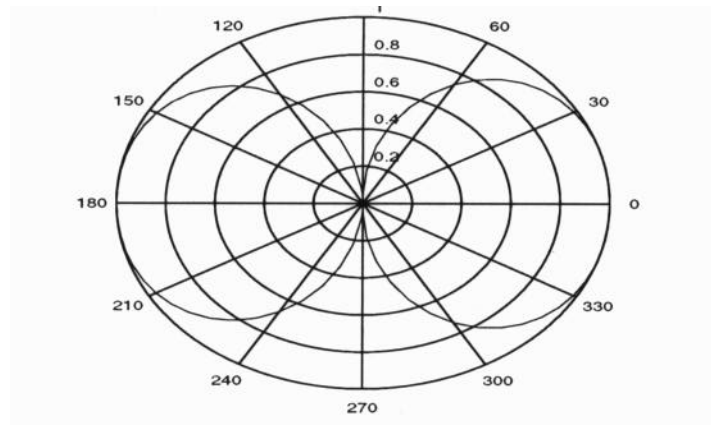


Figure 7(b). Voltage Pattern of an LMS Array, DOA(desired) = 0° ; DOA(interferer) = 45° ; SIR(dB) = -10; Iteration = 70

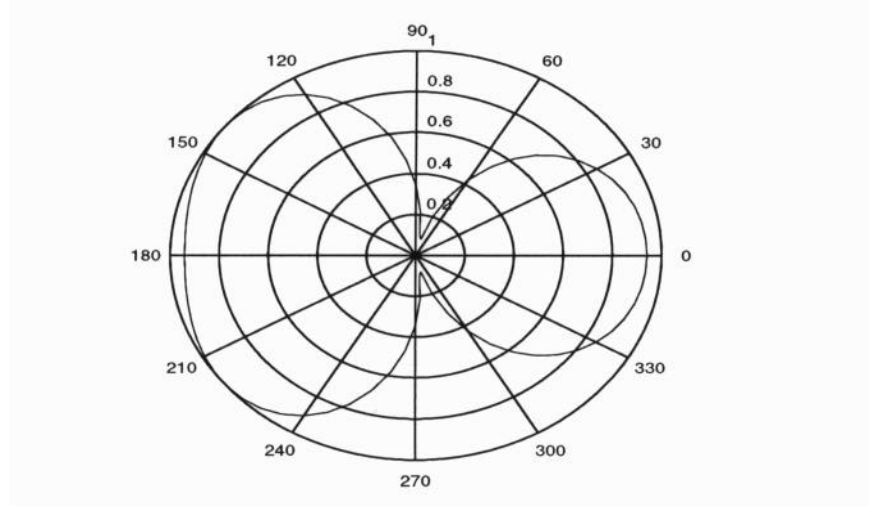


Figure 7(c). Voltage Pattern of an LMS Array, DOA(desired) = 0° ; DOA(interferer) = 45° ; SIR(dB) = -10; Iteration = 350

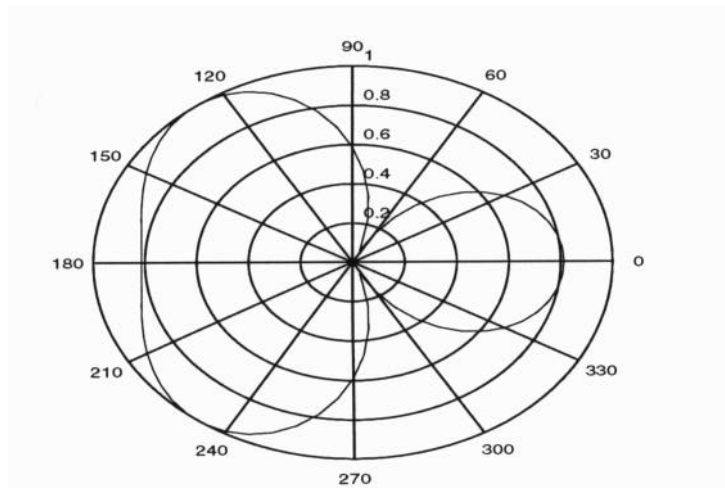


Figure 7(d). Voltage Pattern of an LMS Array, DOA(desired) = 0° ; DOA(interferer) = 45° ; SIR(dB) = -10; Iteration = 750

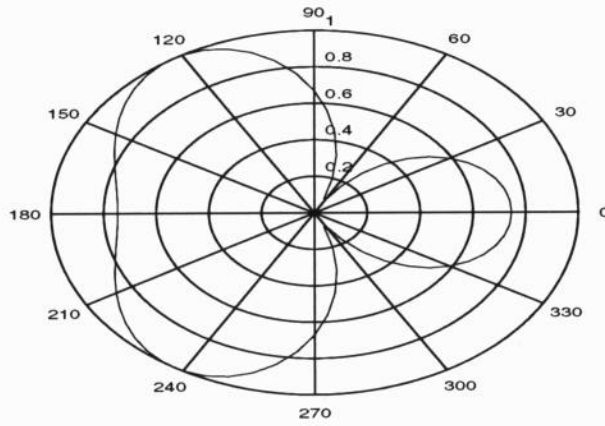


Figure 7(e). Voltage Pattern of an LMS Array, DOA(desired) = 0° ; DOA(interferer) = 45° ; SIR(dB) = -10; Iteration = 1200

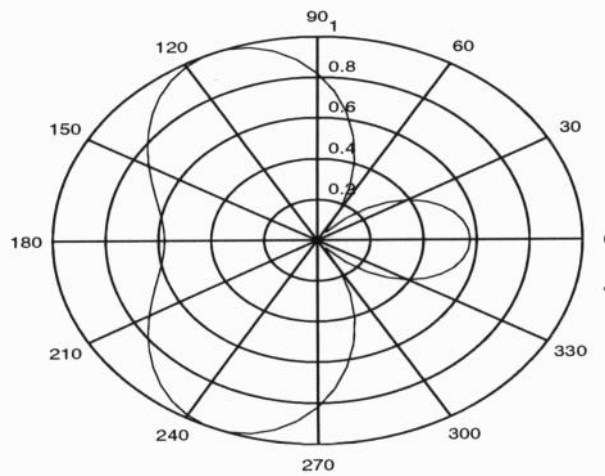


Figure 7(f). Voltage Pattern of an LMS Array, DOA(desired) = 0° ; DOA(interferer) = 45° ; SIR(dB) = -10; Iteration = 3000

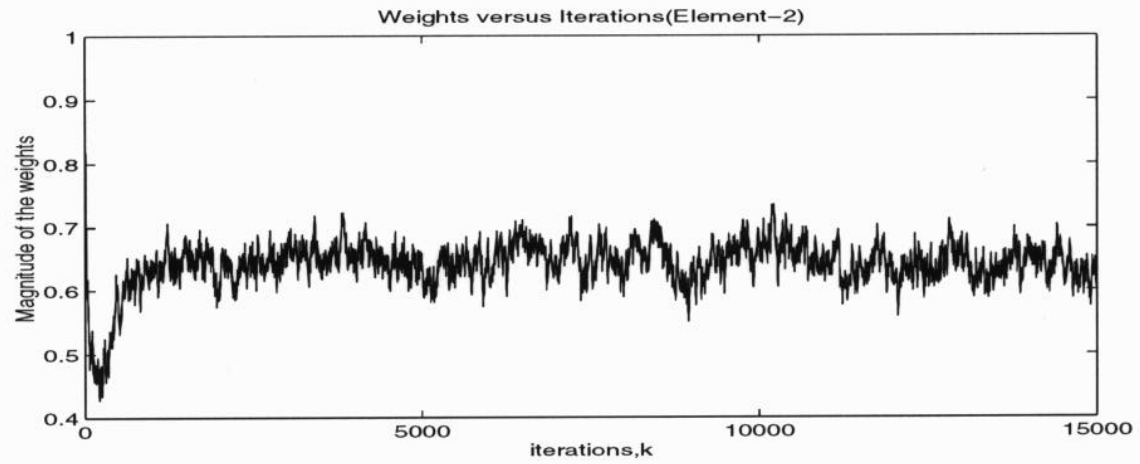
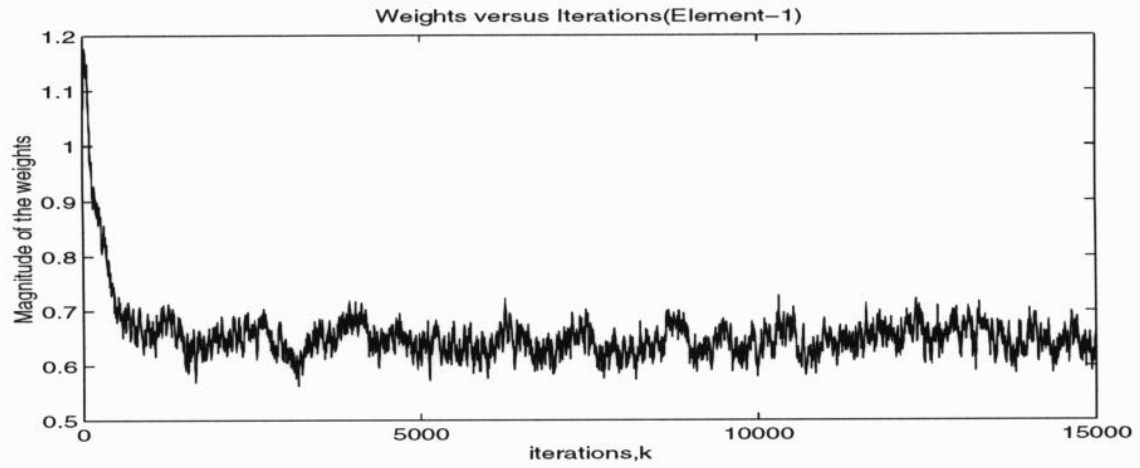


Figure 8 Weights of the adaptive array vs. Number of iterations

By using an initial set of weights of 1 (arbitrary), we can plot the change in the weights as the number of iterations changes. Figure 8 shows a series of such patterns at various times for the weight transients. The purpose of Figure 8 is to show that the weight changes based on the information received from the training sequences. This is important because the weights control the direction of the beam.

4.5. Grating Nulls [Sko80]

As mentioned at the beginning of this chapter, grating nulls are undesirable because interference nulled by the array at one angle may cause additional nulls (grating nulls) to appear at other angles. If the desired signals fall in a grating null, this will result in a low SINR. To illustrate better this concept, we will reuse Figure 6.

The outputs of all the elements are summed to produce an output, Y . Element 1 will be taken as the reference signal with zero phase. The incremented difference in the phase of the signals with respect to adjacent elements is $\psi = \frac{2\pi d \sin(\theta)}{\lambda}$, where θ is the direction of the incoming signal. For this analysis, we will further assume that the amplitudes and phases of the signals at each element are weighted uniformly. As a result, the antenna gain for each element can be normalized to unity. The sum of all the signals from the individual elements, when the phase difference between adjacent elements is ψ , can be written as

$$Y = \sin 2\pi f_c t + \sin(2\pi f_c t + \psi) + \sin(2\pi f_c t + 2\psi) + \dots + \sin(2\pi f_c t + (N-1)\psi) \quad (4.8)$$

where $2\pi f_c$ is the angular frequency of the signal. The sum can be written

$$Y = \sin(2\pi f_c t + (N-1)\frac{\psi}{2}) \frac{\sin \frac{N\psi}{2}}{\sin \frac{\psi}{2}} \quad (4.9)$$

The first factor is a sine wave of frequency $2\pi f_c$ with a phase shift $(N-1)\frac{\psi}{2}$ (if the phase reference were taken at the center of the array, the phase shift would be zero), while the second term represents an amplitude factor of the form $\frac{\sin(\frac{N\psi}{2})}{\sin(\frac{\psi}{2})}$. The field intensity pattern is the magnitude of equation (4.9), or

$$|Y| = \left| \frac{\sin(Nx(d/\lambda)\sin\theta)}{\sin(x(d/\lambda)\sin\theta)} \right| \quad (4.10)$$

The pattern has nulls (zero) when the numerator is zero. The latter occurs when $Nx(d/\lambda)\sin\theta = 0, \pm x, \pm 2x, \dots, \pm nx$, where n is an integer $\neq 0$. The denominator, however, is zero when $x(d/\lambda)\sin\theta = 0, \pm x, \pm 2x, \dots, \pm nx$. Note that when the denominator is zero, the numerator is also zero. The value of the field intensity is apparently indeterminate when both the denominator and numerator are zero. However, by applying L'Hopital's rule (differentiating numerator and denominator separately) it is found that $|Y|$ is a maximum whenever $\sin\theta = \pm n\lambda/d$. These maxima all have the same value equal to N . The maximum at $\sin\theta = 0$ defines the main beam. The other maxima are called the grating lobes, which are typically undesirable. In the case when the spacing is a half-wavelength ($d = \lambda/2$), the first grating lobe ($n = \pm 1$) does not appear in real space since that requires $\sin\theta > 1$, which cannot happen. Grating lobes appear at $\pm 90^\circ$ when $d = \lambda$.

From equation (4.39), $Y(\theta) = Y(\pi - \theta)$. Therefore, an antenna with isotropic elements has a similar pattern in the rear of the antenna as in the front. In order to avoid any ambiguities, the backward radiation is usually eliminated by placing a reflecting screen behind the array. Thus, only the radiation over the forward half of the antenna ($-90^\circ \leq \theta \leq 90^\circ$) needs to be considered. The radiation pattern is equal to the normalized square of the amplitude, or

$$G_a(\theta) = \frac{|Y|^2}{N^2} = \frac{\sin^2[Nx(d/\lambda)\sin\theta]}{N^2 \sin^2[x(d/\lambda)\sin\theta]} \quad (4.11)$$

4.6 Practical Limitations

In Chapter 2, the data presented for SatPCS examples show that most of the proposed satellite constellations for personal communications will be broadcasting at L- and S- Band. At these frequencies the wavelength is in the range of 10 to 20 centimeters. As mentioned previously, the spacing between the antenna is typically between $0.5\lambda - 0.8\lambda$. Consequently, this will be a challenge for the handheld unit designers since they have to be concerned with the actual implementation and design of the handheld unit. Thus, the size of the array becomes the limiting factor in terms of the number of elements that can fit on the handheld unit. In order to mount a linear array on the handheld unit, the maximum number of elements that can conveniently fit limit the antenna to a two element array. Most of the new handheld units are designed to fit into a shirt pocket and are usually light in weight. If multiple elements were used on a handheld unit at L-band, this might result in a bulky handheld unit. Hence, the size of the

handheld unit is a major factor in consumer satisfaction. However, in the case of higher frequencies, such as S-band, a four element array may fit onto the handheld unit. More will be said about the mechanical design of the antenna in Chapter 5. In the following subsections, we will see how these limitations will affect the performance of the overall system.

4.6.1 Degrees of Freedom

The more antenna elements in an array, the more degrees of freedom the antenna possesses in combating interference and multipath fading. For instance, an N -element antenna array has $N-1$ degrees of freedom in its pattern. This puts a limit on the number of things an array can do at a particular time.

Let us define the signal vector in the array as

$$S = Ae^{j2\pi f_c t} \begin{bmatrix} 1 & e^{j\psi} & e^{j2\psi} & \dots & e^{jN\psi} \end{bmatrix} \quad (4.12)$$

where A is the amplitude of the signal and f_c is the carrier frequency. Everything in the squared bracket is known as the steering vector. Each exponential term represents the signal from one antenna element. From eqn (4.12), there are N -elements in the array. Assuming that we ignore the amplitude variation for the sake of simplicity in this analysis (eliminating A from eqn. (4.12)), the received signal would then be the signal from each element multiplied by the complex weight defined in (4.7) and summed to produce the signal output $y(t)$ where:

$$y(t) = e^{j2\pi f_c t} \left[w_1 + w_2 e^{j\psi} + w_3 e^{j2\psi} + \dots + w_N e^{jN\psi} \right] \quad (4.13)$$

Let us define $f(\psi)$ to be the quantity in the square brackets [Com88],

$$f(\psi) = w_1 + w_2 e^{j\psi} + w_3 e^{j2\psi} + \dots + w_N e^{jN\psi} \quad (4.14)$$

where ψ is the angle of arrival for the desired signal. The function $f(\psi)$ is the voltage pattern of the array for any given set of weighting factors, w_N . By factoring out one of the weights, w_1 from the expression in (4.14), we get

$$f(\psi) = w_1 \left[1 + \frac{w_2 e^{j\psi}}{w_1} + \frac{w_3 e^{j2\psi}}{w_1} + \dots + \frac{w_N e^{jN\psi}}{w_1} \right] \quad (4.15)$$

In (4.15), the weight w_l will have no effect on the shape of the pattern since the bracket term is the one that is dependent on ϵ , the angle of arrival for the desired signal. Hence, w_l can only control the overall amplitude and phase of the entire pattern. Since there are $N-1$ coefficients in the bracketed term, excluding w_l , we see that there are $N-1$ degrees of freedom in $f(\epsilon)$.

To understand how an adaptive array performs differently with different degrees of freedom, we will use the following example. Assume that the Signal-of-Interest (SOI) is arriving from the 45° direction. There exists an interfering signal(uncorrelated) arriving from the 0° direction. We will further assume a SIR = 10 dB, where the SOI is 10 times stronger than the interfering signal.

Figure 9 illustrate examples of the antenna pattern calculated for arrays with different numbers of elements. Figure 9(a) shows a two element array with the SOI coming from 45° while the interference is arriving from 0° . Figure 9(d) shows the pattern of an array with eight elements. Comparing Figure 9(a) for two elements, we see that the array with eight elements is more effective in nulling the interference compared to the array with two elements. Also, the array is able to adjust the main lobe and point it toward the DOA of the SOI. From Figure 9(b), we see that the main lobe is gradually moving toward the DOA of the desired signal and from Figure 9(c), we notice that it has already successfully pointed the main lobe in the desired direction. The obvious conclusion is that the more elements the array has, the more effective it will be against the interference because it has more degrees of freedom in terms of controlling the antenna pattern. However, the tradeoff is that the larger the number of elements in the array, the more complex the array will be and the more space it will occupy. Furthermore, having more elements will cause all the weights to take longer to converge. The issue of weight convergence will be further discussed in Chapter 5.

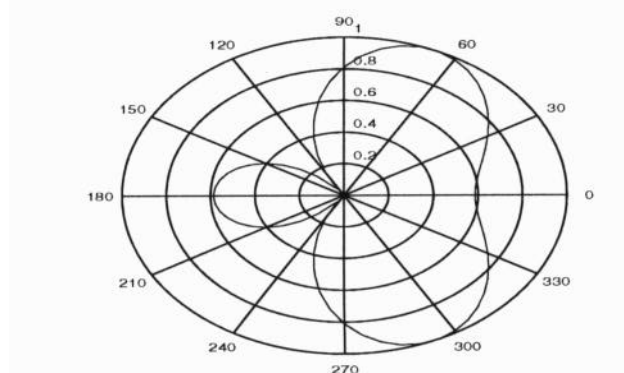


Figure 9(a) 2 Element Array Voltage Pattern; DOA(desired)=45°; DOA(interferer)=0°; SIR(dB)=10

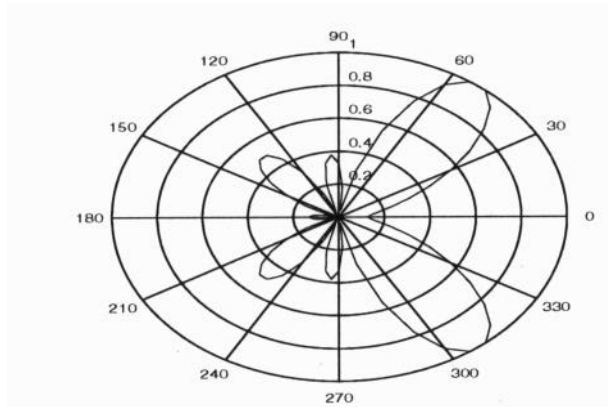


Figure 9(b) 4 Element Array Voltage Pattern; DOA(desired)=45°; DOA(interferer)=0°; SIR(dB)=10

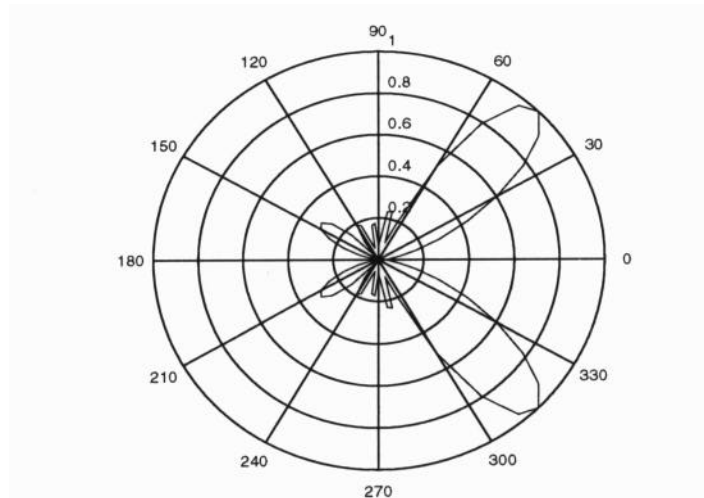


Figure 9(c) 6 Element Array Voltage Pattern; DOA(desired)=45°; DOA(interferer)=0°; SIR(dB)=10

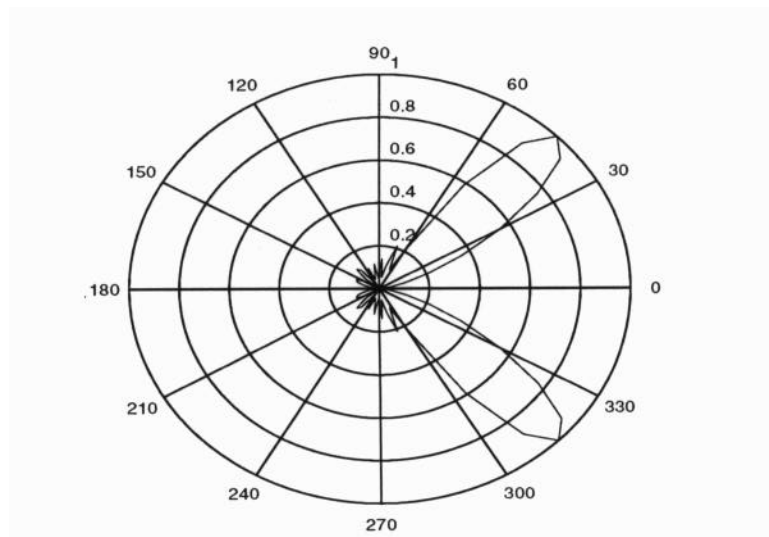


Figure 9(d) 8 Element Array Voltage Pattern; DOA(desired)=45°; DOA(interferer)=0°; SIR(dB)=10

4.6.2 Array Null Depth

To illustrate this concept, we will again simulate an adaptive array with the given specification. Let us assume a two element antenna array, with the SOI arriving from the 30° direction. There is an interfering signal (uncorrelated) arriving from the direction of 0°. In this particular simulation, we will vary the strength of the interfering signal by changing the Signal to Interference ratio (SIR). For Figure 10(a), we will use a two element array while making the SOI 100 times weaker than the interfering signal. In Figure 10(b), the SOI is 10 times weaker than the interfering signal. In Figure 10(c) the strength of the interfering signal is similar to the SOI, while in Figure 10(d), the interfering signal is 10 times weaker than the SOI. From Figure 10(a) to (d), we notice that the depth of the null generated by the array increases as the strength of the interference increases also. This is because the weights of the adaptive arrays are functions of the strength of the interfering signals.

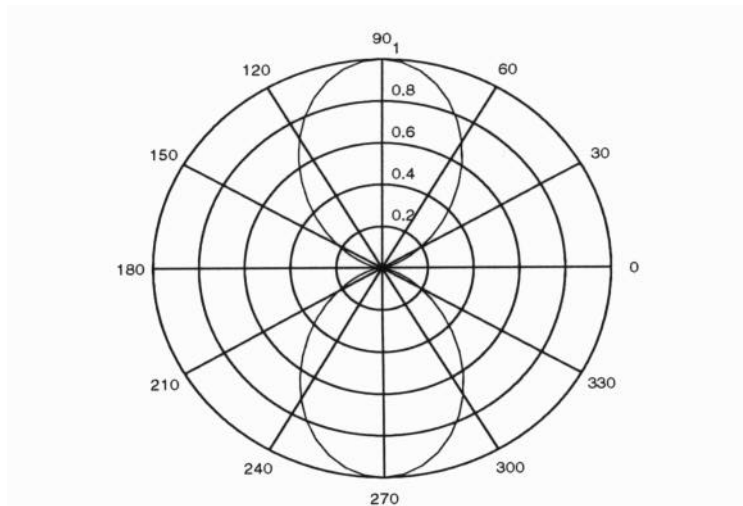


Figure 10(a) 2 Element Array Voltage Pattern; DOA(desired) = 30° ; DOA(interferer) = 0° ; SIR(dB) = -20

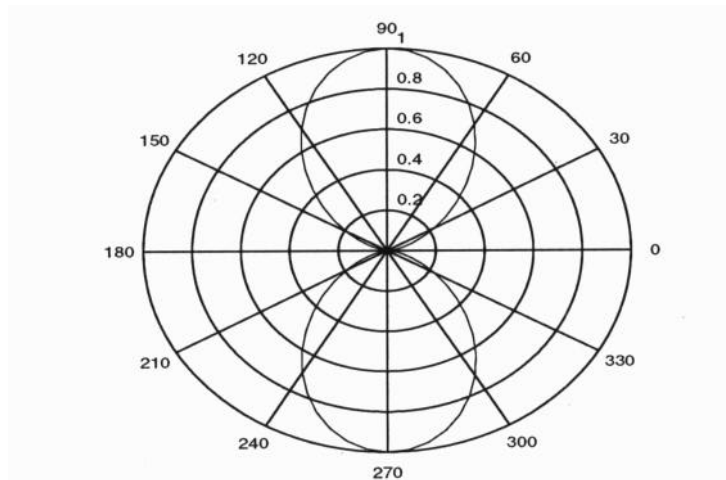


Figure 10(b) 2 Element Array Voltage Pattern; DOA(desired) = 30° ; DOA(interferer) = 0° ; SIR(dB) = -10

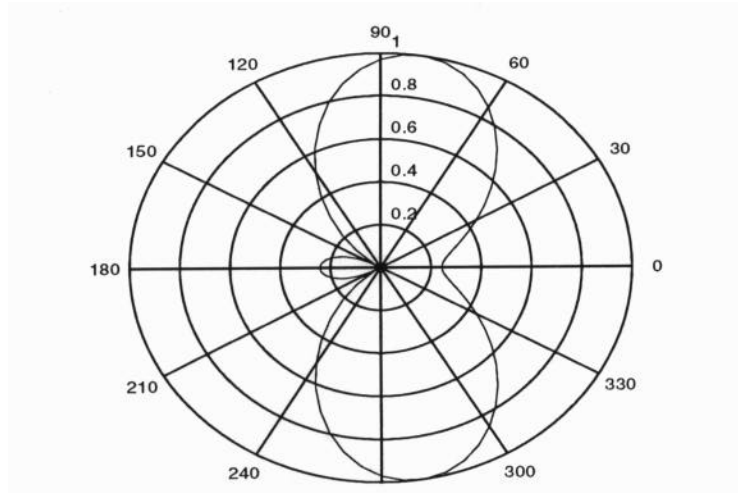


Figure 10(c) 2 Element Array Voltage Pattern; DOA(desired) = 30°; DOA(interferer) = 0°; SIR(dB) = 0

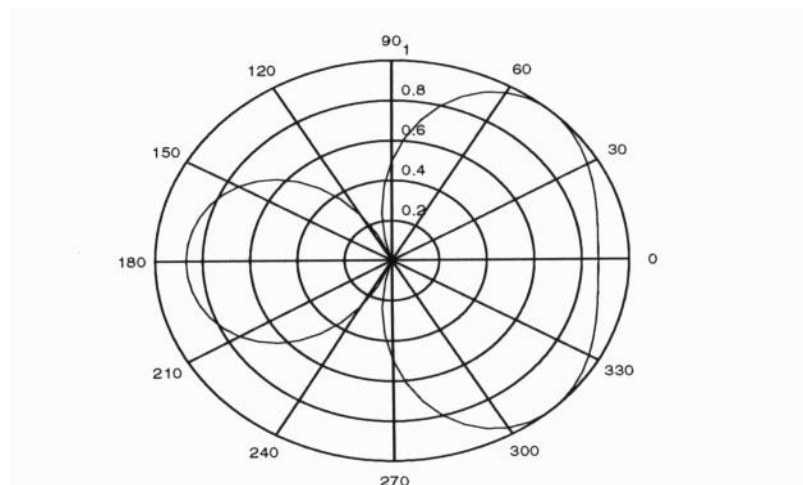


Figure 10(d) 2 Element Array Voltage Pattern; DOA(desired) = 30°; DOA(interferer) = 0°; SIR(dB) = 10

To illustrate this effect analytically, we will need to make the following assumptions. We will assume that there exist three signals present at the array, one desired signal and two interference signals. To simplify the analysis, we will assume these two interfering signals are uncorrelated with the desired signal to illustrate the relationship between the SIR and the depth of the null generated by the array. We will also assume that uncorrelated white Gaussian noise is present in each element signal. Using equations (4.1) - (4.5), we will define the signals as follows:

Let the Signal of-Interest be defined as SOI

$$SOI = A_{SOI} e^{j2\pi f_c t + \phi_{SOI}} \quad (4.16)$$

where A_{SOI} is the amplitude of the SOI. The interfering signals are defined as the Signal-Not-of-Interest, $SNOI_1$ and $SNOI_2$,

$$SNOI_1 = A_{SNOI1} e^{j2\pi f_c t + \phi_{SNOI1}} \quad (4.17)$$

$$SNOI_2 = A_{SNOI2} e^{j2\pi f_c t + \phi_{SNOI2}} \quad (4.18)$$

where ϕ_{SOI} , ϕ_{SNOI1} and ϕ_{SNOI2} are the phase shifts associated with the different elements and are related to the angles of arrival, ϵ_{SOI} , ϵ_{SNOI1} and ϵ_{SNOI2} of the signals. We will then assume a noise vector given by, N

$$N = [n_1(t) \quad n_2(t)]^T \quad (4.19)$$

where $n_1(t) = n_2(t) = \epsilon$.

The respective steering vector associated with each signal is given as follows:

$$U_{SOI} = \begin{bmatrix} 1 \\ e^{-j\epsilon_{SOI}} \end{bmatrix} \quad (4.20)$$

$$U_{SNOI1} = \begin{bmatrix} 1 \\ e^{-j\epsilon_{SNOI1}} \end{bmatrix} \quad (4.21)$$

$$U_{SNOI2} = \begin{bmatrix} 1 \\ e^{-j\epsilon_{SNOI2}} \end{bmatrix} \quad (4.22)$$

The resulting signal, S_T at each element will be

$$S_T = SOI + SNOI_1 + SNOI_2 + \epsilon \quad (4.23)$$

We will further assume that all the signals are statistically independent and have zero mean, thus the covariance matrix, Φ , is given by the expected value of the outer product of

$(S_T - \mu)(S_T - \mu)^T$ [Sta94]. However, since the mean, μ , is zero, the covariance matrix is given as follows:

$$\begin{aligned} \Phi &= E[S_T^* S_T^T] = \epsilon^2 I + A_{SOI}^2 U_{SOI}^* U_{SOI}^T + A_{SNOI1}^2 U_{SNOI1}^* U_{SNOI1}^T + A_{SNOI2}^2 U_{SNOI2}^* U_{SNOI2}^T \\ &= \begin{bmatrix} \epsilon^2 + A_{SOI}^2 + A_{SNOI1}^2 + A_{SNOI2}^2 & A_{SOI}^2 e^{-j\theta_{SOI}} + A_{SNOI1}^2 e^{-j\theta_{SNOI1}} + A_{SNOI2}^2 e^{-j\theta_{SNOI2}} \\ A_{SOI}^2 e^{j\theta_{SOI}} + A_{SNOI1}^2 e^{j\theta_{SNOI1}} + A_{SNOI2}^2 e^{j\theta_{SNOI2}} & \epsilon^2 + A_{SOI}^2 + A_{SNOI1}^2 + A_{SNOI2}^2 \end{bmatrix} \end{aligned} \quad (4.24)$$

In the case of the LMS algorithm, which will be discussed in Chapter 5, a reference signal, $r(t)$ is required for the array structure. Here, we will assume that the reference signal, $r(t)$ is correlated with the desired signal and is defined as follows:

$$r(t) = \text{Re}\{e^{j(2\pi f_c t + \theta_{SOI})}\} \quad (4.25)$$

The reference correlation vector is then

$$S = E[X^* r(t)] = A_{SOI} R U_{SOI}^* \quad (4.26)$$

and the optimal vector, W , is then given by [Com88]

$$W = \Phi^{-1} S \quad (4.27)$$

where Φ^{-1} is given as

$$\Phi^{-1} = \frac{1}{D} \begin{bmatrix} \epsilon^2 + A_{SOI}^2 + A_{SNOI1}^2 + A_{SNOI2}^2 & -A_{SOI}^2 e^{j\theta_{SOI}} - A_{SNOI1}^2 e^{-j\theta_{SNOI1}} - A_{SNOI2}^2 e^{-j\theta_{SNOI2}} \\ -A_{SOI}^2 e^{j\theta_{SOI}} - A_{SNOI1}^2 e^{-j\theta_{SNOI1}} - A_{SNOI2}^2 e^{-j\theta_{SNOI2}} & \epsilon^2 + A_{SOI}^2 + A_{SNOI1}^2 + A_{SNOI2}^2 \end{bmatrix} \quad (4.28)$$

where D is the determinant of Φ ,

$$D = (\epsilon^2 + A_{SOI}^2 + A_{SNOI1}^2 + A_{SNOI2}^2)^2 - \left| A_{SOI}^2 e^{j\theta_{SOI}} + A_{SNOI1}^2 e^{-j\theta_{SNOI1}} + A_{SNOI2}^2 e^{-j\theta_{SNOI2}} \right|^2 \quad (4.29)$$

where $||$ represents the modulus.

Given all the information required for (4.29), we find that the weight vector as obtained from (4.27) is given by

$$\mathbf{W} = \frac{A_{SOI} R}{D} \begin{bmatrix} \epsilon^2 + A_{SNOI1}^2 (1 - e^{j(\theta_{SOI} - \theta_{SNOI1})}) + A_{SNOI2}^2 (1 - e^{j(\theta_{SOI} - \theta_{SNOI2})}) \\ -A_{SNOI1}^2 e^{j\theta_{SNOI1}} - A_{SNOI2}^2 e^{j\theta_{SNOI2}} + (\epsilon^2 + A_{SNOI1}^2 + A_{SNOI2}^2) e^{j\theta_{SOI}} \end{bmatrix} \quad (4.30)$$

To show the dependence of the weights on the strength of the interference, we will define ζ_{SNOI1} and ζ_{SNOI2} as the Interference-to-Noise ratios, INR for $SNOI_1$ and $SNOI_2$. The respective INR can be represented as follows:

$$\zeta_{SNOI1} = \frac{A_{SNOI1}^2}{\epsilon^2} \quad (4.31)$$

$$\zeta_{SNOI2} = \frac{A_{SNOI2}^2}{\epsilon^2} \quad (4.32)$$

We will further define the SNR for the SOI as

$$\zeta_{SOI} = \frac{A_{SOI}^2}{\epsilon^2} \quad (4.33)$$

By some manipulation of eqn (4.26) and dividing by σ^4 , we get

$$\mathbf{W} = \frac{\sqrt{\zeta_{SOI}} (R / \epsilon)}{D / \epsilon^4} \begin{bmatrix} 1 + \zeta_{SNOI1} [1 - e^{j(\theta_{SOI} - \theta_{SNOI1})}] + \zeta_{SNOI2} [1 - e^{j(\theta_{SOI} - \theta_{SNOI2})}] \\ -\zeta_{SNOI1} e^{j\theta_{SNOI1}} - \zeta_{SNOI2} e^{j\theta_{SNOI2}} + (1 + \zeta_{SNOI1} + \zeta_{SNOI2}) e^{j\theta_{SOI}} \end{bmatrix} \quad (4.34)$$

where D is also a function of ζ_{SOI} , ζ_{SNOI1} and ζ_{SNOI2}

$$D = (\epsilon^2 + \zeta_{SOI} \epsilon^2 + \zeta_{SNOI1} \epsilon^2 + \zeta_{SNOI2} \epsilon^2)^2 - \left| \zeta_{SOI} \epsilon^2 e^{j\theta_{SOI}} + \zeta_{SNOI1} \epsilon^2 e^{j\theta_{SNOI1}} + \zeta_{SNOI2} \epsilon^2 e^{j\theta_{SNOI2}} \right|^2 \quad (4.35)$$

To show the relationship between the weights and the strength of the interfering signal, we used eqn (4.34) and plotted the magnitude of the weight versus the INR of $SNOI_2$. The dependence of the weights, W, on ζ is shown in Figure 11. The conditions for the simulation (as shown in Figure 11) are as follows: ζ_{SOI} is 0 dB, ζ_{SNOI1} is 20 dB and a random direction of arrival was

arbitrarily chosen for all three signals. Then, by varying the ζ_{SNOI_2} , the weight decreases as the strength of the interferer increases, as seen in Figure 11.

From eqn(4.34) and with the knowledge of \mathbf{W} , the array pattern can be computed. In order to compute the pattern, we assume a unit amplitude test signal propagating into the array from an angle θ . This signal will produce an output signal, $y(t)$:

$$y(t) = \mathbf{W}^T \text{SOI} = e^{j(2\pi f_c t + \pi \text{soi})} \mathbf{W}^T \begin{bmatrix} 1 \\ e^{-j\pi} \end{bmatrix} = e^{j(2\pi f_c t + \pi \text{soi})} [w_1 + w_2 e^{-j\pi}] \quad (4.36)$$

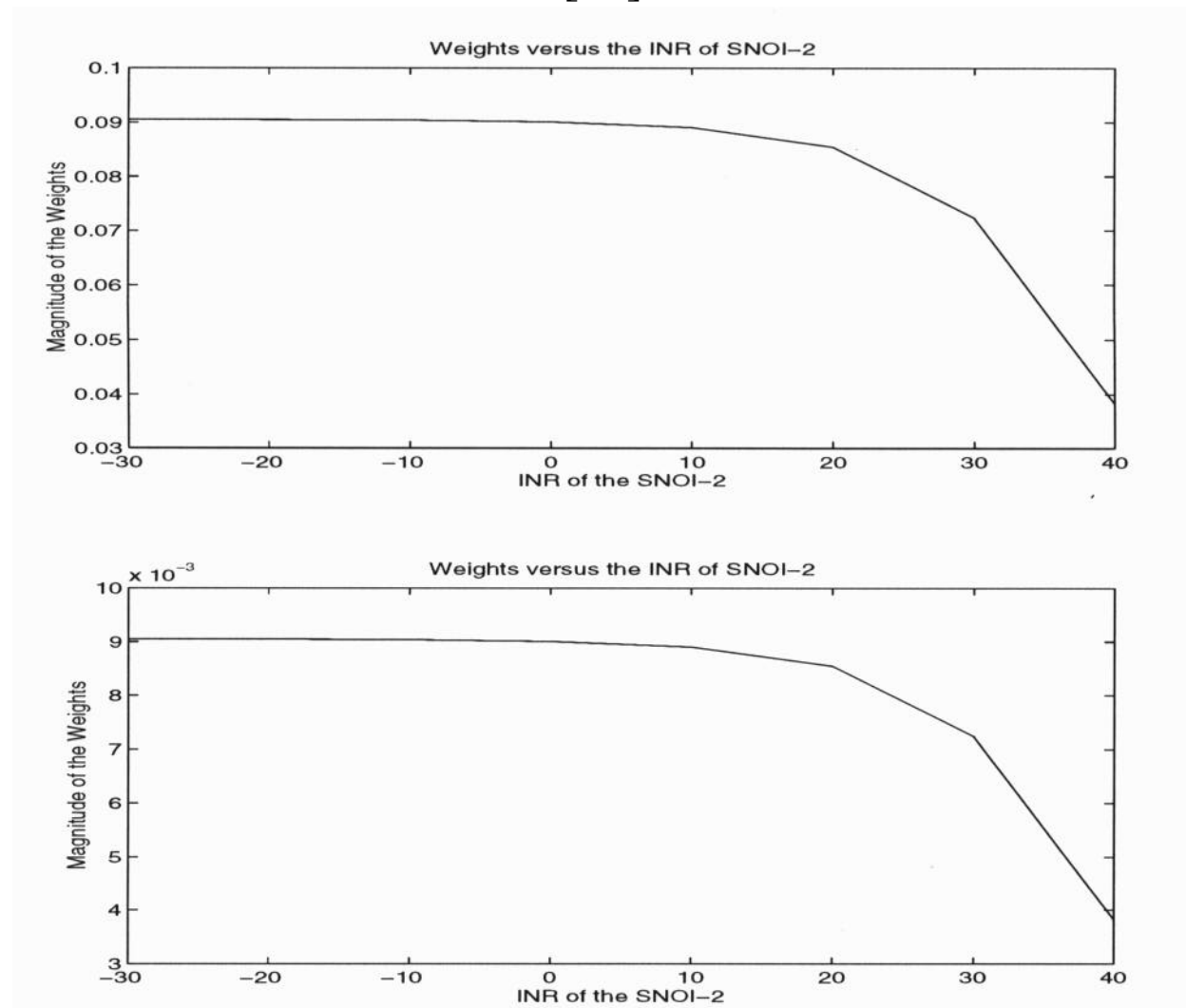


Figure 11 Weights converging as INR of SNOI₂ increases

where the voltage pattern is given by the magnitude of $y(t)$ as a function of t . Hence, the Signal-to-Interference plus noise ratio is given by

$$SINR = \frac{P_{SOI}}{P_n + \sum_{i=0}^n P_{SNOIi}} \quad (4.37)$$

But, in order to calculate the SINR, we must first determine the power associated with each signal and the noise. From eqn. (4.39), we see that the output power of the SOI is given by

$$y_{SOI}(t) = e^{j(2\pi f_c t + \theta_{SOI})} W^T \begin{bmatrix} 1 \\ e^{-j\theta_{SOI}} \end{bmatrix} = e^{j(2\pi f_c t + \theta_{SOI})} [w_1 + w_2 e^{-j\theta_{SOI}}] \quad (4.38)$$

$$P_{SOI} = \frac{1}{2} E [y_{SOI}(t)]^2 = \frac{A_{SOI}^2}{2} |w_1 + w_2 e^{-j\theta_{SOI}}|^2 \quad (4.39)$$

Similarly, the output power for the interference and noise is given as follows:

$$P_{SNOI1} = \frac{A_{SNOI1}^2}{2} |w_1 + w_2 e^{-j\theta_{SNOI1}}|^2 \quad (4.40)$$

$$P_{SNOI2} = \frac{A_{SNOI2}^2}{2} |w_1 + w_2 e^{-j\theta_{SNOI2}}|^2 \quad (4.41)$$

and

$$P_n = \frac{\xi_n^2}{2} [|w_1| + |w_2|]^2 \quad (4.42)$$

From the eqn (4.34) to (4.42) and Figure 11, we see that the weights are a function of ζ_i . We see that as ζ_{SNOI} increases, the weight drops to a small value. As a result of this dependence, the null increases as the strength of the interfering signal increases.

The principal advantage of having the null depth depend on the strength of the interferer is that stronger interference automatically results in a deeper null; thus, the array gets additional protection as interference power increases. However, the drawback is that if the interference signal changes with time (such as a signal having envelope modulation), there will be a time variance in the weights of the array. Time varying weights are not good because they may modulate the desired signal [Com83].

Also in this case, we know that the two element array is limited to one degree of freedom. If there exists more than one interferer, as shown in this example, the array will null out the interfering signal with the strongest signal strength [Com88].

The examples in this chapter illustrate the effect of uncorrelated signals. In the case of multipath, the result would be different because the signals are correlated. This case will be addressed in Chapter 5.

4.7 Adaptive Algorithms

An adaptive algorithm is an algorithm that varies the weights of the antenna array based on the received data in order to maximize the signal strength of the SOI. The algorithm is crucial in steering the main beam of the antenna array. Different algorithms have different characteristics, i.e. different convergence rates, computation complexity, and effectiveness.

Another characteristic of the adaptive algorithm is that it operates in either a block mode or an iterative mode. In a block processing technique, a new solution (weights) is calculated periodically using estimates of statistics obtained from the most recently available block of data. The latter technique utilizes the current weight vectors, $\mathbf{w}(k)$ and calculates new weight vectors $\mathbf{w}(k+1)$ at the next iteration. The iterative approach is more accurate in the sense that it can constantly track a changing environment as the new information is being sampled at every iteration.

Compton [Com88], Widrow [Wid67], Agee [Age83], Petrus [Pet94], Proakis [Pro95] and Liberti [Lib95] have described numerous adaptive algorithms that utilize the two different processing techniques to approximate the weights of the array. Some of these algorithms include the Spectral Self-coherence Restoral Algorithm (SCORE), the Constant Modulus Algorithm (CMA), the Recursive Least Squares Algorithm (RLS), the Switched Diversity Algorithm, the Least Mean-Square Algorithm (LMS) and many more. Determining the unique characteristics of these algorithms is beyond the scope of this thesis. However, to demonstrate the effectiveness of the adaptive array in combating interference (uncorrelated) and multipath (correlating) fading, we will use the LMS algorithm for our simulation in Chapter 5.

4.8 Adaptive Arrays and SatPCS

Table 13. Satellite Characteristics

	IRIDIUM	GLOBALSTAR	ODYSSEY	Teledesic
Orbit Class	LEO	LEO	MEO	LEO
Altitude (km) [Tor96]	780	1410	10354	695-705

Period [Pra86]	(minutes)	100.1	114	358.7	98.8
Satellite Time [Pra86]	Visibility (minutes)	11.1	16.4	94.5	3.5
Elevation (degrees) [Pra86]	Angle	8.2	10	20	40
Satellite (degrees per second) [Pra86]	Movement	0.06	0.05	0.016	0.06

Table 13 shows a few of the proposed satellite constellations and their orbital characteristics. This table shows that LEOs have a shorter satellite visibility time compared to MEOs. The reason for this difference is because the latter is at a higher altitude, as a result it does not move as fast as a LEO. Consequently, LEOs will experience more handoffs compared to MEOs. In the case of IRIDIUM and Teledesic, we observed that the satellite remains in the user's visibility for approximately 11 minutes, after which the user's call will be handed off to another IRIDIUM satellite. As a result, the handheld system would need a mechanism that can facilitate the handoff to a "new" satellite without dropping the call. As previously mentioned, an omni directional antenna does not require the user to point the antenna at the satellite since it receives signals from all direction. However, omni directional antennas are also extremely susceptible to interference and multipath, as a result, a proposed solution is to use an adaptive antenna array.

Nevertheless, using adaptive arrays on the handheld unit requires the antenna beam to point at the right satellite. If the satellite moves more than 2 degrees within the time the weights are required to converge, the adaptive array will not have the necessary time required to form the beam. As a result, the convergence rate of the weights in the adaptive array will play a significant role in determining the effectiveness of adaptive arrays on a handheld system. Simulations performed on MATLAB (will be discussed in Chapter 5) will illustrate that a two element array (LMS) will be able to adapt to the changing environment as fast as 15 ms for a given set of conditions. The conditions for this particular convergence rate will be further discussed in Chapter 5.

4.9 Summary

Satellite personal communication systems experience some of the problems that occur in terrestrial systems. Interference and multipath fading are just two of the issues discussed in this

chapter. This chapter shows one technique for combating such problems, namely, the use of adaptive antenna arrays. However, this technique is not without its practical limitations as has been shown in the previous discussions. Issues such as the grating nulls, spacing of the elements, and number of degrees of freedom are just a few of the many factors that limit the performance of the adaptive antenna array.

In the following chapter, we will illustrate that adaptive arrays are most effective when dealing with interference signals that are uncorrelated with the signal of interest (SOI). In the case of multipath, where the interfering signal incident on the antenna element is a phase shifted version of the SOI, it is correlated with the SOI and the adaptive array has difficulty nulling out the multipath as effectively as it would with an uncorrelated signal. Besides this, we will also discuss the convergence rate and its importance in SatPCS.

Chapter 5 Adaptive Algorithms, Simulations and Results

In satellite personal communication system (SatPCS), interference can be caused by other users within the same cell, by other satellites, or by scattering, diffraction and reflection. Most of the handheld units for current terrestrial systems utilize an omni-directional antenna, which is susceptible to both interference and multipath. To overcome these problems, we proposed mounting adaptive arrays on a handheld unit and applying it to SatPCS. As mentioned in Chapter 4, adaptive antenna arrays have the ability to null out the interfering signal (uncorrelated) and steer the main beam in the direction of the Signal-of-Interest (SOI). In this chapter, we will look at how effective the antenna array is against multipath and interference. This is accomplished by conducting several computer simulations.

5.1 The Least Mean Square (LMS) Algorithm

5.1.1 Introduction

As discussed briefly in Chapter 4, adaptive algorithms are responsible for processing the weights of the adaptive array based on the input data in order to maximize the signal strength of the SOI. In most digital communication systems, the performance index of the receiver is usually the probability that received bits are in error, Bit Error Rate (BER). In the case of an adaptive array, the weight vectors need to be chosen in such a way that the BER is minimized.

However, this performance index is quite difficult to implement in real time and can be difficult to evaluate directly at the array output. As a result, two other criteria are used to evaluate the performance of the adaptive array. The first technique, developed by Widrow et al. [Wid67], measures the minimum mean square error (MMSE) between the actual array output and an ideal array output and will be further discussed in section 5.1.2. The other technique, which is beyond the scope of this thesis, is to maximize the SINR at the output of the array. This is the concept adopted by Applebaum[App76] and Shor [Sho66].

As mentioned in Chapter 4, there are numerous algorithms that can be used to adapt the weights of the antenna array. Two of the most well known adaptive algorithms are the Least Mean Square algorithm (LMS) and the Recursive Least Squares algorithm (RLS). The LMS algorithm attempts to minimize the Mean Square Error (MMSE) of the error signal, $\epsilon(k)$ (will be discussed in section 5.1.2), while the RLS tries to minimize the time-averaged weighted squared error of $\epsilon(k)$ [Pro95]. These algorithms are similar in that they try to determine an optimal set of weighting factors which maximize the power of the desired signal while minimizing the power of the noise and interference. Both of these techniques are iterative and provide a best possible estimate with each iteration until the weights have adapted/converged. The LMS algorithm is much more simple than the RLS algorithm. However, the tradeoff is that the RLS algorithm has the ability to adapt the weights much faster.

Other algorithms such a Self-Coherence Restoral (SCORE) and Constant Modulus Algorithms (CMA) are classified as blind adaptive algorithms [Pet94][Age83][Age85], which do not require any training sequences to adapt to the environment. These algorithms have their own unique characteristics, however, these characteristics are beyond the scope of this thesis.

5.1.2 Minimum Mean Square Error (MMSE)[Wid67],[Com88]

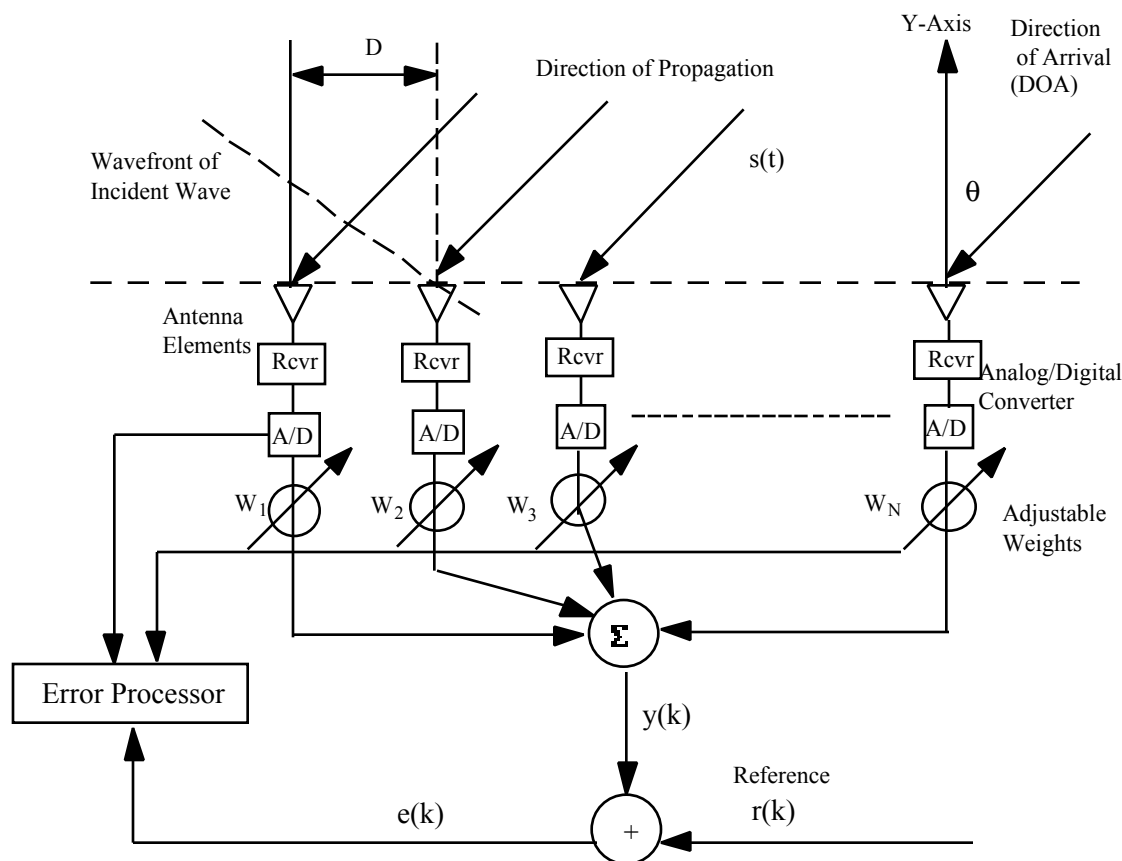


Figure 12 The LMS Adaptive Antenna Array

The figure above is similar to Figure 6 in Chapter 4. For convenience, this figure is reused to illustrate how the LMS algorithm works. The incident waves are defined as $s(t)$. We will assume that the receiver will downconvert the signal to its Intermediate Frequency (IF) while the Analog-to-Digital converter (A/D) will downconvert the signal to its baseband equivalent. As they reach the antenna elements, the waves are converted to electrical signals, $X(t)$. From Figure 12, we define the input signals as $X_1(t), X_2(t), \dots, X_n(t)$. These signals are then multiplied by the input weights w_1, w_2, \dots, w_n , which in this case are complex. The output signal $y(t)$ is the weighted sum of the input signals

$$y(t) = \sum_{i=1}^n X_i(t) w_i \quad (5.1)$$

where n is the number of the weights; or using vector notation

$$y(t) = \mathbf{W}^T \mathbf{X}(t) \quad (5.2)$$

where \mathbf{W}^T is the transpose of the weight vector.

$$\mathbf{W} = [w_1 \quad w_2 \quad \dots \quad w_n]^T \quad (5.3)$$

and the signal input vector is

$$\mathbf{X}(t) = [X_1(t) \quad X_2(t) \quad \dots \quad X_n(t)] \quad (5.4)$$

For digital communication systems, the input signals are in discrete time sampled data form, and thus the output is written as

$$s(k) = \mathbf{W}^T \mathbf{X}(k) \quad (5.5)$$

where the index k indicates the k^{th} sampling instant. In order that adaptation takes place, a reference signal $r(t)$ when continuous, or $r(k)$ when sampled, must be supplied by the adaptive array. [Com88] discusses different ways of generating this reference signal.

The difference between the desired response and the output response forms the error signal $\epsilon(k)$:

$$\epsilon(k) = r(k) - \mathbf{W}^T \mathbf{X}(k) \quad (5.6)$$

This signal is used as a control signal for the weight adjustments and adaptation.

The purpose of the weight adaptation is to find a set of weights that will permit the output response of the adaptive element at each instant of time to be equal to, or as close as possible to, the desired response. A set of weights, \mathbf{W} , is found to be minimal when

$$MMSE = \sum_{k=1}^N \epsilon^2(k) \quad (5.7)$$

When the input signals can be regarded as stationary stochastic variables, we are always interested in finding a set of weights that will minimize the mean square error. The mean square error is given by

$$E[\epsilon^2(k)] = \bar{\epsilon}^2 \quad (5.8)$$

The set of weights that minimizes the mean-square error can be calculated by squaring both sides of (5.6) and taking the expected values on each side.

$$\begin{aligned} E[\epsilon^2(k)] &= E[r^2(k) + \mathbf{W}^T \mathbf{X}(k) \mathbf{X}^T(k) \mathbf{W} - 2\mathbf{W}^T r(k) \mathbf{X}(k)] \\ &= E[r^2] + \mathbf{W}^T \Phi(X, X) \mathbf{W} - 2\mathbf{W}^T \Phi(X, r) \end{aligned} \quad (5.9)$$

where

$$\Phi(X, X) = E[\mathbf{X}(k) \mathbf{X}^T(k)] = \begin{bmatrix} X_1 X_1 & X_1 X_2 & \dots & X_1 X_n \\ X_2 X_1 & \ddots & & \vdots \\ \vdots & & \ddots & \vdots \\ X_n X_1 & \dots & \dots & X_n X_n \end{bmatrix} \quad (5.10)$$

and

$$\Phi(X, r) = E[X(k)r(k)] = E \begin{bmatrix} X_1 r \\ X_2 r \\ \vdots \\ X_n r \end{bmatrix} \quad (5.11)$$

The symmetric matrix $\Phi(X, X)$ is a matrix of cross correlations and autocorrelations of the input signals to the adaptive array, and the column matrix $\Phi(X, r)$ is the set of cross correlations between the n input signals and the desired response signal.

The mean square error defined in (5.9) is a quadratic function of the weight values. The components of the gradient of the mean square error function are the partial derivatives of the mean square error with respect to the weight values. Differentiating (5.9) with respect to \mathbf{W} yields the gradient $\nabla E[\epsilon^2]$, a linear function of the weights.

$$\nabla E[\epsilon^2] = 2\Phi(X, X) \mathbf{W} - 2\Phi(X, r) \quad (5.12)$$

When the choice of the weights is optimized, the gradient is zero. Thus,

$$\begin{aligned}\Phi(X, X)\mathbf{W}_{LMS} &= \Phi(X, d) \\ \mathbf{W}_{LMS} &= \Phi^{-1}(X, X)\Phi(X, r)\end{aligned}\tag{5.13}$$

The optimum weight vector \mathbf{W}_{LMS} is the one that gives the least mean square error. Eqn (5.13) is the Weiner-Hopf Equation. The computation of $\Phi^{-1}(X, X)$ and $\Phi(X, r)$ is not feasible in a practical system; therefore, the above solution is implemented as an adaptive algorithm so that \mathbf{W}_{LMS} optimizes gradually, leading to the LMS algorithm.

5.1.3 Basic Description

The LMS algorithm was first introduced by Widrow et al [Wid67] and operates with *a priori* knowledge of the direction of arrival and the spectrum of the signal, but with no knowledge of the noise and interference in the channel. This algorithm is useful when the interference contains some spectral correlation with the SOI. Minimization of the MMSE can be accomplished by a gradient-search technique; the particular method that the LMS algorithm uses is known as the steepest decent technique. For this particular technique, the changes in the weight vector are made along the direction of the estimated gradient vector.

The basic description of the LMS Algorithm is as follows[Wid67]:

$$e(k) = r(k) - \mathbf{X}^T(k)\mathbf{W}(k)\tag{5.14}$$

$$\mathbf{W}(k+1) = \mathbf{W}(k) + 2\mu e(k)\mathbf{X}(k)\tag{5.15}$$

Where

$e(k)$ = error signal between the reference, $r(k)$ and the weighted input

$\mathbf{W}(k)$ = weight vector before adaptation

$\mathbf{W}(k+1)$ = weight vector after adaptation

μ = scalar constant controlling rate of convergence and stability ($\mu < 0$)

From (5.15) we can see that the LMS algorithm does not require squaring, averaging or differentiating and hence can be implemented in most practical systems. Its popularity is accredited to the fact that it is simple, easy to compute and efficient. However, the drawback is that the weights for this algorithm take a long time to converge. This will become apparent in the simulations discussed in Section 5.3.

5.1.4 The Convergence Rate of the LMS Algorithm

The parameter μ from (5.15) is the gain constant that regulates the speed and stability of adaptation, in other words it determines the convergence rate. This gain factor is bounded by the limits $0 < \mu < \frac{1}{\lambda_{\max}}$, where λ_{\max} is the largest eigenvalue of the correlation matrix Φ . The simulations in Section 5.3 will analyze the effects of the parameter μ .

5.2 Simulation Assumptions

All of the simulations for this thesis were performed on UNIX based SUN/HP workstations with the use of MATLAB. Some of these MATLAB programs were developed with the assistance of Mansoor Ahmad [Man96]. All of the antenna arrays modeled are omnidirectional arrays. In practice, two sets of arrays are used. One set of arrays will be used to cover the 0 to 180 degree region. This is accomplished with the use of a reflecting screen mounted on the back of the array, making the array one sided.

In a satellite based personal communication system there is the problem of interference from both correlated and uncorrelated signals. Interference signals in this context will be constrained to uncorrelated signals, which are a result of interference arriving from other users within the same coverage areas or from other satellites. Multipath signals are considered as correlated signals because they are principally phase shifted versions of the Signal of Interest (SOI). They arrive at the receiver via different paths due to reflection from scattering surfaces such as the ground, buildings, and vehicles.

The simulation is divided into two parts, the first simulation shows how an LMS based adaptive antenna performs in the presence of uncorrelated interference. In the second part of the simulation, we will demonstrate the use of the same antenna and analyze its performance in the presence of multipath (correlated signals). This is equivalent to using a Ricean fading model. Vatlaro used a similar model in calculating the Carrier-to-Interference ratio for his analysis of some of the different proposed LEOs [Vat95]. Allnutt [All95] demonstrated that in a GEO, this multipath component can cause as much as 7 dB fading as a result of signal cancellation. To simplify the model, only a single interferer will be present in our analysis. In the first simulation, the interferer will have a signal with a given Signal-to-Interference Ratio (SIR) and a BPSK modulated signal. This interference signal will be generated separately from the SOI since it is uncorrelated with the SOI. For the second part of our simulation, we will assume that the multipath signal is a phase shifted replica of the SOI. As a result, this signal is correlated with the SOI.

The noise in the system is modeled by a Gaussian noise channel. To obtain the noise amplitude, E_b/N_0 was specified for a given Energy per Symbol (bit), E_b . This is accomplished by taking the carrier amplitude as unity, and defining the amplitude of the pulse sample as $\sqrt{2P} = \sqrt{2E_b/T}$, where T is the symbol period. Also, taking the sample rate as f_s , the bandwidth of a single sided spectrum of that bit stream is $\frac{f_s}{2}$, so that the frequencies in the corresponding double sided spectrum range from $-\frac{f_s}{2}$ to $\frac{f_s}{2}$. The noise variance (noise power), is defined as follows:

$$\sigma_N^2 = \frac{N_0 f_s}{2}$$

The noise variance is used in the MATLAB simulation to generate the necessary noise.

5.3 Simulations & Results

5.3.1 LMS Algorithm in a TDMA System

The LMS algorithm was defined in section 5.1. These simulations attempt to show that the adaptive antenna array is effective in combating both interference and multipath fading.

As shown in Figure 12, a reference signal, $r(k)$ is required to form the beam of the antenna. This reference signal is usually a stable locally generated carrier frequency which exhibits high correlation with the SOI. This implies that there will be at least one strong component incident on the array. The locally generated reference frequency can be generated by the use of a local oscillator, or it can be generated with one of the techniques mentioned by Monzingo [Mon90]. For this simulation, the reference signal is assumed to be the baseband equivalent of the carrier or SOI.

In the TDMA or packet data system, a training sequence is required to train the weights of the adaptive array. We can take advantage of the fact that digital data can be stored (analog signals cannot be stored without adding quantization noise), and as a result the transmitter can send pre-determined training sequences (for a short period of time). These are stored at the receiver to adjust the weights in the mobile environment. This stored data is used as a reference.

The training sequence can be stored in a TDMA frame or a packet as overhead, in which case a fixed number of sequences will be used. The drawback of such a system is a reduction in the information data rate at that particular time frame since the information data in the frame will

be reduced with the addition of these training bits. The length of these training sequences is dependent on numerous parameters in the antenna array and the algorithm. Alternatively, a variable length training sequence can be transmitted regularly to train the weights, and when the MMSE falls below the desired level, the training sequence will stop. This technique will require a more complicated processor to check the MSE at the receiver. The main disadvantage of using the training sequence is that it may result in an interruption of the call in progress, hence affecting the quality of the call. However, it will be apparent in the following results that adaptive arrays are excellent implementations for rejecting interference and multipath. The following figure shows the transmission scheme for an adaptive array used with TDMA or packet data transmission systems.



Figure 13 A TDMA frame for an adaptive array

This LMS simulator operates on the baseband equivalent of the signals. The quadrature noise is generated as specified in Section 5.2. Also, the noise is assumed to be independent between the antenna elements; therefore, it is generated separately and independently for each element. This is done to simplify the simulator and to demonstrate the effectiveness of the array; moreover, another random component will make the interpretation of the result more difficult. Since narrowband arrays are analyzed, the data rate, R_b , for this BPSK modulated signal is kept at 200 kbps. The reference signal used is the complex baseband equivalent of the carrier.

5.3.1.1 Adaptive Array in the Presence of Interference (Uncorrelated)

The assumptions and conditions of simulations are similar to those mentioned in Sections 5.2 and 5.3, respectively. The SOI is a BPSK signal, generated independently from the interference signal. Fading due to the channel was not modeled because it would only add another random component into the interpretation of the results. The interference signal is generated as an independent source transmitting an uncorrelated data sequence. In this simulation, the SOI is seen as arriving from 45° while the interference is coming from 0° .

The first set of simulation results are for a two element linear array with spacing between them equal to half a wavelength. A BPSK modulated SOI with an E_b/N_0 of 10 dB was used for all the following simulations. The convergence factor μ was chosen as 0.001. The results are shown in Figure 14. From Figure 14(a), we can see a null forming in the direction of the interferer. The Signal-to-Interference ratio, SIR is taken as 5 dB. Also, Figure 14(b) shows the output Signal-to-Interference ratio (SINR) as a function of the number of iterations. After 5000

iterations, we observed that the weight converges and that the SINR levels off at approximately 8 dB.

In Figure 15(a) to (d), the same simulation conditions apply, but this time we vary the strength of the interfering signal (by varying the SIR). This is accomplished by varying the amplitude of the interfering signal. As the SIR changes, we noticed that the depth of null also changes. In Figures 15(a) and (b), the interference is much stronger than the signal, thus the null is very deep. In Figure 15(c), the depth of the null decreases when the strength of the interferer is similar to that of the SOI. In Figure 15(d), since the interfering signal is much smaller than the SOI, we see that the null decreases in depth. This shows that the shape of the beam is a function of the interfering signal strength, as

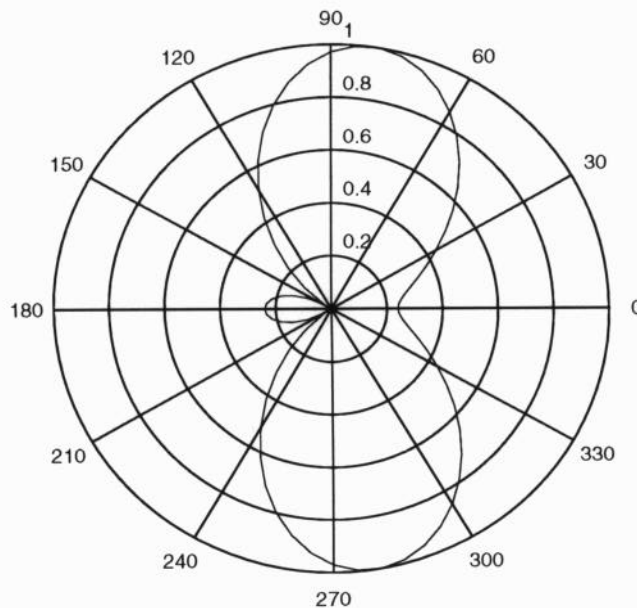


**Figure 14(a) Voltage Pattern of an Adaptive Array DOA(desired)=45°;
DOA(interferer)=0°; SIR(dB) = 5**

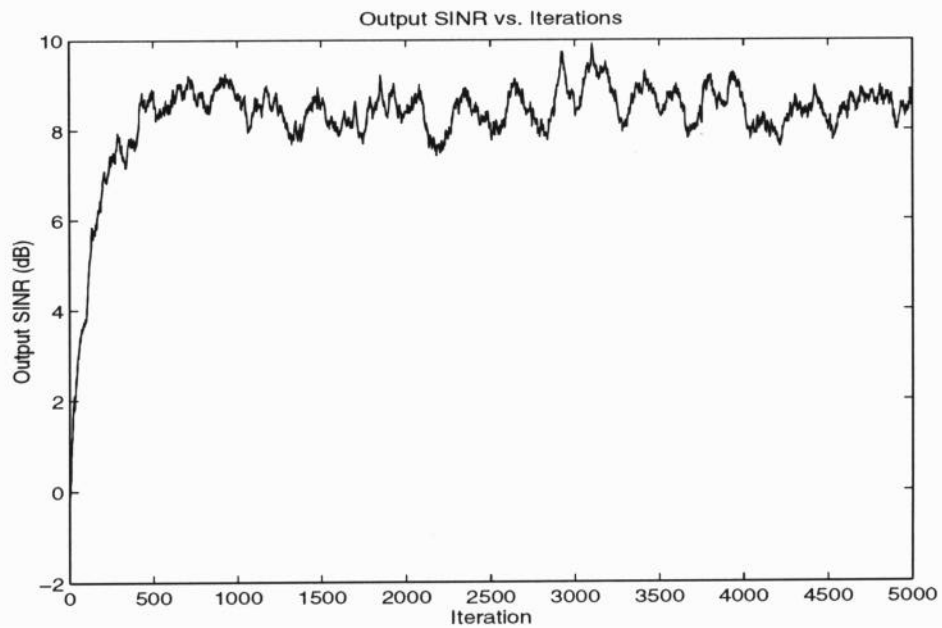


Figure 14(b) Output SINR versus number of iterations (training sequences)

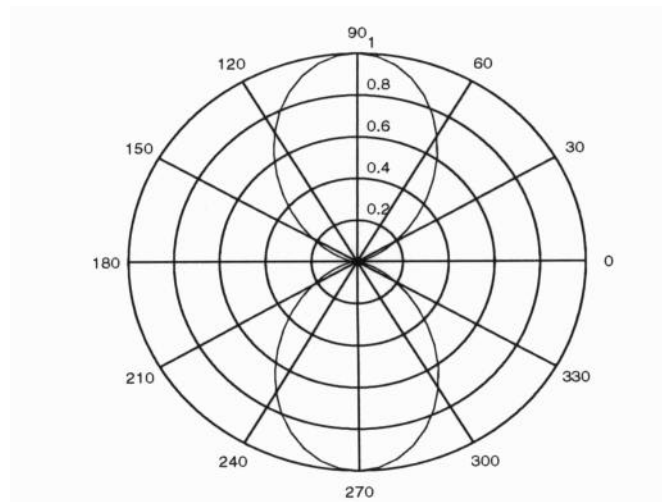
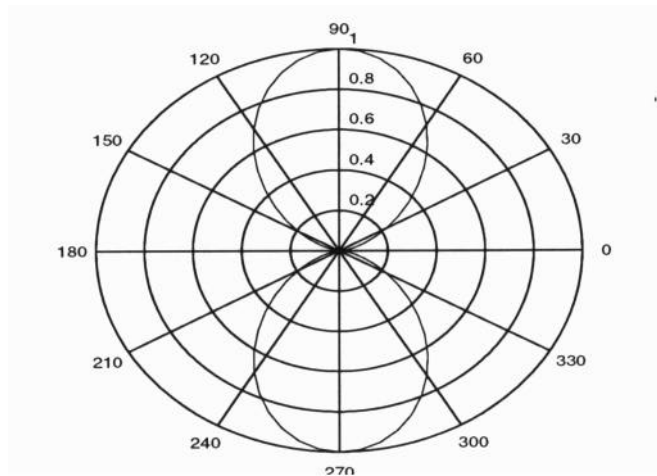
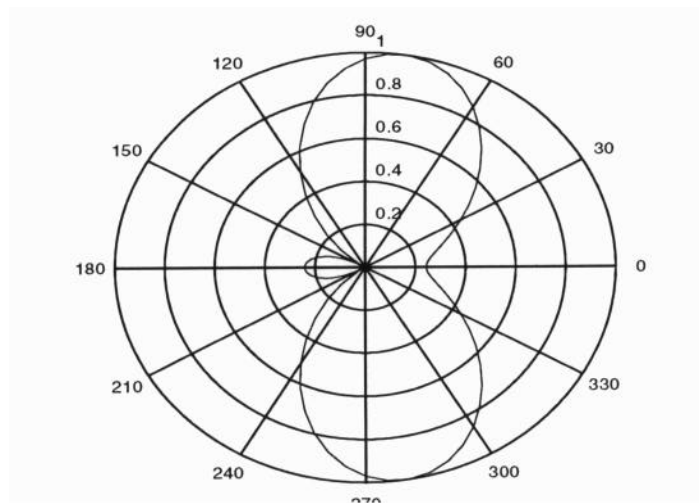


Figure 15(a) 2 Element Array Voltage Pattern; DOA(desired) = 30° ; DOA(interferer) = 0° ; SIR(dB) = -20



**Figure 15(b) 2 Element Array Voltage Pattern; DOA(desired) = 30° ; DOA(interferer) = 0° ;
SIR(dB) = -10**



**Figure 15(c) 2 Element Array Voltage Pattern; DOA(desired) = 30° ; DOA(interferer) = 0° ;
SIR(dB) = 0**

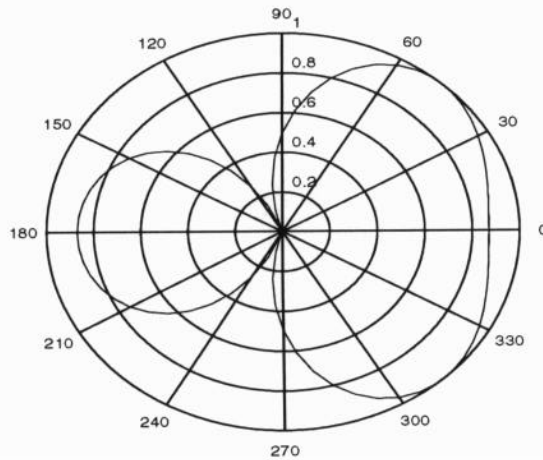


Figure 15(d) 2 Element Array Voltage Pattern; DOA(desired) = 30° ; DOA(interferer) = 0° ; SIR(dB) = 10

mentioned in section 4.4.2. As the interfering signal becomes stronger, the array increases its null depth and vice versa. As long as the signal is not correlated with the reference signal, $r(t)$, the feedback system attempts to remove it from the array output by forming a null on this signal.

There are advantages and disadvantages of having the null depth depend on the interfering signal strength. The advantage is that stronger interference automatically results in a deeper null; thus the array gets additional protection as the interference power increases. The drawback is that if the interference signal changes with time (such as a signal having envelope modulation) there is a time variance in the weights of the array. Time-varying weights are not good because they may modulate the desired signal. [Com 83].

Moreover, we can see from Figures 14 and 15 that since this is a two element linear array, the antenna only has one degree of freedom, hence, it can only put a null in the direction of the interference. If there is more than one interferer, the array will pick the strongest interferer and automatically put a null in that direction. However, if the number of elements is increased to N , the array will have $N-1$ degrees of freedom and thus it will be able to null out $N-1$ interferers.

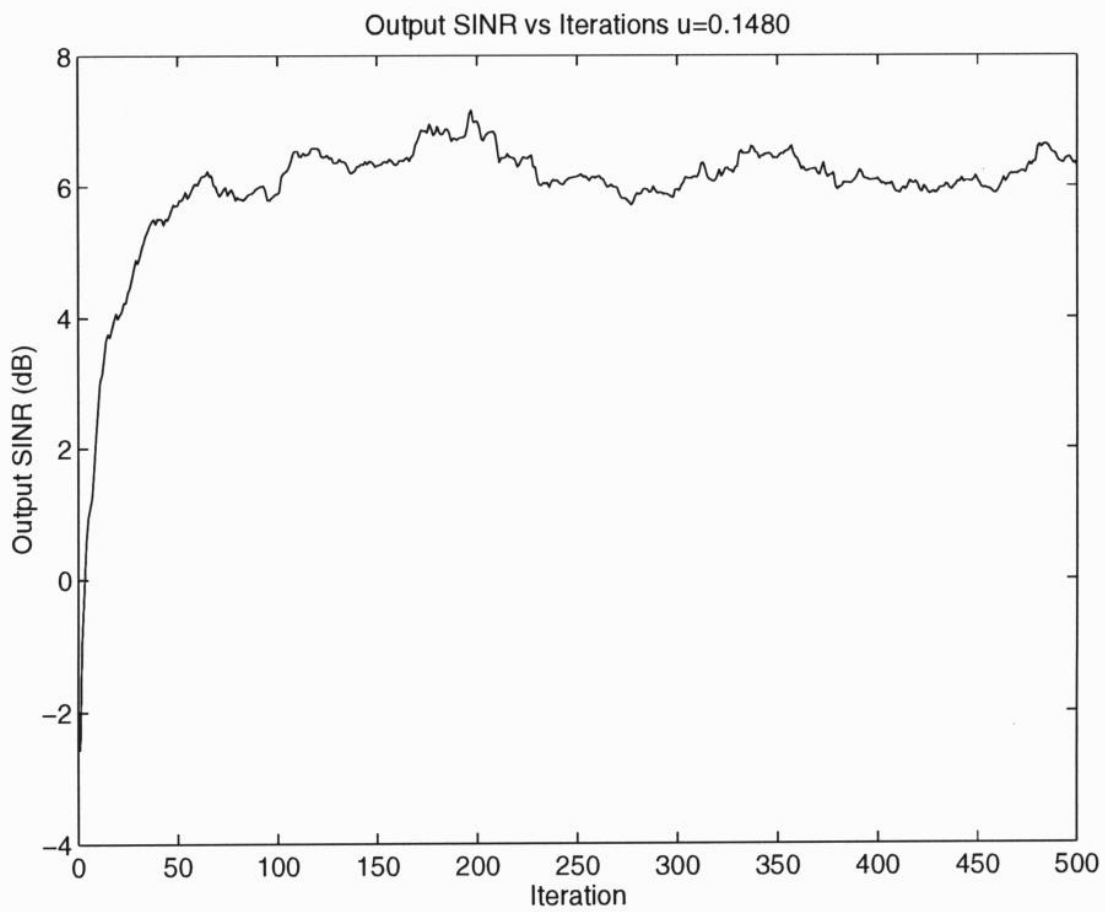


Figure 16(a) Output SINR versus number of iterations. $\mu = 0.1480$

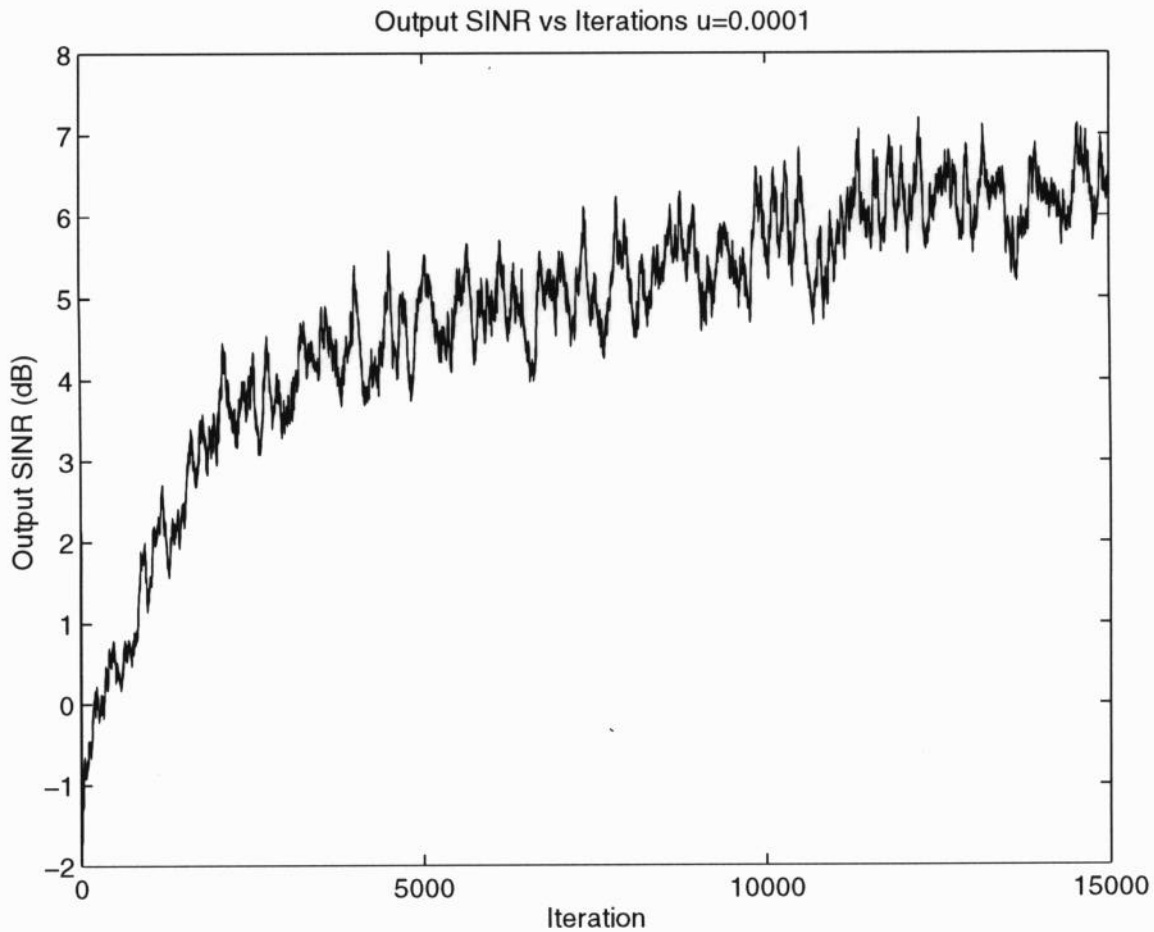


Figure 16(b) Output SINR versus number of iterations. $\mu = 0.0001$

To see the convergence rates of the weights, we will use two different gain/convergence factors, a μ of 0.0001 and 0.1480. Similarly, we will use the same two element linear arrays, with an E_b/N_0 of 10 dB, a bit rate of 9.6 kbps and SIR of 5 dB, and we will compare the adaptation of the weights. We noticed in Figure 16(a) that the simulation associated with a factor of 0.1480. The weights require approximately 100 iterations to converge, however, the output SINR is 5.5 dB. In Figure 16(b), we see that for a simulation associated with a convergence factor of 0.0001, the weights require more than 15000 iterations to converge, and the output SINR is 7 dB. This implies that for this particular scenario for a μ of 0.0001, 15000 iterations is not sufficient to cause the weights to adapt and more iterations are required. This also shows that as μ is increased, and as long as it stays within the theoretical bound, the weights will converge faster. The main disadvantage of making μ larger is that the weights will not converge or there will be significant variation (ripple) in the output SINR.

The faster the convergence rate, the less time the array takes to form an adaptive beam. In Table 13 of Chapter 4, Teledesic (the LEO system with the lowest altitude); has a satellite visibility time of 3.8 minutes. This means that the user needs to have an handheld array that can form the beam before the satellite moves out of visibility. By analyzing the result above, we notice that for a 9.6 kbps system, the number of iterations required for a convergence factor of 0.1480 is 100 iterations. In terms of time, these 100 iterations translate to 10 ms. Since all the LEOs will move less than 1 degrees per second, the user with the handheld array will have sufficient time to form the beam and track the satellite.

To look at the performance of different numbers of antenna elements in the presence of increasing interferers, the output SINR versus the number of interferers was calculated. The interfering signals are all generated independently of each other, and as a result, are uncorrelated with each other. All the signals incident on the array elements are BPSK modulated signals. These simulations were conducted with an E_b/N_0 of 10 dB, where the amplitude of the interferers is 1/5 of that of the SOI. The SOI is coming from a 45° angle, while the directions of the interferers are arbitrary. Based on these conditions and assumptions, the results are plotted in Figure 17. The convergence factor used for this simulation is 0.001 and 10000 iterations were used. We notice that as the number of

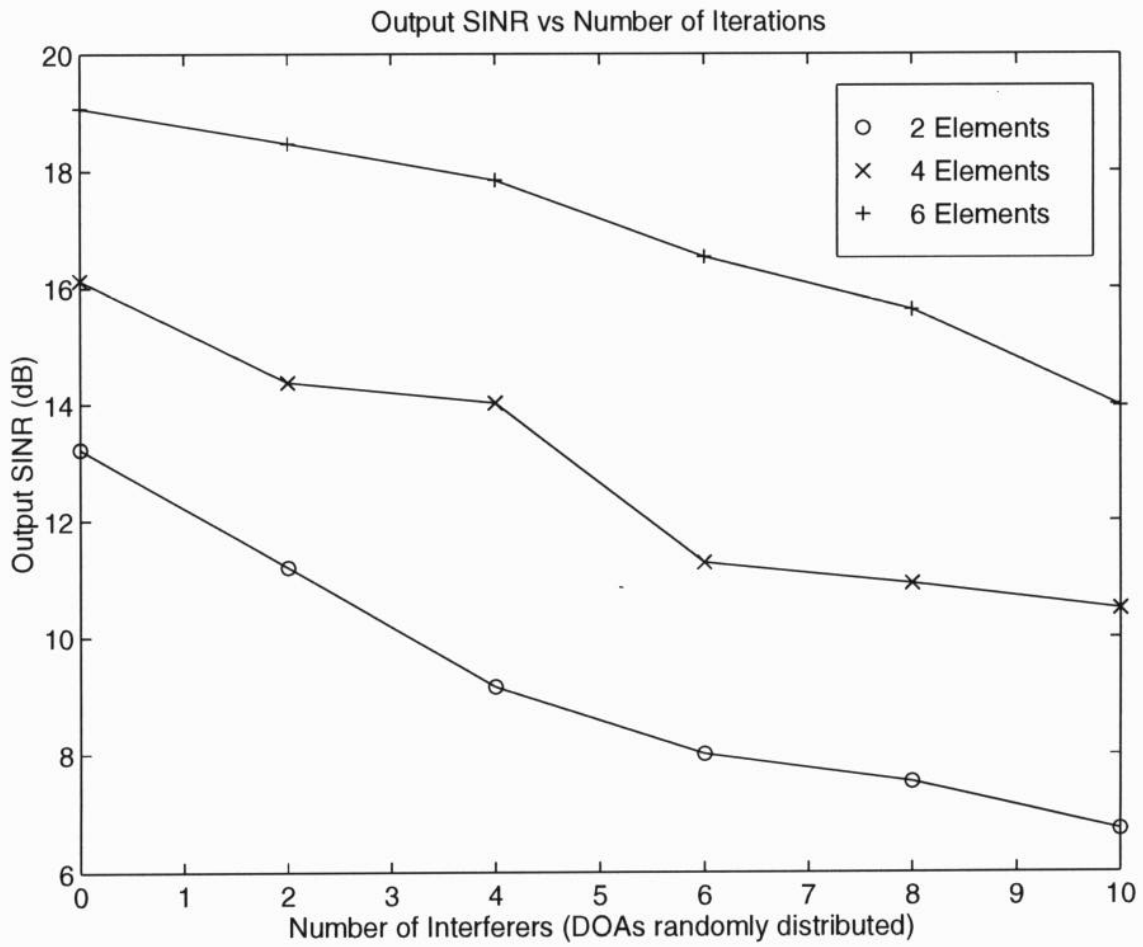
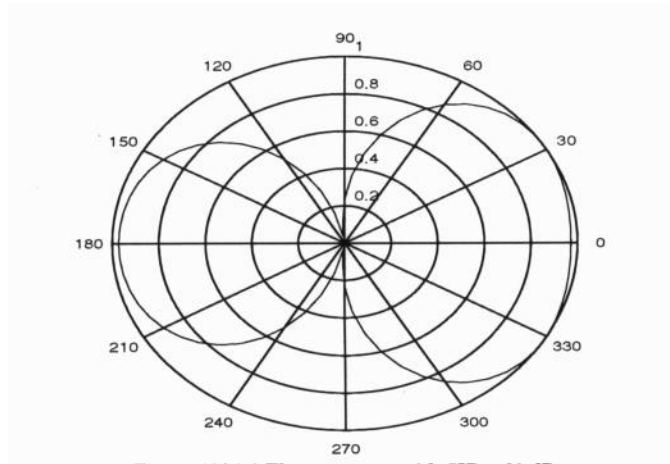
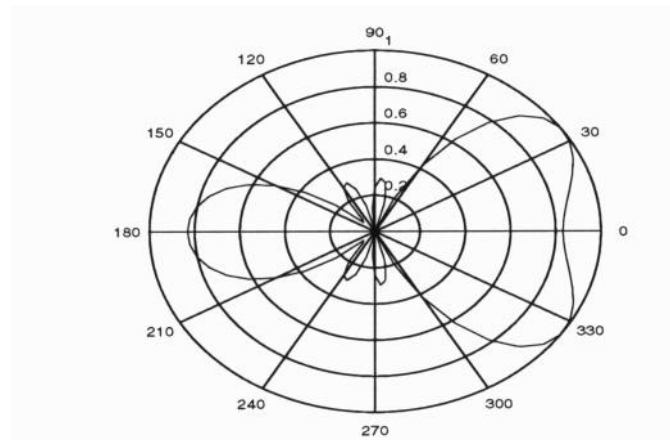


Figure 17 Output SINR versus number of interferers for several different arrays



**Figure 18(a) 2 Element array with SIR = 20 dB Voltage Patern; DOA(desired)=30°;
DOA(interferer)= 0°**



**Figure 18(b) 4 Element array with SIR = 20 dB Voltage Patern; DOA(desired)=30°;
DOA(interferer)= 0°**

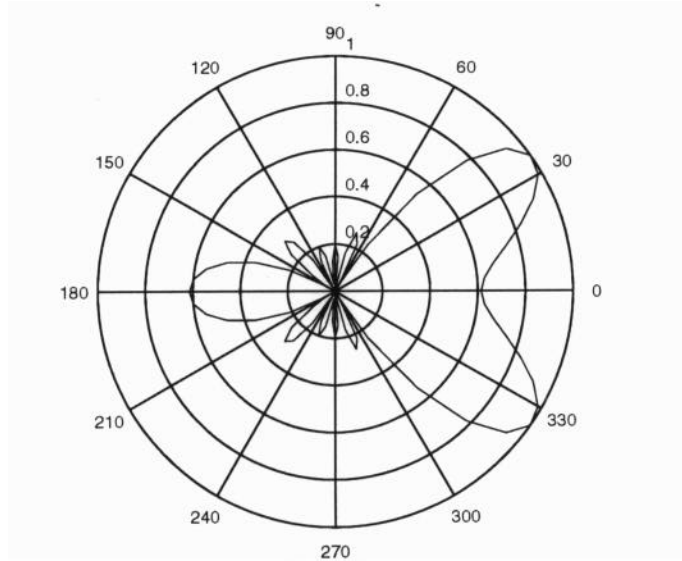


**Figure 18(c) 6 Element array with SIR = 20 dB Voltage Patern; DOA(desired)=30°;
DOA(interferer)= 0°**

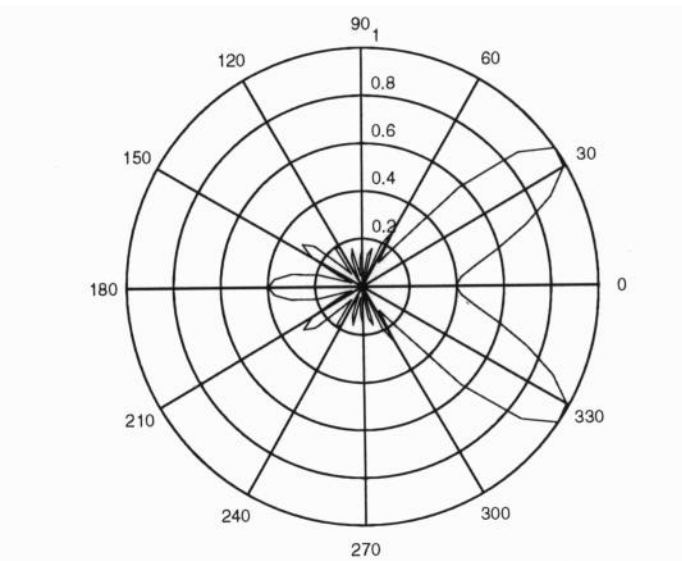


**Figure 18(d) 8 Element array with SIR = 20 dB Voltage Patern; DOA(desired)=30°;
DOA(interferer)= 0°**

interferers increases, the output SINR decreases. Also, a larger number of elements results in a higher gain, which in turn produces a larger output SINR.

Similarly, we can apply the same conditions, but instead analyze the effect of having a varying number of antenna elements but with only one interferer. For convenience, Figure 9 will be reused and labeled as Figure 18. Again, in this particular simulation, the SOI is a BPSK modulated signal arriving from a Direction of Arrival of 30° . The interferer is coming from the 0° direction. The variable for this particular simulation will be the number of elements in the adaptive array. In Figure 18, we observed that the voltage pattern changes and the array steers the main beam toward the direction of the SOI. This is due to the fact that as the number of elements increases, the more degrees of freedom the array possesses, and hence a higher gain results and essentially producing a higher output SINR.

5.3.1.2 Adaptive Array in the Presence of Multipath (Correlated)

In the second part of this simulation, instead of using an uncorrelated interferer, we will use an attenuated and phase shifted version of the SOI as our interfering multipath signal. Similar to the previous simulations, the LMS algorithm is used in the adaptive array. The signals are all BPSK signals. However, instead of using an uncorrelated interfering signal, multipath is used as the interfering source. This multipath signal is generated by using a phase shifted replica of the SOI, with a different DOA. In this simulation, a BPSK modulated SOI is used as the source signal, arriving from a 30° DOA. The multipath is taken as 3 dB weaker than the SOI and is arriving from a DOA of 0° . This multipath signal is shifted by $\frac{\pi}{2}$ compared to the SOI. A convergence parameter, μ of 0.001 and an E_b/N_0 of 10 dB were used for this simulation. The voltage pattern of the array and the output SINR versus the number of iterations is plotted in Figures 19(a) and (b).

For comparative reasons, we simulated another adaptive array, but instead of using a multipath signal that is shifted by $\frac{\pi}{2}$, a new multipath signal phase shifted by π was used. All previous parameters, conditions and assumptions apply to this simulation also. The result is plotted in Figures 20(a) and (b).

In Figure 19(a) and 20(a), we observe that the voltage pattern does not null out the interfering signal as well as it did with an uncorrelated signal. This is probably because the reference signal, $r(k)$, is correlated with the multipath signal. In Figures 19(b) and 20(b), we notice that the SINR, where the multipath signal is shifted by $\frac{\pi}{2}$, resulted in a mean output SINR of 15 dB, while in the case where the multipath signal is shifted by π , the mean output SINR is 8 dB. This demonstrates that depending on the phase of the multipath signal incident on the array, the signals might add constructively or destructively.

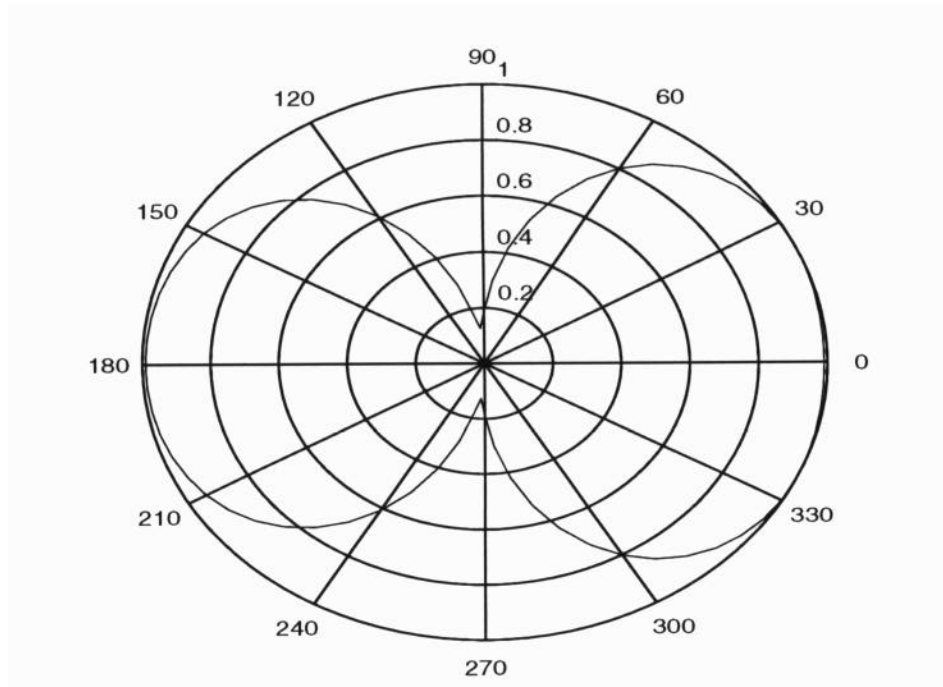


Figure 19(a) Voltage Pattern of Adaptive Array (with Multipath phase shifted by $\pi/2$) DOA(desired) = 30° ; DOA(interferer) = 0° ; SIR(dB)=3

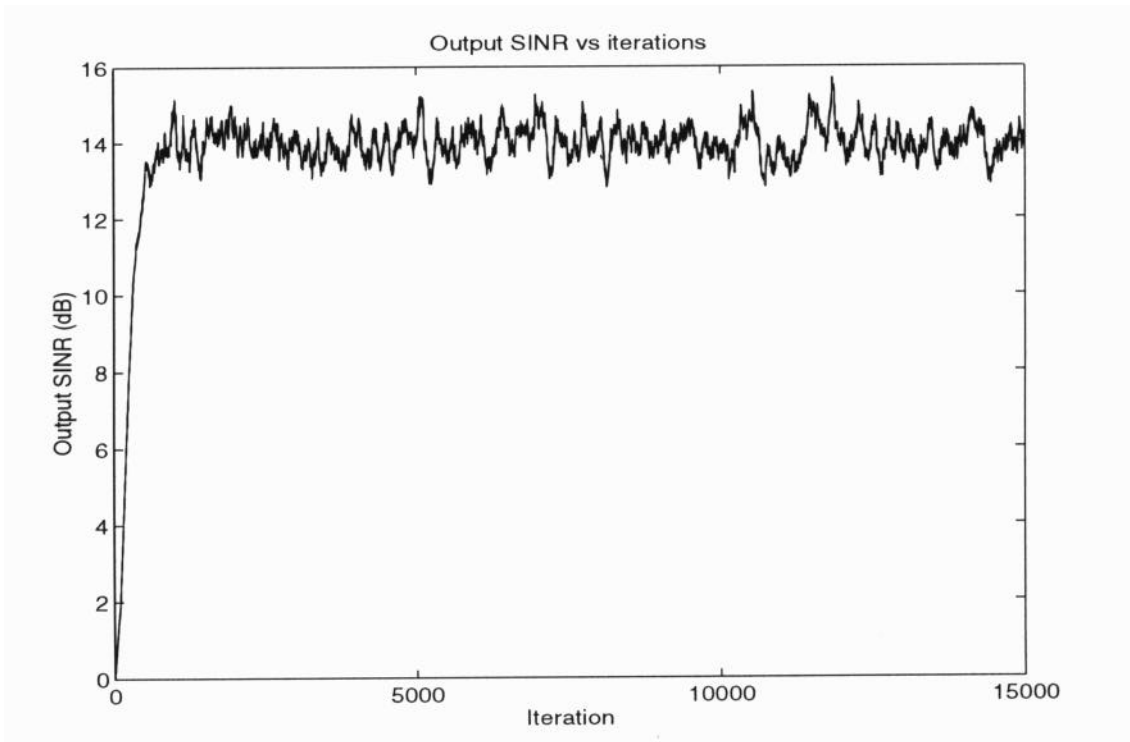


Figure 19(b) Output SINR versus number of iterations

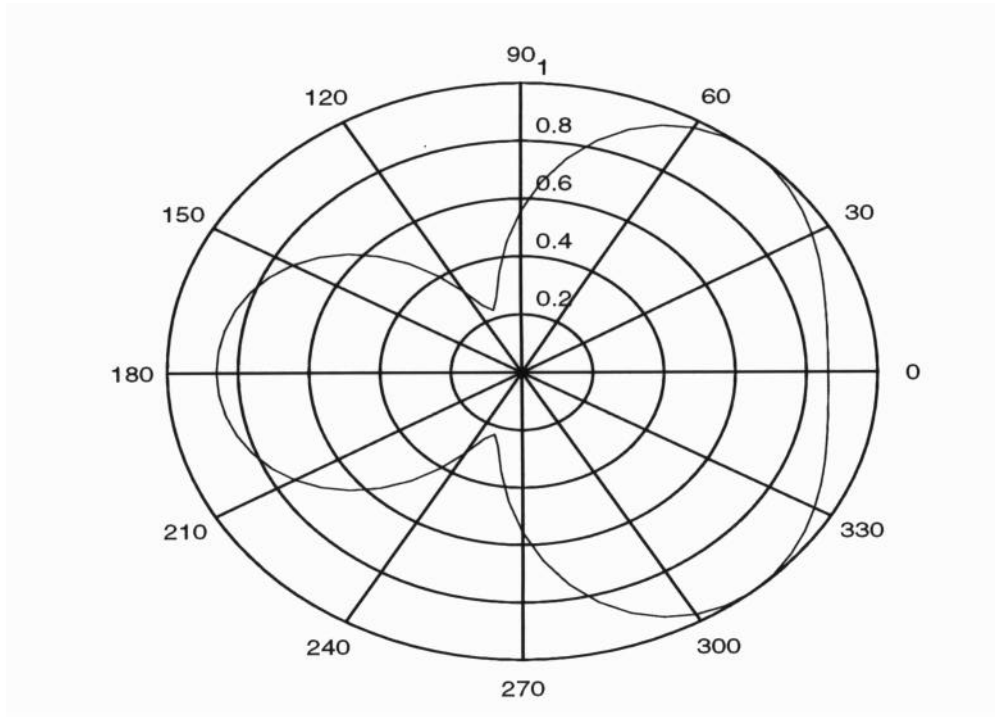


Figure 20(a) Voltage Pattern of Adaptive Array (with Multipath phase shifted by π)
DOA(desired) = 30° ; DOA(interferer) = 0° ; SIR(dB)=3

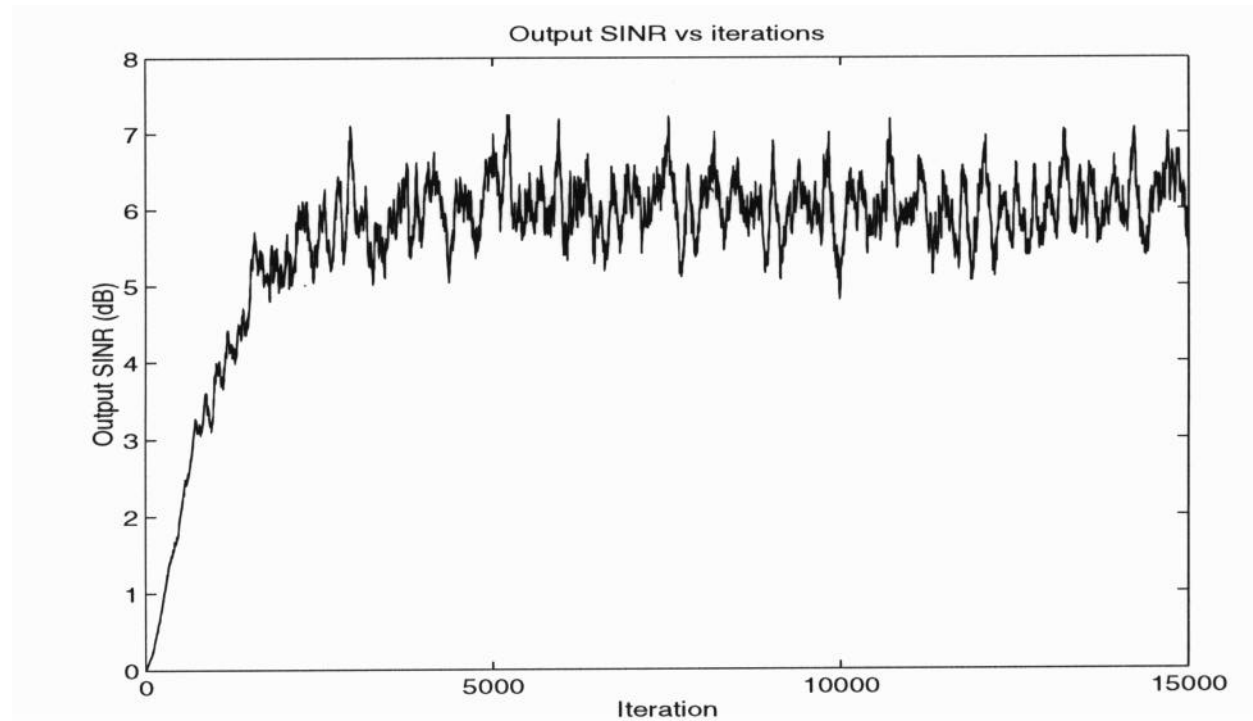


Figure 20(b) Output SINR versus number of iterations

In view of this, the array must be modified to overcome this problem. The following section (Section 5.4) proposes the use of a diversity combining technique where the multipath signals will always be added constructively.

5.4 Adaptive Array for Combating Multipath

Numerous techniques have been proposed to combat multipath fading with an adaptive antenna. Shan [Sha85] uses a preprocessing scheme for the sensor outputs that will restore the rank of the signal covariance matrix so that the multipath signal will be completely coherent with the SOI. The method is based on combining measurements and overlapping the subarrays. Gabriel [Gab84] proposed the use of the Burg maximum entropy method and the maximum likelihood method. He then tried to relate them to a nonlinear adaptive array that consisted of a generic sidelobe canceller and directional gain constraint technique.

However, the approaches mentioned above require more than two antenna elements. To restrict the array to only two radiating elements, because of the issue of space on a handheld unit

at L-Band, Berkebile et al. [Ber96] propose the use of switched antenna diversity. This method allows the handheld unit to determine which of the arriving signals are stronger, and then to switch to this antenna for a given time interval. In the case where there is no direct Line-of-Sight (LOS) present, numerous multipath signals might be incident on the handheld terminal. When this occurs, the antenna with the strongest incident signal will be selected to receive the stronger component. At the end of the predetermined time interval, the signals from each antenna are again compared, and the system again decides which antenna to select.

In a diversity combiner antenna design, a phase shifter is added to set the relative phase of the signals from the two antenna elements before they are combined [Ber96]. Figure 21 shows a block diagram of a two element phased array. The antenna consists of two radiating elements, an electronic switch that can be used to transmit and receive, a two bit phase shifter, and some logic circuits to control the optimum phase setting.

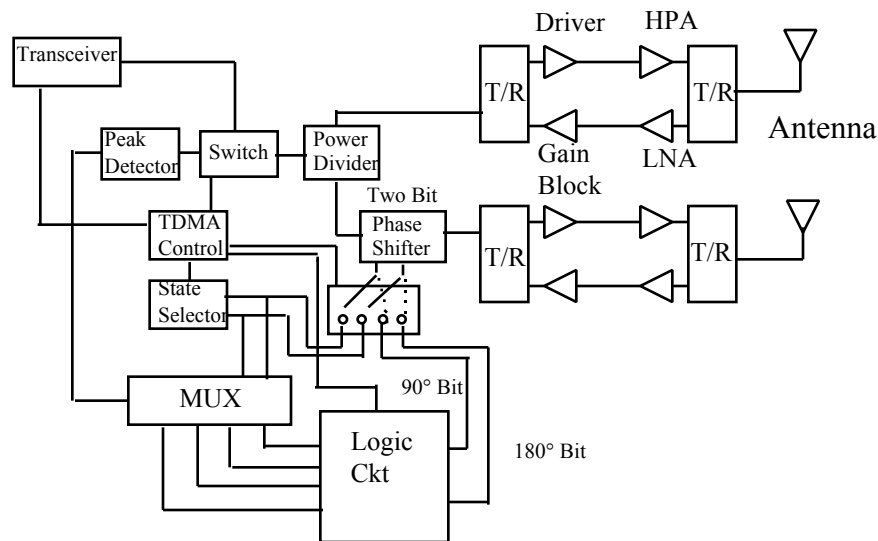


Figure 21 A block diagram of the two element phased array [Ber96]

In order to select the optimum phase shifter setting, the system samples the signal received from the satellite at regular time intervals. The stronger of the two signal is then selected and the phase of that antenna element is fixed. Then, the phase of the other antenna element is varied using the Two-Bit Phase Shifter. After this phase shift, the signals are combined and passed through to the peak detector. By using comparators, the phase setting corresponding to the highest combined received power is determined [Ber96]. The phase shift state that yields the best received power or signal-to-noise ratio is then used for the receive function during operation. The system is configured in such a way that the test is repeated after a short interval to compensate for any movement by the user.

The diversity combiner will produce a better result compared to an adaptive array that only utilizes LMS algorithm. This is because the diversity combiner will phase shift the input signal to produce the best maximum possible output SINR while the LMS adaptive array output SINR will depend on the incoming multipath and the relative SOI phase.

5.5 Conclusion

From the simulations of the antenna arrays, we observed that an LMS based adaptive antenna array can null out an uncorrelated signal successfully; however, in the presence of multipath, the SOI might add destructively or constructively with the multipath signal depending on the phase of the multipath.

Nevertheless, a modification to the antenna architecture is required to reject both interference and multipath. As proposed by Berkebile et al. [Ber96], the antenna can be modified according to Figure 21, by using a diversity combiner. In this architecture, the logic circuit in the handheld system determines the strongest incident signal for every particular time interval. It then selects the antenna element n which this signal component is impinging. After which, the phase of the other signal is varied either by 90° or 180° depending on which will produce the maximum power or signal-to-noise ratio at the receiver. As a result, we can conclude that the array is effective in combating interference and that with the proper modifications, it can also reject multipath signals.

Also, as shown in Figure 14 and 15, the simulated LMS adaptive array requires training sequences to train the weights of the adaptive array. We noticed that by using a larger step size (larger convergence factor), the final output SINR is smaller compared to when a larger step size is used. From the simulation results shown in Figure 16, we observed that given a convergence factor of 0.1480, the time required for a 9.6 kbps SatPCS can be as low as 10 ms. This result assumes that the user is stationary, however, if the user is constantly moving, the adaptive array might not be able to converge as fast. Using the same MATLAB program, we simulated the two element array but vary the initial weights. This variation can be interpreted as movement on the handheld unit. We observed that the convergence does not depend on the initial weights chosen. The number of iterations required were roughly similar every time the weights were varied. This leads us to the conclusion that rapid movement in the handheld unit will constantly cause the weights in the array to change. Whether the weights will converge will depend on how fast the user is moving. Thus, the LMS algorithm is not feasible for LEOs, but it is suitable for a MEO system, which normally takes a few hours to move across the sky. However, a mobile user using either system might experience the same problem since the environment is changing too rapidly for the weights to converge. To overcome this problem, blind adaptive algorithms can be used to overcome the need for training sequences. Blind adaptive algorithms are algorithms that exploit the characteristics of the signal envelope and utilize this information to train the weights to the

changing environment. Moreover, since some of the proposed satellite constellations utilize CDMA as the multiple access technique, the PN codes (which, by design of the CDMA standard are known by both the transmitter and the receiver) can be utilized to train the adaptive array weights instead of using external training sequences. As a result, the LMS algorithm can be used as a blind adaptive algorithm (the LMS algorithm is not inherently blind, but for this particular application it becomes blind).

Chapter 6 Conclusions and Future Work

6.1 Summary and Conclusions

This thesis began by presenting an overview of some of the different proposed satellite mobile communication systems. These systems are classified according to the type of orbit they occupy, the type of service they plan to provide and the multiple access techniques or frequency bands they plan to use.

As discussed in Chapter 2, each system has its own advantages and disadvantages. From the type of service these systems plan to provide to the orbital location and number of satellites for global coverage, these systems pose a challenge for the engineers that are involved in the design. These Satellite Personal Communication Systems (SatPCS) utilize the same concepts that are applied in cellular communications in terrestrial networks. Similarly, they also experience some of the same problems associated with cellular communication, for instance, interference, multipath fading, frequency planning and much more. However, due to the fact that satellites are constantly moving in space (except for GEOs), there are additional considerations such as Doppler shift and handoff from cell to cell and satellite to satellite. Additionally, other regulatory issues will come into play. However, the latter is beyond the scope of this thesis.

One of the more serious problems concerning both space and terrestrial communication systems is the issue of interference. Interference from coherent, correlated signals is known as

multipath, while interference from incoherent, uncorrelated signals is simply termed interference. These interfering signals (both correlated and uncorrelated to the SOI) can result in significant link degradation and lead to poor quality reception. To overcome this problem, one of the more common techniques is to utilize space diversity with adaptive antenna arrays. These arrays can be mounted on the handheld unit to replace the omni-directional antenna, which radiates in all directions.

Adaptive arrays are phased array antennas that can automatically adjust the element weightings to null out interfering signals. These arrays require algorithms that can process the input information and determine which is the SOI and which is the SNOI. For this thesis, we looked only at the LMS algorithm. We simulated a two element LMS adaptive array (limited by space) and demonstrated that the array does null out the interfering signal. However, we also showed that in the presence of multipath signals, the SOI might experience cancellation from the multipath component depending on the phase of the multipath signal.

Consequently, modifications had to be made to the handheld unit to overcome the problem of multipath. Numerous alternatives were mentioned, but the diversity combiner technique was selected because of its simplicity. As a result, the technique was discussed in general terms, but since it requires hardware implementation, the performance cannot be evaluated. The proposed technique utilizes a digital processor that phase shifts one of the multipath components and then combines the two signals together.

6.2 Future Work

Much work has been done in the area of adaptive antenna arrays; however, there is still much to be done. This thesis looked at how adaptive arrays can be mounted on handheld units to combat both interference and multipath signals. It focuses on the Least Mean Square algorithm (LMS) and how the convergence factor affects the rate of convergence of the weights in the adaptive array. The LMS algorithm is easy to implement in a practical sequence, but it requires the use of training sequences, sometimes as much as 5000 bits, in order for the weights to adapt fully. In low data rate (less than 200 kbps) systems, this will result in an interruption of the call in progress.

Consequently, future work should focus on blind adaptive algorithms that do not require the use of training sequences. This can be done by taking advantage of some of the inherent characteristics of the signal itself. One technique uses the Constant Modulus Algorithm (CMA), which exploits the constant modulus (amplitude) property of FM, PSK, or FSK waveforms by minimizing the variation of the signal amplitude at the array output [Pet94]. In the case of a CDMA system, the LMS algorithm can also take advantage of the PN sequence (which, by design of the CDMA standard, is known by both the transmitter and receiver) to train the array

weights, thus making the array “blind.” As a result, some more work can be done to compare the performance of these different algorithms and determine which one will produce the best output SINR.

Moreover, this thesis has not considered the implementation of adaptive arrays on a handheld unit. As a result, numerous issues such as how the antenna elements are to be mounted on the handheld unit were not discussed. Since most of the proposed SatPCSs are operating in the L-Band, and the antenna elements need to be spaced by no less than $\lambda/2$, there is a problem of space with which the antenna designers have to deal. For instance, at L band, the spacing required between two elements is approximately 12 cm. However, in S-band systems, only 6-7 cm spacings are required between the two elements. As a result, at higher frequencies, more elements can be mounted on the handheld unit. At Ka-Band, the spacing between two elements can go as low as 1.2 cm. This will allow for better performance for the handheld system. More analysis and research can be done to compare the performance of hardware implementation on these arrays on handheld units. More work can also be done to compare the performance of adaptive arrays with LEO and MEO systems.

None of the proposed SatPCS systems had been implemented when this thesis was written, so much information about the systems, such as channel characterization, could not be obtained. Also, the link margins required cannot be determined because too many factors, including the surroundings and the systems’ elevation angle, play a crucial role in determining the link margin. More research can be conducted by collecting empirical data regarding the channel characteristics in a LEO and MEO system. In the case of the LMS algorithm, studies can be done to find out how often the weights need to be adjusted in the adaptive array in a mobile environment, and also to compare urban and rural locations and to determine the propagation models required for SatPCS.

References

- [ABI96] _____. *“Wireless World Strategic Outlook: Intelligence for the wireless revolution, 1996 to 2000,”* Allied Business Intelligence, Feb. 1996
ISBN 1-883742-16-1.
- [Abr96] Farrokh Abrishamkar and Zoran Siveski. *“PCS Global Mobile Satellites,”* IEEE Communications Magazine, September 1996.
- [Age83] J.R. Treichler and B.G. Agee. *“A new approach to multipath correction of constant modulus signals,”* IEEE Trans on ASSP., vol. ASSP-31, no. 2, pp. 459-472, April 1983.
- [Ana94] Fulvio Ananasso and Marco Carosi. *“Architecture and networking issues in satellite systems for personal communications,”* International Journal of Satellite Communications, Vol. 12, 1994, pp. 33-44.
- [Ana95] Fulvio Ananasso and Francesco Delli Priscoli. *“The Role of Satellites in Personal Communication Systems,”* IEEE Journal on selected areas in Communications, Vol. 13, No.2 Feb. 1995, pp 180-196.

- [All93] R. Allnutt, R.M. Dissanayake A. et. al. “*A Study of Satellite Motion Induced Multipath Phenomena*,” IMSC’93, 337-339, June 1993.
- [All95] R. Allnutt and T. Pratt. “*A Study in Small Scale Antenna Diversity in combating the Effects of Satellite Motion Induced Multipath Fading for Handheld Satellite Communications Systems*,” IEE Antennas and Propagation Conference, 4-7 April 1995.
- [Ana94] Fulvio Ananasso and Marco Carosi. “*Architecture and Networking Issues in Satellite Systems for Personal Communications*,” International Journal of satellite communications, Vol. 12, 33-44 (1994).
- [Bai96] Thomas Baird & Wes Bush. TRW Space and Electronics Group “*Odyssey System Overview*,” February 1996.
- [Ber96] J. Berkebile et. al.. “*A Two-Element Phased-Array Antenna for Reducing Multipath Effects in Handheld SATCOM Units*,” Microwave Journal, January 1996.
- [Bos95] Charles W. Bostian. “*Satellite Cellular Integration*,” Proceedings of the AIAA/ESA Workshop, Sept 1995.
- [Böt95] A. Böttcher, A. Jahn, E. Lutz and M. Werner. “*Analysis of Basic System Parameters of Communication Networks based on Low Earth Orbit Satellites*,” IEEE Journal on selected areas in communications, Vol. 13, No.2, Feb. 1995.
- [Col85] R.E. Collin. *Antennas and Radiowave Propagation*. McGraw-Hill Book Company, 1985.
- [Com83] R.T.Compton. “*Adaptive Array Behavior with Sinusoidal Envelope Modulated interference*,” IEEE Transactions on Aerospace and Electric systems, AES-19, no. 5 (September 1983): 677.
- [Com88] R.T. Compton. *Adaptive Antennas-concepts and performance*. Prentice Hall, New Jersey 07632, 1988.

- [Com93] Gary M. Comparetti. *"A technical comparison of several global mobile satellite communication systems,"* IOS Press, Space Communications 11, 1993, pp. 97-104.
- [Cor92] _____. *"A statistical model for land mobile satellite channels and its application to nongeostationary orbit systems,"* IEEE Trans. Veh. Technol., Special issue on "Future PCS technologies," vol 43, no.3, pp 738-742, Aug. 1994.
- [Cor et al. 95] Giovanni E. Corazza and Francesco Vatalaro. *"An Approach to Transmission Performance Evaluation for Satellite Systems Adopting Non-Geostationary constellations,"* Proceedings of the AIAA/ESA Workshop, Sept 1995.
- [Cou97] Leon W. Couch II. *Digital and Analog Communication Systems*, 5th edition Prentice Hall, New Jersey 07458.
- [Cul93] C. Cullen, X. Benedicto, R. Tafazolli and B. Evans. *"Network and common channel signalling aspects of dynamic satellite constellations,"* IEEE Journal on selected areas in communications, Vol. 13, No.2, Feb. 1995.
- [Dis93] Allnutt, R.M. Dissanayake A. et.al. *"Propagation considerations on L-band handheld communications service offerings on L-band handheld communications service offerings via satellite,"* ICAP'93, Edinburg, Scotland, 1993.
- [Enr93] Enrico Del Re, Romano Fantacci and Giovanni Giambene. *"Performance Analysis of a Dynamic Channel Allocation Technique for Satellite Mobile Cellular Networks,"* International Journal of Satellite Communications, Vol. 12, 33-44 (1994).
- [Enr95] Enrico Del Re, *"Mobile Satellite Communications for Seamless PCS"* IEEE Journal on selected areas in communications, vol. 13, No. 2, Feb 1995.
- [Gab76] W.F. Gabriel. *"Adaptive arrays-an introduction"*, Proc. IEEE, pp239-271, Feb 1976.
- [Gab84] W. Gabriel. *"Spectral Analysis and Adaptive Array Superresolution Techniques,"* Proceedings of the IEEE, Vol.68, No. 6, June 1984.

- [Gaf94] L.M. Gaffney et. al. “*Non-GEO Mobile Satellite Systems: A risk assesment*,” 4th International Mobile Satellite Conference 1995, Ottawa, Canada, June 6-8, 1995, pp. A-23-A-27.
- [Gri95] Tren Griffin. “*Teledesic Presentation*,” Satellite Summit ‘96, London, England, June 24-26, 1996.
- [Gru91] Jerry L. Grubb. “The traveler’s dream come true,” *IEEE Communications*, November 1991, pp. 48-51.
- [Har94] Todd Hara , Orbital Communications Corporation. “*ORBCOMM Low Earth Orbit Mobile Satellite Communications System*,” submitted in response to TCC-94, Papers for Digital Technology for the Tactical Commander.
- [Har95] Nicholas Hart et. al. “*A Discussion on Mobile Satellite Systems and the Myths of CDMA and Diversity Revealed*,” 4th International Mobile Satellite Conference 1995, Ottawa, Canada, June 6-8, 1995, pp 469-475.
- [Hir95] Edward Harshfield. “*The GLOBALSTAR System*,” Applied Microwave and Wireless, Summer 1995.
- [How96] Glen Howell and Paromita Mazumder. “*ORBCOMM’s LEO Mobile Satellite System*,” Project Report, VPI&SU, 1996.
- [ICO96] Documents retrieved from ICO’s World Wide Web server at URL <http://www.i-co.co.uk/>, spring 1996.
- [Inm95] Documents retrieved from Inmarsat’s World Wide Web server at URL <http://www.worldserver.pipex.com/inmarsat/>, July 1996.
- [Iri96] Iridium’s website, at URL <http://www.iridium.com>.
- [Jer94] M.C. Jeruchim, P.Balaban, K. Sam Shanmugan. “*Simulation of Communication Systems*,” 2 edition. Penum press, New York, January 1994.
- [Lia96] KengJin Lian. “*The IRIDIUM system*,” Project Report, VPI&SU, Spring 1996.

- [Lib95] Joseph Liberti. "CDMA Cellular Communications Systems employing Adaptive Antennas," Ph. D. dissertation, VPI&SU, 1995.
- [Lod91] John Lodge. "Mobile Satellite Communication Systems: Toward Global Personal Communications," IEEE Communications Magazine, Nov. 1991, pp.24-30.
- [Lutz93] E. Lutz et al. "Analysis of Basic Parameters of Communication Networks based on Low Earth Orbit Satellites," IEEE Journal on selected areas in communications, Nov. 1993.
- [Man96] Mansoor Ahmad. "LMS based Adaptive Antenna Algorithms for TDMA and CDMA Systems," Master's Project, VPI&SU, 1996.
- [Mar91] Gerard Maral, Jean-Jacques De Ridder, Barry Evans and Madhavendra Richharia. "Low Earth Orbit Satellite Systems for Communications," International Journal of satellite communications, Vol. 9, 209-225 (1991).
- [Mai95] K Maine, C. Devieux and P. Swan. "Overview of IRIDIUM satellite network," Satellite Communication Division, Motorola Inc., Chandler, AZ, USA, published at WESCON/95, p. 483-490, 1995, ISBN: 0 7803 2636 9.
- [Maz93] M Mazzella, M Cohen, D Rouffet, M Louie, KS Gilhousen. "Multiple Access techniques and spectrum utilization of the Globalstar Mobile Satellite System," 4th IEE Conference on Telecommunications London, UK, 1993 ISBN: 0 85296 568 0 pp. 306-311.
- [Mon80] R.A. Monzingo and T.W. Miller. *Introduction to adaptive arrays*, New York, Wiley 1980.
- [Nic89] Edmond Nicolau and Dragos Zaharia. *Adaptive Arrays*, Elsevier, New York, 1989.
- [Pra86] T. Pratt and C.W. Bostian. *Satellite Communications*, John Wiley and Sons, New York, 1986.
- [Pro95] J.G. Proakis. *Digital Communications*, 3rd edition. McGraw-Hill, Inc. New York 10020, 1995.

- [Pet94] Paul Petrus. “*Blind Adaptive Antenna Arrays for Mobile Communications,*” Master’s Thesis, VPI&SU, 1994.
- [Rap95] Theodore Rappaport. *Wireless Communications: Principles and Practice.*, Prentice Hall, New Jersey, 1996.
- [Rod96] Dennis Roddy. *Satellite Communications.*, McGraw Hill, New York, 1996.
- [Sha85] T.J. Shan and T. Kailath. “*Adaptive Beamforming for Coherent Signals and Interference,*” IEEE Transactions on ASSP, Vol. 33, No. 3, June 1985.
- [Sko90] Merrilli Skolnik. *Introduction to Radar Systems*, 2nd edition McGraw-Hill, New York, 10020, 1990.
- [Sta94] Henry Stark and John Woods. *Probability, Random Processes, and Estimation Theory for Engineers*, Prentice Hall, New Jersey, 2nd edition, 1994.
- [Ste91] David E. Sterling and Hohn E. Hatlelid. “*The Iridium system- A revolutionary satellite communications system developed with innovative applications of technology,*” *MilCom*, 1991.
- [Stu81] G.A. Thiele, and W.L. Stutzman. *Antenna theory and design*, Wiley, New York, 1981.
- [Stu95] Mark Sturza. “*Architecture of the Teledesic Satellite System,*” 4th International Mobile Satellite Conference 1995, Ottawa, Canada, June 6-8, 1995, pp. 212-218.
- [Swa93] Peter A. Swan and Paul N. Cloutier. “Global Personal Communications this decade with Iridium,” *Space Technology*, Vol. 13, No. 4, 1993, pp. 423-425.
- [Tor96] Tor E wolff. <http://www.idt.unit.no/~torwi/>, July, 1996.
- [Tuc94] Edward Tuck et. al. “*The calling SM Network: A global wireless communication system,*” International Journal of Satellite Communications, Vol 12, No.1, Jan.-Feb., 1994. pp. 45-61.
- [Wid67] B. Widrow et. al. “*Adaptive antenna systems,*” Proc. IEEE, Vol. 55, No. 12, Dec. 1967.

- [Wil96] A.E. Williams, R.K. Gupta, and A.I. Zaghloul. “*Evolution of Personal Handheld Satellite Communications*,” Applied Microwave and Wireless, Summer 1996.
- [Woo96] Lloyd Wood. “Lloyd’s satellite constellations,” retrieved from URL <http://www.ee.surrey.ac.uk/Personal/L.Wood/constellations/overview.html>.
- [Vat et.al 95] Francesco Vatalaro, Giovanni E. Corazza, Carlo Caini and Carlo Ferrarelli. “*Analysis of LEO, MEO, and GEO Global Mobile Satellite Systems in the Presence of Interference and Fading*,” IEEE Journal on selected areas in communications, Vol. 13, No.2, Feb. 1995.

Vitae

Keng-Jin Lian was born on November 8, 1972 in Taiping, Perak, Malaysia. It was there that Keng-Jin spent the first 18 years of his life attending primary and secondary school. After completing his secondary education, Keng-Jin was awarded a scholarship by the STARR Foundation which allowed him to pursue a higher education in the United States of America. Upon completion of his Bachelor of Science in Electrical Engineering at Virginia Polytechnic Institute and State University (VPI&SU), Keng-Jin stayed on to work on his Masters in Electrical Engineering under the guidance of Dr. Timothy Pratt. After completing his thesis and graduate coursework, Keng-Jin will return to Malaysia to celebrate Chinese New Year with his family, something that he hasn't done for the last six years. After that, he will return to United States, where he will be working at Hughes Network Systems in Germantown, Maryland.